The anatomy of Teleocrater rhadinus, an early avemetatarsalian from the lower portion of the Lifua Member of the Manda Beds (Middle Triassic)

Nesbitt, Sterling; Butler, Richard; Ezcurra, Martin; Charig, Alan; Barrett, Paul

DOI:
10.1080/02724634.2017.1396539

License:
Other (please specify with Rights Statement)

Document Version
Peer reviewed version

Citation for published version (Harvard):
Nesbitt, S, Butler, R, Ezcurra, M, Charig, A & Barrett, P 2018, 'The anatomy of *Teleocrater rhadinus*, an early avemetatarsalian from the lower portion of the Lifua Member of the Manda Beds (Middle Triassic)', *Journal of Vertebrate Paleontology*, vol. 37, no. sup1, pp. 142-177. https://doi.org/10.1080/02724634.2017.1396539

The anatomy of *Teleocrater rhadinus*, an early avemetatarsalian from the lower portion of the Lifua Member of the Manda Beds (~Middle Triassic)

STERLING J. NESBITT,*[,1] RICHARD J. BUTLER,[2] MARTÍN D. EZCURRA[2,3], ALAN J. CHARIG, [4,†] and PAUL M. BARRETT[4]

[1]Department of Geosciences, Virginia Polytechnic Institute and State University, Blacksburg, Virginia, 24061, U.S.A. sjn2104@vt.edu;

[2]School of Geography, Earth and Environmental Sciences, University of Birmingham, Edgbaston, Birmingham B15 2TT, U.K.;

[3]CONICET−Sección Paleontología de Vertebrados, Museo Argentino de Ciencias Naturales, C1405DJR Buenos Aires, Argentina;

[4]Department of Earth Sciences, The Natural History Museum, Cromwell Road, London, SW7 5BD, U.K.

*Corresponding author

[†]Deceased

ABSTRACT—Bird-line archosaurs (=Avemetatarsalia, the clade containing birds, dinosaurs, pterosaurs, and their kin) originated in the Triassic Period. However, the earliest evolution of this group is poorly documented because fossils are extremely rare and consist mostly of postcrania. Here, we document the osteology of *Teleocrater rhadinus*, an early avemetatarsalian from the lower portion of the Middle Triassic Lifua Member of the Manda Beds of the Ruhuhu Basin, southwestern Tanzania. Material of *Teleocrater rhadinus* includes the holotype partial skeleton comprising a single individual including cervical, trunk, and caudal vertebrae, pectoral, pelvic, forelimb, and hind limb material, and referred specimens representing parts (skull elements, vertebrae, pectoral, pelvic, and limb elements) of at least three other individuals collected from a bonebed. Character states of the skull elements, vertebrae, girdles, and limbs indicate that *Teleocrater rhadinus* represents the first documented non-ornithodiran avemetatarsalian known from well-preserved, associated material. Furthermore, *Teleocrater rhadinus* forms part of a newly recognized clade, Aphanosauria~~Silesauridae~~, which also contains formerly enigmatic archosaur taxa from across Pangea, including *Dongusuchus efremovi* from the Middle Triassic of Russia, *Yarasuchus deccanensis* from the Middle Triassic of India, and *Spondylosoma absconditum* from the ?Middle Triassic of Brazil. This new clade and other new discoveries from the Middle to Late Triassic elucidate the sequence of character acquisitions at the base of Avemetatarsalia and fill a crucial gap in the understanding the anatomical transformations that enabled dinosaurs to flourish later in the Mesozoic.

INTRODUCTION

Archosauria, the clade that includes extant crocodylians and birds, has a deep evolutionary history that stretches back to the late Early Triassic, over 247 million years ago (Gower and Sennikov, 2000; Butler et al., 2011; Nesbitt, 2011; Nesbitt et al., 2011). In the 15 million years following their origin, archosaurs became the largest, most diverse group of terrestrial vertebrates and extended their range across Pangea (Fraser, 2006; Sues and Fraser, 2010; Sookias et al., 2012; Turner and Nesbitt, 2013). By the early part of the Late Triassic (c. 230 Ma), nearly all the major groups of Triassic archosaurs were present (Rogers et al., 1993; Furin et al., 2006). This diversification has been viewed as an example of an adaptive radiation (Benton, 1983, 2010; Brusatte et al., 2008a, b, 2010; Nesbitt, 2011; Ezcurra, 2016).

Archosauria is divided into two lineages: archosaurs more closely related to crocodylians (= 'crocodile-line archosaurs', = Pan-Crocodylia, = Pseudosuchia) and archosaurs more closely related to birds (= 'bird-line archosaurs', = Ornithosuchia, = Avemetatarsalia, = Pan-Aves) (Gauthier, 1986; Benton, 1999; Gauthier and de Queiroz, 2001). Of these two lineages, the pseudosuchians have been interpreted as the first to increase in diversity and disparity (Brusatte et al., 2008a) and a number of major clades (ornithosuchids, aetosaurs, crocodylomorphs) appeared in the fossil record for the first time by the Late Triassic. Pseudosuchians have a relatively good fossil record in the Middle Triassic and a widespread distribution across Pangea (Butler et al., 2011; Nesbitt, 2011; Nesbitt et al., 2011; Butler et al., 2014). By contrast, the fossil record of

avemetatarsalians is limited prior to the Late Triassic: although previously thought to extend into the Middle Triassic, recent radiometric dating of the Chañares Formation of Argentina pushed much of their early fossil record into the early Late Triassic (Marsicano et al., 2016). Consequently, the first half of Triassic avemetatarsalian evolutionary history is represented by only a handful of derived dinosauriform occurrences (*Asilisaurus kongwe*, *Nyasasaurus parringtoni*, *Lutungatali sitwensis*). To complicate matters further, character support at the base of Archosauria has typically been weak (Sereno, 1991; Juul, 1994; Brusatte et al., 2010; Nesbitt, 2011; Nesbitt et al., 2014) and the identification of its sister-taxon is debated (Nesbitt, 2011; Ezcurra, 2016), so it has been difficult to distinguish the earliest archosaurs from their closest relatives, the non-archosaurian archosauriforms.

The Middle Triassic Manda Beds archosaur assemblage is helping to resolve some of the outstanding questions posed by the poorly sampled fossil record of early archosaurs. Most archosaurs from this assemblage include cranial and postcranial remains, which are essential for untangling the order of character acquisition in archosaur clades. The pseudosuchian component of the Manda Beds archosaur assemblage includes *Parringtonia gracilis* (Huene, 1939; Nesbitt and Butler, 2012; Nesbitt et al., 2017a), *Mandasuchus tanyauchen* (Butler et al., 2017), *Stagonosuchus nyassicus* (Huene, 1938; Lautenschlager and Desojo, 2011), *Nundasuchus songeaensis* (Nesbitt et al., 2014), *Hypselorhachis mirabilis* (Butler et al., 2009), and several other species that await description. By contrast, only three avemetatarsalians are also known from the assemblage, *Asilisaurus kongwe* (Nesbitt et al., 2010), *Nyasasaurus parringtoni* (Nesbitt et al., 2013a), and *Teleocrater rhadinus* (Nesbitt et al., ~~in review~~2017b).

Teleocrater rhadinus was first described by AJC in his unpublished PhD dissertation (Charig, 1956), and subsequently appeared widely in the literature as a nomen nudum (see Moody and Naish, 2010; Butler et al., 2017). Nesbitt et al. (2017b~~in review~~) formally erected the taxon and provided brief discussions of its anatomy and phylogenetic position. Here, we fully describe the osteology of the holotype (NHMUK PV R6795) and referred material of ~~*Teleocrater*~~ *T. rhadinus*. Furthermore, we provide a detailed examination of its phylogenetic position and discuss its impact on the evolution of character states from the base of Archosauria through to the origin of Dinosauria. *Teleocrater* is part of the lower Lifua Member (Fig. 1) archosauromorph assemblage, which also includes an allokotosaurian archosauromorph and likely *Hypselorhachis mirabilis* (see Smith et al., 2017; Nesbitt et al., 2017b~~in review~~).

Institutional Abbreviations—**ISI**, Indian Statistical Institute, Kolkata, India; **MCP**, Museu de Ciências e Tecnologia da Pontifícia Universidade Católica do Rio Grande do Sul, Porto Alegre, Brazil; **MSM**, Arizona Museum of Natural History, Mesa, Arizona, U.S.A. (formerly Mesa Southwest Museum); **NHMUK**, Natural History Museum, London, U.K.; **NMT**, National Museum of Tanzania, Dar es Salaam, Tanzania; **PIN**, Borissiak Paleontological Institute of the Russian Academy of Sciences, Moscow, Russia; **PVL**, Instituto Miguel Lillo, Tucuman, Argentina; **PEFO**, Petrified Forest National Park, Arizona, U.S.A.; **SAM**, Iziko South African Museum, Cape Town, South Africa; **TTU**, Texas Tech University Museum, Lubbock, U.S.A.; **UMZC**, University Museum of Zoology, University of Cambridge, Cambridge, U.K.; **ZPAL**, Institute of Paleobiology of the Polish Academy of Sciences, Warsaw, Poland.

SYSTEMATIC PALEONTOLOGY

ARCHOSAURIA Cope, 1869 sensu Gauthier and Padian, 1985

AVEMETATARSALIA Benton, 1999

Definition— The most inclusive clade containing *Passer domesticus* Linnaeus, 1758 but not *Crocodylus niloticus* Laurenti, 1768 (modified from Benton, 1999).

Comments—Equivalent clade names include Ornithosuchia (Gauthier and Padian, 1985; de Queiroz and Gauthier, 1990) and Pan–Aves (Gauthier and de Queiroz, 2001). We do not use Ornithosuchia for the reasons outlined by Sereno (1991).

~~SILENDASAURIA~~ APHANOSAURIA Nesbitt, Butler, Ezcurra, Barrett, Stocker, Angielczyk, Smith, Sidor, Niedźwiedzki, Sennikov, and Charig, ~~in review~~2017b

Taxonomic Content—*Teleocrater rhadinus* Nesbitt, Butler, Ezcurra, Barrett, Stocker, Angielczyk, Smith, Sidor, Niedźwiedzki, Sennikov, and Charig, 2017b~~in review~~, *Yarasuchus deccanensis* Sen, 2005, *Dongusuchus efremovi* Sennikov, 1988, and *Spondylosoma absconditum* Huene, 1942.

Definition—The most inclusive clade containing *Teleocrater rhadinus* Nesbitt, Butler, Ezcurra, Barrett, Stocker, Angielczyk, Smith, Sidor, Niedźwiedzki, Sennikov, and Charig, 2017b~~in review~~ and *Yarasuchus deccanensis* Sen, 2005 but not *Passer domesticus* Linnaeus, 1758 or *Crocodylus niloticus* Laurenti, 1768 (Nesbitt et al., ~~in review~~2017b).

Diagnosis—Epipophyses present on post-axial anterior cervical vertebrae (Nesbitt, 2011:character 186, state 1; abbreviated to e.g., 'N186-1' hereafter; and Ezcurra, 2016: character 336, state 1; abbreviated to e.g., 'E336-1' hereafter); dorsal end of neural spines of cervical vertebrae blade-like, but with adjacent, rounded expansions with a rugose texture (N191-3, ambiguous when *Dongusuchus efremovi* is included); anterior and middle postaxial cervical neural spines with a strong anterior overhang (E343-1); posterior cervical vertebrae with an articulation surface just dorsal to the parapophysis (= divided parapophysis of Nesbitt [2011]) (N193-1; E314-1); dorsally opening pit lateral to the base of the neural spine of trunk vertebrae (E361-1); elongated deltopectoral crest of the humerus greater than 30% the length of the shaft (N230-1); wide distal end of the humerus greater than 30% of humerus length (N235-1); extensive contact between the ischia on the midline but the dorsal margins are separated (E485-1; N191-1, but ambiguous); rounded outline of the posteroventral portion of the ischium (N293-1); longitudinal groove on the dorsal surface of shaft of the ischium (E484-1); femur with a scar for the M. iliofemoralis externus near the proximal surface (homologous with the anterior trochanter in dinosauromorphs) (N308-1; E520-1); proximal surface of the femur with a straight transverse groove (N314-1; E495-1); distal articular surface of the femur concave (E512-2); calcaneal tuber taller than broad (N376-0).

Remarks—~~Silendasauria~~Aphanosauria, meaning 'secret reptiles' in Greek, contains a group of long-necked Triassic-aged archosauriform taxa that have been discovered across Pangea from fragments or partial skeletons, but not recognized as a natural group until the naming of *Teleocrater* (Nesbitt et al., 2017b~~, in review~~).

TELEOCRATER RHADINUS Nesbitt, Butler, Ezcurra, Barrett, Stocker, Angielczyk, Smith, Sidor, Niedźwiedzki, Sennikov, and Charig, ~~in review~~2017b

Figures 2–26

"*Teleocrater tanyura* gen. et sp. nov."; Charig, 1956:177, plates 33–40.

"*Teleocrater* Charig 1957: 28 (nomen nudum)"; Charig et al., 1965:215.

"*Teleocrater rhadinus* Charig 1967"; Charig in Appleby et al., 1967:709.

"*Teleocrater*"; de Ricqlès et al., 2008:61, 63, plate 2.1.

Formatted: Spanish (Argentina)

Teleocrater rhadinus Nesbitt, Butler, Ezcurra, Barrett, Stocker, Angielczyk, Smith, Sidor, Niedźwiedzki, Sennikov, and Charig, ~~in review~~2017b

Holotype—NHMUK PV R6795 (field number 48b of F. R. Parrington), a disarticulated but associated partial skeleton, including: four cervical, ~~seven~~ eight trunk, and 16~~7~~ caudal vertebrae, two rib fragments, one from the cervical and one from the trunk region, partial right scapula, partial coracoid, complete right radius and ulna, partial left ilium, both femora, both tibiae, left fibula, two proximal ends of metatarsals, isolated phalanges, and associated fragments (Figs. 3, 8, 11–13, 16, 17, 19, 21, 23–25; Tables 1, 2).

Referred Specimens—Left maxilla (NMT RB495; Fig. 2); right frontal (NMT RB496; Fig. 2); left quadrate (NMT RB493; Fig. 2); braincase (NMT RB491; will be described elsewhere); axis (NMT RB504; Fig. 4); anterior cervical vertebrae (NMT RB505; NMT RB506; Fig. 5); middle cervical vertebrae (NMT RB511; NMT RB512;

Fig. 6); posterior cervical vertebra (NMT RB514; Fig. 7); anterior trunk vertebra (NMT RB500); posterior trunk vertebrae (NHMUK PV R6796, NMT RB516; Fig. 9); second sacral vertebra (NMT RB519; Fig. 10); right scapula (NMT RB480; Fig. 13); left humeri (NMT RB476; NMT RB477; Fig. 14); distal half of left humerus (NHMUK PV R6796; Fig. 15); left ulnae (NMT RB485; NMT RB486); metacarpal (NMT RB484; Fig. 18); left ilium (NMT RB489; Fig. 19); left ischium (NMT RB479; Fig. 20); right femur (NMT RB498; Figs. 22, 23); left tibia (NMT RB481); right fibulae (NMT RB482; NMT RB488); right calcaneum (NMT RB490; Fig. 26) (Tables 3, 4).

Locality and Horizon—The holotype specimen was found in a fluviolacustrine mudstone–sandstone sequence in the lower portion of the Lifua Member of the Manda Beds, near the confluence of the Mkongoleko and Rutikira rivers, Ruhuhu Basin, Tanzania (Fig. 1). The exact locality is not known but was mapped as locality B9 of Stockley (1932) by F. R. Parrington and recorded as "1/2 hours march west village of Mkongoleko. South of river Mkongoleko" (field notes of F. R. Parrington, 1933, UMZC). The holotype specimen was found at the same locality as the holotype and associated remains of '*Stanocephalosaurus*' *pronus* (Howie, 1970).

The referred specimens were discovered in 2015 within 1 km of the mapped position of Stockley's (1932) locality B9, in the lower portion of the Lifua Member of the Manda Beds (locality Z183; Smith et al., 2017; exact locality information available from the authors because of possible fossil poaching in the area). However, the precision of the locality data provided by Stockley (1932), as well as the reliability of Parrington's attributions of his localities to Stockley's original localities, is unclear (see Sidor et al., 2017). Therefore, the recently collected specimens could have come from the exact same

locality as the holotype, or from a new locality nearby.

On the basis of comparisons with the tetrapod fauna from subzone B of the *Cynognathus* Assemblage Zone of South Africa, the base of the Lifua Member is considered to be Anisian in age (Lucas, 1998; Hancox, 2000; Abdala et al., 2005; Rubidge, 2005; Hancox et al., 2013; Nesbitt et al., 2017b) though it might possibly be as young as earliest Carnian (Marsicano et al., 2016).

Diagnosis—*Teleocrater rhadinus* differs from all other archosauriforms except *Yarasuchus deccanensis* and *Dongusuchus efremovi* in possessing the following combination of character states (*asterisk indicates possible autapomorphy): anterior cervical vertebrae with large anterior neural canal openings, which are sub-elliptical in outline with the long axis of the ellipse oriented mediolaterally, whereas the posterior neural canal openings are elliptical with the long axis oriented dorsoventrally*; anterior cervical vertebrae at least 1.5 times longer than anterior to middle trunk vertebrae; olecranon process present, but forms only a short expansion; preacetabular process of the ilium arcs medially to create a distinct pocket on the medial surface; small concave ventral margin of the ischial peduncle of the ilium; long M. iliofibularis crest of the fibula, extending for more than 35% of the length of the bone; anterior edge of the proximal portion of fibula curved laterally. *Teleocrater rhadinus* can be further distinguished from *Yarasuchus deccanensis* in possessing a more posteriorly directed scapula glenoid. *Teleocrater rhadinus* and *Dongusuchus efremovi* can be differentiated on the basis of femoral morphology, with the former taxon possessing a more rounded lateral portion of the proximal portion in anterolateral view, a concave medial surface on the proximal end, a lower ratio of total femoral length to minimum midshaft diameter

(~12), and the possession of a posteromedial tuber of the proximal portion that is mediolaterally convex.

Taphonomic Comments—The holotype of *Teleocrater rhadinus* consists of a single, disarticulated skeleton that was surface-collected alongside temnospondyl remains (field notes of F. R. Parrington, 1933, UMZC). The areal extent of the collection surface was not recorded, but is likely to have been several meters. With the exception of two sacral ribs that likely belong to a dicynodont, all of the material pertains to a single taxon. None of the remains attributed to *T. rhadinus* are duplicated, elements from alternate sides of the body, when present, correspond in size (e.g., both tibiae are the same length), and the preservation style and color of the remaining matrix is common to all of the bones that compose the holotype.

The referred specimens of *Teleocrater rhadinus* were found weathered out and in situ within a bonebed in association with a mixed vertebrate assemblage that also includes a much larger, long-necked archosauromorph (anterior cervical vertebra, NMT RB549; quadrate, NMT RB550) that is likely an allokotosaurian (sensu Nesbitt et al., 2015; Nesbitt et al., 2017b), a partial skeleton of *Cynognathus crateronotus* (NMT RB459; Wynd et al., 2017), a dicynodont (NMT RB554), temnospondyl skull fragments (NMT RB551), and small indeterminate reptiles (humerus, NMT RB552; femur, NMT RB553). Differences in size between the referred specimens of *T. rhadinus* indicate that at least three individuals are preserved. None of the referred specimens were found in articulation, but their relatively similar size, consistent morphology, morphological similarity to the closely related taxon *Yarasuchus deccanensis* (see Nesbitt et al., 2017b, ~~in review~~ Supplemental Information), and their overlap with the holotype indicate

that all of this material is referable to the same taxon, *T. rhadinus*. Although very well preserved in general, some of the referred vertebrae are missing parts of the neural spines, vertebral processes, and the edges of the anterior and posterior articular surfaces of the centra.

Skeletal Maturity—Determining the ontogenetic age of the *Teleocrater rhadinus* specimens is challenging. The vertebrae of the holotype and the referred specimens have closed neurocentral sutures indicating that none of the specimens of *T. rhadinus* were young individuals, assuming that they followed the same sutural closing patterns documented in *Alligator mississippiensis* (Brochu, 1996; Ikejiri, 2012) and other crocodile-line archosaurs (Irmis, 2007). However, some *T. rhadinus* individuals clearly grew to sizes that were considerably larger (~30%) than the holotype, as evidenced by a referred large middle cervical vertebra (NMT RB512; Fig. 6). Additionally, histological data from a humerus (NMT RB476) and fibula (NMT RB488) presented by Nesbitt et al. (2017b~~in review~~) indicate that the sampled animals were in a rapid growth stage, but no growth marks are present; thus, the skeletal maturity of the sampled individuals cannot be confirmed histologically.

DESCRIPTION

Skull

Maxilla (Referred)—The front of the skull is represented by a nearly complete referred left maxilla (NMT RB495; Fig. 2) missing only parts of the posterior portion of the dorsal process. We assign this bone to *Teleocrater rhadinus* based on its ~~appropriate~~

Formatted: Font: Italic

size, which is commensurate with that ~~with the~~of other associated elements of the taxon (including other skull bones; see below), and the presence of an antorbital fossa on the posterodorsal margin of ~~the posterior of~~ the maxilla (present in crown Archosauria; Nesbitt, 2011). No ~~other~~ character states specifically ~~clearly~~support the assignment of this specimen to ~~an~~ A~~a~~vemetatarsalia~~n~~. In lateral view, the maxilla has a long posterior process and an anteroposteriorly restricted dorsal process. The antorbital fenestra has a gently rounded anterior border and a straight ventral border. The maxilla also bears an antorbital fossa that excavates the dorsal process and the dorsolateral portion of the posterior process along nearly its full length. The presence of these two character states supports the placement of ~~*Teleocrater*~~ *T. rhadinus* within Archosauria (Nesbitt, 2011). The preserved portion of the dorsal process is directed primarily dorsally but with a small posterior component. The excavation of the dorsal process by the antorbital fossa is more extensive anteriorly, whereas the fossa becomes ~~narrower~~ shallower posteriorly. The anterior edge of the dorsal process has a roughened, well-defined surface for articulation with either the maxillary (= posterodorsal) process of the premaxilla or the ventral process of the nasal. The maxilla appears therefore to be excluded from the border of the external naris, as also occurs in proterochampsids (e.g., *Chanaresuchus bonapartei*; PULR 07), *Euparkeria capensis* (SAM-PK-K5867), ctenosauriscids (e.g., *Arizonasaurus babbitti*: Nesbitt, 2005a; Nesbitt et al., 2011), and the pterosaur *Dimorphodon macronyx* (NHMUK PV OR41212). The anterior portion of maxilla is continuously rounded in lateral view, and there may have been a notch between the maxilla and premaxilla, resembling the condition in *Gracilisuchus stipanicicorum* (MCZ 4117), but unlike that in *Euparkeria capensis* (SAM-PK-K6047) where there is a continuous ventral margin

between the premaxilla and the maxilla. In *T. rhadinus* ~~*Teleocrater*~~, the anterior-most extent of the maxilla in lateral view bears a large, anteriorly opening foramen. This anteriorly opening foramen is also present in *Asilisaurus kongwe* (NMT RB159) and *Silesaurus opolensis* (ZPAL Ab III/361/26) and may be homologous to the anteriorly opening foramen on the lateral surface of the anterior end of the maxilla of ~~*Euparkeria*~~ *E. capensis* (SAM-PK-K6047).

———Much of the lateral surface of the maxilla is flat with a slightly rugose surface texture. A row of foramina ~~runs~~ extends parallel to the ventral margin of the maxilla for most of its length, and a few anteroposteriorly elongated foramina lie immediately ventral to the antorbital fossa. The ventral margin of the posterior process is straight and parallel with the dorsal margin, as in ~~*Euparkeria*~~ *E. capensis* (SAM-PK-K6047) and ~~*Chanaresuchus*~~ *C. bonapartei* (PVL 4586). The antorbital fossa is dorsoventrally deepest anteriorly near the dorsal process of the maxilla and disappears near the posterior extent of the posterior process. The boundary between the lateral surface of the maxilla and the antorbital fossa consists of a simple change in slope, as in most archosauriforms (e.g., ~~*Euparkeria*~~ *E. capensis*; SAM-PK-K6047), and there is no laterally expanded ridge defining the edge of the fossa unlike that present in ~~*Gracilisuchus*~~ *G. stipanicicorum* (MCZ 4117), *Eoraptor lunensis* (PVSJ 512), and several basal neotheropods, such as *Coelophysis bauri* (MCZ 4326, 4327). Posteriorly, the posterior process of the maxilla expands slightly dorsally and ventrally immediately posterior to the termination of the antorbital fossa, resembling the condition in some non-eucrocopodan archosauriforms (e.g., *Proterosuchus fergusi*: RC 846; *Erythrosuchus africanus*: BP/1/5207). A weakly developed, posteroventrally directed ridge is present on

the lateral surface at the posterior end of the maxilla near the articular surface for the jugal (Fig. 2).

The medial surface of the dorsal process bears a rimmed, triangular fossa that extends dorsally along much of the preserved height of the process and ventrally to the base of the palatal process. This deep fossa is also present in ~~*Euparkeria*~~ *E. capensis* (SAM-PK-K6050; Gow, 1970) and might be homologous to fossae in the same position in ~~*Asilisaurus*~~ *A. kongwe* (NMT RB159) and ~~*Silesaurus*~~ *S. opolensis* (ZPAL Ab III/361/26). The medial surface of the dorsal process surrounding the deep fossa is flat. The palatal process is oriented horizontally and extends anteriorly beyond the most anterior extent of the lateral surface of the maxilla, such that the palatal process is visible in lateral view. The extent of the medial expansion of the palatal process indicates that it likely met its antimere on the midline, as in nearly all archosaurs (Nesbitt, 2011), and that it was more medially expanded than that of ~~*Euparkeria*~~ *E. capensis* (Gow, 1970). The delicate medial flange of the palatal process is dorsoventrally compressed and lacks grooves on its medial surface. A small groove, with a parallel ridge ventral to it, lies immediately ventral to the palatal process. This groove possibly marks the articular surface for the palatal process of the premaxilla, as in *Asperoris mnyama* (Nesbitt et al., 2013b).

In medial view, the posterior process of the maxilla is divided into two major sections, a robust, mediolaterally broad, tooth-bearing ventral portion that tapers posteroventrally, and a mediolaterally thin dorsal lamina that extends along the posterior two-thirds of the posterior process and forms the ventral margin of the antorbital fenestra. In dorsal view, a distinct groove separates the thin dorsal lamina from the tooth-bearing

ventral portion, as also occurs in most other archosaurs (e.g., *Xilousuchus sapingensis*, Wu, 1981; Nesbitt et al., 2011; *Postosuchus kirkpatricki*, Weinbaum, 2011). A distinct anteroposteriorly elongated articular surface for the palatine is present, and lies about halfway between the posterior extent of the posterior process and the posterior margin of the dorsal process.

The tooth-bearing ventral margin of the maxilla is not well preserved. However, it is clear that the interdental plates were well separated and closely associated with the ridge that divides the tooth-bearing margin from the rest of the medial surface. At least 12 rounded alveoli are preserved, and a maximum of 13 or 14 tooth positions would have been present in the complete bone. The first alveolus is the smallest, and the size of the alveoli increases from the first to the fourth alveoli. Alveolus size decreases posteriorly from the fourth alveolus. A single, partially erupted broken tooth is present in the fourth alveolus. The tooth is mediolaterally compressed, slightly posteriorly recurved, and serrated on at least the ~~anterior~~ mesial edge (Fig. 2D). Tooth implantation appears to be thecodont, but this condition can only be confirmed once a fully erupted tooth crown is found.

Frontal (Referred)—A right frontal (NMT RB496; Fig. 2) is referred to *Teleocrater rhadinus* based on the similarity of size of the surrounding material also referred to *T. rhadinus* ~~*Teleocrater rhadinus*~~ and character states consistent with an avemetatarsalian phylogenetic position (Nesbitt et al., 2017b). The frontal is nearly complete but missing the anterior portion that would have articulated with the nasal. The entire element is gently ~~bowed~~ arched~~s~~ dorsally at the orbital margin ~~where~~and the ventral surface is concave in lateral view. The dorsal surface is slightly concave

mediolaterally so that the midline and the orbital margin are raised slightly above the rest of the dorsal surface, as also occurs in some other archosauriforms (e.g., *Chanaresuchus bonapartei*, PULR 07; *Gracilisuchus stipanicicorum*, MCZ 4117). The frontal participates in the orbital margin. A lateral embayment anterior to the orbital margin represents the articular surface for the prefrontal. Posterior to the orbital margin a second lateral embayment represents the articular surface for either the postfrontal or postorbital. This more posterior articular surface is overhung by the frontal dorsally and the articulation takes the form of a deep ventral slot. The lateral surface of the orbital margin is slightly rugose, like that of ~~*Chanaresuchus*~~ *C. bonapartei* (PULR 07), *Silesaurus opolensis* (ZPAL Ab III/1223), and *Arizonasaurus babbitti* (Nesbitt, 2005a), and is not as dorsoventrally thin as that of *Asilisaurus kongwe* (NMT RB159). Posteriorly, the articulation with the parietal is located on the posteromedial edge of the frontal suggesting that a midline projection of the parietal intervened between the frontals, as in *Coelophysis bauri* (CM 31374). A similar condition also appears to be present in ~~*Asilisaurus*~~ *A. kongwe* (NMT RB159), but the anterior extent of the parietal is not as long as in the latter taxon. By contrast, an almost transversely straight frontoparietal suture is present in most other archosauriforms, including *Euparkeria capensis* (Ewer, 1965), ~~*Chanaresuchus*~~ *C. bonapartei* (PVL 4647), *Herrerasaurus ischigualastensis* (PVSJ 407), and ~~*Gracilisuchus*~~ *G. stipanicicorum* (MCZ 4117). In *T. rhadinus*~~*Teleocrater*~~, the dorsal surface of the posterior portion of the frontal bears a posteriorly opening depression with an anterior bounding ridge. A similar, but better-defined, depression is present in the same position in ~~*Asilisaurus*~~ *A. kongwe* (NMT RB159), and is also present in many early dinosaurs (Langer and Benton, 2006; Langer et al., 2010; Brusatte et al., 2010b). This

depression, referred to as the supratemporal fossa, has often been considered a synapomorphy of Dinosauria (Langer et al., 2010; Brusatte et al., 2010b), but is now synapomorphic for a more inclusive group of avemetatarsalians (Nesbitt et al., 2017b~~in review~~).

The medial margin, or midline, is slightly thickened relative to the rest of the element. In medial view, the midline suture possesses thin grooves and ridges that radiate from the center of the medial surface.

Ventrally, the entire length of the frontal possesses a laterally ~~laterally~~ bowed ridge (the crista cranii) that marks the medial edge of ~~medially defines~~ ~~the roof of~~ the orbital cavity roof. The orbital fossa likely continued onto the prefrontal and the postfrontal/postorbital, as also occurs in other archosauriforms. Medial to this ridge, a depression marks the anterior portion of the cerebrum (olfactory tract) and anteriorly, this depression expands laterally to form the dorsal and lateral extent of the impression of the primary olfactory bulb.

Quadrate (Referred)—The referred left quadrate (NMT RB493; Fig. 2) of *Teleocrater rhadinus* is nearly complete, missing only ~~some~~ part of the thin ~~edges~~margin of the pterygoid process. The quadrate referred to *T. rhadinus* was found closely assocated with the other remains of the taxon and ~~the~~its size is consistent with that of the other skull bones assigned to *T. rhadinus*. There are no clear character states that allow the quadrate to be assigned to ~~an early~~ A~~a~~vemetatarsalia~~n~~. The total height of the quadrate is 36 mm. ~~The~~ Its posterior edge ~~of the quadrate~~ is moderately arched posteriorly in lateral view. No crests are present on the posterior margin of the quadrate. In posterior view, the ventral portion of the quadrate expands medially and laterally and

Formatted: Font: (Default) Times New Roman, 12 pt

Formatted: Font: Italic

Formatted: Font: Italic

distally it terminates in two distinct and rounded condyles for articulation with the mandibular glenoid. The medial condyle extends further ventrally than the lateral condyle and a broad anteromedial groove separates the two, resembling the condition in *Chanaresuchus bonapartei* (PVL 4575) and *Lewisuchus admixtus* (CRILAR-Pv 552). By contrast, the two ventral quadrate condyles extend for an approximately equal distance in *Silesaurus opolensis* (ZPAL Ab III/361) and *Gracilisuchus stipanicicorum* (MCZ 4117). In ventral view, the two condyles are anteroposteriorly compressed, like those of *Asilisaurus* kongwe (NMT RB15), and are not as anteroposteriorly thickened as in *Silesaurus opolensis* (ZPAL Ab III/362/36). ~~Anteriorly~~In anterior view, a thin ridge separates the condylar articular surfaces from the rest of the quadrate body. Just dorsal to this ridge, a distinct crest rises from above the medial side of the lateral condyle and extends anteromedially to form part of the ventral border of the pterygoid process. A similar crest has been reported in pseudosuchians (e.g., *Arizonasaurus babbitti*, Nesbitt, 2005a; *Batrachotomus kupferzellensis*, Gower, 1999; crocodylomorphs, Walker, 1990; Iordansky, 1964) and is also present in some avemetatarsalians (e.g., *Allosaurus fragilis*, Madsen, 1976). A shallow fossa lies between the ventral termination of the crest and the anterodorsal rim of the condylar articular surfaces. Lateral to the lateral condyle, the ventral end of the quadrate bears an anteriorly directed flange, the lateral surface of which would have articulated with the quadratojugal, although there is no distinct articular surface preserved. The dorsal surface of this flange forms the ventral margin of a seemingly large foramen that would have been formed between the quadrate and the quadratojugal; this paraquadratice ~~quadratojugal~~ foramen is present in most Triassic archosauriforms (e.g., *Batrachotomus kupferzellensis*, Gower, 1999). A small fossa is

present posteromedial to the medial border of the paraquadratice ~~quadratojugal~~ foramen. The medial border of the ~~quadrate quadratojugal~~ is foramen transitions dorsally into the anterodorsal process of the quadrate, which likely articulated with the squamosal, as in other archosauriforms (e.g., ~~*Euparkeria*~~ *E. capensis*, SAM-PK-K5867; ~~*Batrachotomus*~~ *B. kupferzellensis*, Gower, 1999). The anterolateral process is triangular in posterolateral view, laterally convex, mediolaterally compressed, and has a slightly concave medial surface.

~~Anteromedially,~~ The head of the quadrate is continuous with the thin pterygoid process. The medial surface of the pterygoid process bears a fossa that is deepest posteriorly and is framed by two low ridges, one dorsally oriented and defining the medial edge of the quadrate and one defining the ventral border of the pterygoid process, as also occurs in other archosauriforms (e.g., ~~*Silesaurus*~~ *S. opolensis*, ZPAL Ab III/361).

~~Axial~~ Vertebral Column

Charig (1956) assigned 28 vertebrae (Figs. 3, 5, 8, 11; Table 1) to the holotype along with one fragmentary trunk rib (Fig. 12)~~. No sacral ribs or chevrons are preserved~~. A cervical rib was found with the holotype (Fig. 12), but Charig (1956) did not refer it to that specimen. By contrast, we consider the cervical rib to be part of the holotype (see below). None of the vertebrae were found in articulation, but Charig (1956) assigned positions to each of the vertebrae within the column on the basis of their overall morphology and relative size, and these positional identifications were written directly onto the specimens using a lettering scheme, presumably by AJC. These identifications should be viewed as provisional pending the discovery of articulated axial remains, but

are mostly followed herein. Charig (1956) assigned the correct relative order, but some of the vertebrae were assigned to the wrong regions (see below). Two of the vertebrae (labeled 'CeA–B') are clearly cervical vertebrae on the basis of their extreme elongation and parapophysis position (Fig. 3). Eleven vertebrae were identified as trunk vertebrae (labeled 'DA–K'), but we suggest that 'DA' and 'DB' belong to the cervical series rather than the trunk based on their lengths and the position of the parapophyses, and that 'DK' belongs to the anterior caudal series. Moreover, there are two distinct ~~morphs~~ morphologies of trunk vertebrae, which differ primarily in their elongation, suggesting that more than one part of the trunk column is represented and that vertebrae with morphologies transitional between them might have been lost taphonomically. The remaining 15 vertebrae (labeled 'CaA–O') are middle or distal caudal vertebrae~~s~~ and their relative sizes suggest they may form a continuous series, or one in which only small gaps are present. No sacral ~~or proximal caudal~~ vertebrae are present in the holotype, but the second sacral vertebra is represented in the referred material. All of the available vertebrae include centra that are effectively complete, though none possess a complete neural arch. Some of the vertebrae are represented solely by centra ('CeB', 'DA', 'DC', 'DF'). The neurocentral junctions are fused in all of the available vertebrae from the holotype and referred material.

Ten vertebrae preserved among the referred specimens are described, including an axis, two anterior cervical vertebrae~~s~~, two middle cervical vertebrae~~s~~, a posterior cervical vertebra, an anterior trunk vertebra ~~vertebra~~, two posterior trunk vertebrae, and a second primordial sacral vertebra. Other vertebrae were found at the same locality, but are duplicates of the specimens described. All of these vertebrae are very well preserved and

the cervical vertebrae are mostly complete. The trunk vertebrae lack their neural spines and ~~the those~~that of the sacrum~~al~~ lacks the distal half of the neural spine. The sacral vertebra is fused to its ribs.

Cervical Vertebrae (Holotype)—Charig (1956) regarded 'CeA' (Fig. 3) as an anterior cervical vertebra and 'CeB' (Fig. 3) as a more posterior cervical vertebra on the basis of their relative sizes and on the greater elongation of ~~'CeA' relative to 'CeB'~~the former. We agree with these identifications based on comparisons to both the referred specimens and *Yarasuchus deccanensis*, and specifically identify 'CeB' as from the middle cervical region. 'CeA' consists of a centrum, which is anteriorly complete, and a partial neural arch, lacking the tips of the prezygapophyses, the tips of the diapophyses, part of the neural spine apex, and the left postzygapophysis; 'CeB' consists of the complete centrum and the base of the neural arch, with the ventral portions of the vertebral laminae.

Although incomplete, the centrum of 'CeA' is exceptionally elongate, with a minimum length/posterior height ratio of approximately 3.6. This extreme elongation led Charig (1956) to question whether this vertebra was referable to the holotype individual, but based on its general morphology and the size of its articular surfaces he maintained this assignment. We confirm this assignment based on similarity to the referred material (see below). *Yarasuchus deccanensis* also possesses elongated anterior cervical vertebrae, but the minimum length/posterior height ratio is approximately 2.6 (ISI R334/9), and thus proportionally shorter than in *Teleocrater rhadinus*. In lateral view, the centrum is strongly curved along its length, with the posterior articular surface offset ventrally so that the dorsal margin of the posterior articular surface lies in a similar plane to the

ventral margin of the anterior articular surface, as also occurs in most other Permo-Triassic archosauromorphs (Ezcurra, 2016). The ventral margin of the centrum is strongly concave in lateral view, reflecting ~~this~~ the ventral offset of the posterior end. Centrum elongation and the presence of a ventrally offset posterior centrum articular surface ~~alsoboth~~ co-occur in dinosauriforms (e.g., *Marasuchus lilloensis*, Sereno and Arcucci, 1994a; *Eoraptor lunensis*, Sereno et al., 2013) among avemetatarsalians, in some pseudosuchians (e.g., *Qianosuchus mixtus*, Li et al., 2006), and in allokotosaurians (Nesbitt et al., 2015) and tanystropheids (Wild, 1973) among non-archosauriform archosauromorphs. The lateral surfaces of the centrum are weakly concave anteroposteriorly, almost flat dorsoventrally, and exhibit no pneumatic features. They are separated from the ventral surface by sharp breaks in slope that form distinct ridges along the anterior and middle part of the centrum, resembling the condition in ~~*Yarasuchus*~~ *Y. deccanensis* (ISI R334). In ventral view, the centrum is constricted to produce a thin, elongate, and spool-shaped outline. A deep concavity, defined by the anterolateral ridges, occupies the anterior half of the ventral surface, whereas the posterior half of the ventral surface is mediolaterally convex and bears a short, low midline keel that terminates prior to the posterior end of the centrum. The postaxial cervical vertebrae of proterochampsids (e.g., *Chanaresuchus bonapartei*, MCZ 4037), *Euparkeria capensis* (SAM-PK-K5867), *Gracilisuchus stipanicicorum* (PULR 08), ~~*Yarasuchus*~~ *Y. deccanensis* (ISI R334), and *Silesaurus opolensis* (ZPAL Ab III/411-7) also have a median longitudinal keel, but it extends further anteriorly than in *T. rhadinus*~~*Teleocrater gracilis*~~. Although broken, there is evidence for a prominent parapophysis on the left anteroventrolateral edge of the centrum. The posterior articular surface has a sub-circular outline and is deeply concave.

In anterior view, the neural canal of 'CeA' (Fig. 3) has a sub-rectangular outline that is wider than tall, but in posterior view this opening is circular, being narrower in diameter than the anterior opening. The prezygapophyses diverge laterally at an angle of approximately 30 degrees in dorsal view and are connected medially by a continuous horizontal platform (interprezygapophyseal lamina; sensu Wilson, 1999) that forms the floor of a deep fossa. This fossa is continuous with a small prespinal fossa that excavates the anterior base of the neural spine. Both of these fossae are delimited by prominent spinoprezygapophyseal laminae. The spinoprezygapophyseal lamina bifurcates posteriorly, with its dorsal branch merging with the neural spine and a ventral branch merging into the lateral margin of the neural arch, resembling the condition in the anterior postaxial cervical vertebrae of *Lewisuchus admixtus* (CRILAR-Pv 552). By contrast, this ventral branch is absent in the anterior postaxial cervical vertebrae~~s~~ of ~~*Yarasuchus*~~ *Y. deccanensis* (ISI R334/9), ~~*Silesaurus*~~ *S. opolensis* (ZPAL Ab III/1930), early pseudosuchians (e.g., ~~*Gracilisuchus*~~ *G. stipanicicorum*: PULR 08), and non-crown eucrocopodans (e.g., ~~*Chanaresuchus*~~ *C. bonapartei*, MCZ 4037; ~~*Euparkeria*~~ *E. capensis*: SAM-PK-K5867). The left diapophysis is broken, but shows that it was a flange-like structure, ~~that was~~ positioned on the anteroventrolateral edge of the neural arch, nearly touching the parapophysis, as occurs in the anterior postaxial cervical vertebrae~~s~~ of ~~*Yarasuchus*~~ *Y. deccanensis* (ISI R334), but ~~distinctly~~ contrasting with the well separated parapophysis and diapophysis of early archosauriforms (e.g., ~~*Chanaresuchus*~~ *C. bonapartei*, MCZ 4037), early pseudosuchians (e.g., ~~*Gracilisuchus*~~ *G. stipanicicorum*, PULR 08), and ~~*Silesaurus*~~ *S. opolensis* (ZPAL Ab III/1930). The posterior margin of the diapophysis is continuous with a prominent posterior centrodiapophyseal lamina, which

extends on-to the lateral surface of the centrum (the posterior portion of this lamina that extends onto the centrum is also visible in 'CeB'). The diapophysis and spinoprezygapophyseal laminae define a shallow, triangular depression on the lateral surface of the neural arch, in a position equivalent to the prezygapophyseal centrodiapophyseal fossa (sensu Wilson et al., 2011). A prominent postzygodiapophyseal lamina extends posterodorsally from the diapophysis, but is not connected with it. The postzygodiapophyseal lamina forms the dorsal border of a shallow, triangular postzygapophyseal centrodiapophyeal fossa, which is bounded ventrally by the posterior centrodiapophyseal lamina, as occurs in the anterior postaxial cervical vertebrae of *Silesaurus S. opolensis* (ZPAL Ab III/1930) and less conspicuously in *Yarasuchus Y. deccanensis* (ISI R334), but not in *Lewisuchus L. admixtus* (CRILAR-Pv 552). The postzygapophysis of 'CeA' extends slightly beyond the posterior margin of the centrum. A small, posteriorly directed base of an epipophysis is present on the dorsal surface of the articular facet of the postzygapophysis as also occurs in dinosauriforms and a variety of other archosauromorphs (Langer and Benton, 2006; Nesbitt, 2011; Ezcurra, 2016). The postzygapophysis has a sub-triangular cross-section and an elliptical articular surface that is oriented at approximately 45 degrees to the horizontal. In posterior view, the postzygapophyseal facets diverge from each other at an angle of approximately 100 degrees[e] and their dorsal margins form prominent spinopostzygapophyseal laminae. These laminae frame a deep postspinal fossa. The preserved part of the neural spine forms a laterally compressed sheet.

The centrum of 'CeB' is complete and differs from that of 'CeA' in numerous respects (Fig. 3). It is much less elongate, with a length/posterior height ratio of ~2.3 and

it also lacks the extreme curvature produced by the strong offset of the anterior and posterior articular surfaces, although the dorsal margin of the posterior surface of 'CeB' is slightly offset ventrally with respect to that ~~the dorsal margin~~ of the anterior surface, closely resembling the proportions and shape of the postaxial anterior cervical vertebrae~~s~~ of ~~*Yarasuchus*~~ *Y. deccanensis* (ISI R334). The centrum of 'CeB' has a spool-shaped morphology, but its lateral surfaces are more strongly concave anteroposteriorly than in 'CeA'; this may be the result of distortion during fossilization, as it is not present in any of the referred specimens or ~~*Yarasuchus*~~ *Y. deccanensis* (ISI R334). Large, oval parapophyses are positioned on the anteroventrolateral edges of the centrum and have gently concave articular facets. Distinct ridges separate the ventral and lateral centrum surfaces and a shallow concavity excavates the anterior half of the ventral surface, as in 'CeA'. The posterior part of the ventral surface is flat to slightly convex and lacks a midline keel, contrasting with the ~~presence of a keel in the~~keeled anterior–middle cervical vertebrae~~s~~ of proterochampsids (e.g., ~~*Chanaresuchus*~~ *C. bonapartei*, MCZ 4037), ~~*Euparkeria*~~ *E. capensis* (SAM-PK-K5867), ~~*Gracilisuchus*~~ *G. stipanicicorum* (PULR 08), ~~*Yarasuchus*~~ *Y. deccanensis* (ISI R334), and ~~*Lewisuchus*~~ *L. admixtus* (CRILAR-Pv 552). The anterior articular surface is sub-quadrate in outline and is flat to gently concave, whereas the posterior articular surface is sub-circular in outline and ~~is~~ concave. The ventral part of the paradiapophyseal lamina is preserved, and the area dorsal to this ridge is shallowly excavated to form part of the prezygapophyseal centrodiapophyseal fossa.

Vertebrae labeled 'DA' and 'DB' by Charig (1956) belong to the posterior portion of the cervical series rather than the anterior portion of the trunk series based on the

ventral location of their parapophyses (Fig. 8). The centra are shorter relative to the more anterior cervical vertebrae. In 'DA', the centrum has a minimum length/posterior height ratio of approximately 1.7, whereas ~~the centrum of 'DB' has a minimum length/posterior height~~that ratio is ~~of~~ approximately 1.6 in DB, closely resembling the ratios of the posterior cervical vertebrae of ~~*Yarasuchus*~~ *Y. deccanensis* (approximately 1.6, ISI R334) and *Spondylosoma absconditum* (GPIT 479/30/2). The anterior and posterior articular facets of the centra lie in nearly the same ~~anteroposterior~~ dorsoventral plane. Both vertebrae have a flat anterior articular surface and a shallowly concave posterior articular surface. The anterior and posterior articular surfaces of 'DA' and 'DB' are sub-circular in outline. Ventrally, both vertebrae have a poorly developed ridge on the midline, as occurs in the posterior cervical vertebrae~~s~~ of ~~*Yarasuchus*~~ *Y. deccanensis* (ISI R334) and several other archosauriforms (e.g., ~~*Gracilisuchus*~~ *G. stipanicicorum*, PULR 08). The ventral surface of the centrum smoothly transitions into a poorly defined lateral fossa that is overhung by the paradiapophyseal and posterior centrodiapophyseal laminae (in 'DB', but broken in 'DA'). A prominent concave parapophysis is present on the anteroventrolateral edge of the centrum in 'DA' and 'DB'. In both of these specimens, a smaller, circular, and convex additional articular surface is present just dorsal to the parapophysis. On the left sides of 'DA' and 'DB', the smaller articular surface is separated from the parapophysis by a narrow cleft whereas on the right side, the two articular surfaces are touching, but distinct. It is not clear if the parapophysis is divided or if the more dorsally positioned structure is novel. Poposauroids such as *Arizonasaurus babbitti* (Nesbitt, 2005a) and *Poposaurus gracilis* (Weinbaum and Hungerbühler, 2007; Nesbitt, 2011) have a similar structure, as does ~~*Yarasuchus*~~ *Y. deccanensis* (ISI R334).

The condition in ~~*Yarasuchus*~~ *Y. deccanensis* (ISI R334), where the two articular facets are nearly adjacent, is more similar to that of *T. rhadinus* ~~*Telecocrater*~~ than to that of poposauroids in which the two facets are well separated. Some of the taxa with these 'divided parapophyses' have associated ribs that are triple-headed (e.g., ~~*Yarasuchus*~~ *Y. deccanensis*, ISI R334) and we infer that *T. rhadinus* ~~*Telecocrater*~~ also had triple-headed ribs.

Vertebra 'DB' preserves most of the neural arch, but is missing much of the diapophyses and the neural spine. The diapophysis is located well dorsal to the centrum and near to the anteroposterior center of the neural arch. This structure is connected to the following: the parapophysis and additional articular surface via a thin paradiapophyseal lamina; posteroventrally to the centrum by a posterior centrodiapophyseal lamina; anteriorly to the prezygapophysis via a prezygodiapophyseal lamina; and posteriorly to the postzygapophysis by a postzygodiapophyseal lamina. These laminae frame exceptionally deep fossae. Dorsal to the diapophysis, there is a dorsally opening fossa at the base of the neural spine, as also occurs in several archosauromorphs (Ezcurra, 2016). In lateral view, the prezygapophyses of 'DB' project anterodorsally forming an angle of approximately 45 degrees with the horizontal, whereas in the following trunk vertebrae they project less strongly dorsally, forming a shallower angle of around 30 degrees° to the horizontal. Complete postzygapophyses are present only in DB: they are sub-triangular in cross-section, have steeply inclined articular facets that face lateroventrally, and have elongate, sub-elliptical articular surfaces. Stout spinopostzygapophyseal laminae form the lateral borders of a deep, oval postspinal fossa.

Cervical Vertebrae (Referred)—A nearly complete axis (NMT RB504; Fig. 4; Table 3) was recovered from locality Z183. The centrum is moderately elongated with a minimum length/posterior height ratio of approximately 2.7. The ~~axis~~ centrum is likely much shorter than that of the third cervical, given the general length of the other anterior cervical vertebrae (see below); however, no articulated cervical series is currently available. A shorter axis relative to the third cervical vertebra is also known in *Marasuchus lilloensis* (PVL 3870), *Asilisaurus kongwe* (Nesbitt et al., 2010), *Lewisuchus admixtus* (Romer, 1972; Bittencourt et al., 2014), *Silesaurus opolensis* (ZPAL Ab III/1930), and dinosaurs (Gauthier, 1986; Langer and Benton, 2006) and is in contrast to the condition in many pseudosuchians (e.g., *Batrachotomus kupferzellensis*; Gower and Schoch, 2009) and non-crown archosauriforms (e.g., *Chanaresuchus bonapartei*, MCZ 4037; *Euparkeria capensis*, SAM-PK-K5867) where the axis is approximately the same length as the other cervical vertebrae. Anteriorly, the articular surface for the atlas on the centrum is nearly flat, whereas the more ventral articulation with the axis intercentrum is deflected anteroventrally and is slightly convex. The posterior articular surface of the centrum is circular and distinctly concave. A midline ridge is present that extends ventral to the anterior and posterior articular facets of the centrum, as in some dinosauriforms (e.g., ~~*Asilisaurus*~~ *As. kongwe*, NMT RB147) and pseudosuchians (e.g., *Riojasuchus tenuisceps*, PVL 3827). In lateral view, the lateral surface of the centrum bears two parallel ridges with a shallow fossa between them. A short, anteroventrally to posterodorsally trending ridge is present just dorsal to the more dorsal ridge on both sides of the axis. The facet for articulation with the atlantal neural arch is well defined with an overhanging rim, extends slightly anterior to~~of~~ the anterolateral margin of the neural

canal, and is convex. A well-defined ridge extends between the atlantal neural arch articulation facet and the lateral edge of the postzygapophysis. The postzygapophyses diverge at an angle of approximately 45 degrees from the midline in dorsal view as in the other anterior cervical vertebrae and a thin interpostzygapophyseal lamina connects the two structures (Fig. 4). The postzygapophyseal facets are flat, ovoid, and extend just posterior to the posterior articular surface of the centrum, as also occurs in ~~*Euparkeria* *E.*~~ *capensis* (SAM-PK-K5867), ~~*Marasuchus* *M.*~~ *lilloensis* (PVL 3870), ~~*Silesaurus* *Si.*~~ *opolensis* (ZPAL Ab III/1930), early dinosaurs (e.g., ~~*Herrerasaurus* *H.*~~ *ischigualastensis*, PVSJ 407), and early pseudosuchians (e.g., ~~*Gracilisuchus* *G.*~~ *stipanicicorum*, PULR 08; ~~*Turfanosuchus* *Tu.*~~ *dabanensis*: IVPP V3237). Epipophyses lie on the dorsal surfaces of the postzygapophyses, as in most dinosauriforms and some pseudosuchians (Langer and Benton, 2006; Nesbitt, 2011). The epipophyses taper posteriorly and extend slightly posterior to the posterior extent of the postzygapophyses. The neural spine is anteriorly rounded in lateral view and rises posterodorsally to an apex that lies dorsal to the postzygapophyses. This posterodorsally extended neural spine is also present in proterochampsids (e.g., ~~*Chanaresuchus* *C.*~~ *bonapartei*: MCZ 4037), most pseudosuchians (e.g., ~~*Arizonasaurus* *Ar.*~~ *babbitti*: Nesbitt, 2005a), and some dinosauriforms (e.g., ~~*Silesaurus* *Si.*~~ *opolensis*, Piechowski and Dzik, 2010; ~~*Herrerasaurus* *H.*~~ *ischigualastensis*: Sereno and Novas, 1994; *Allosaurus* ~~*Al.*~~ *fragilis*, Madsen, 1976), whereas some non-archosaurian archosauriforms (e.g., ~~*Euparkeria* *E.*~~ *capensis*, SAM-PK-K5867) and some dinosauriforms (e.g., ~~*Lewisuchus* *L.*~~ *admixtus*, Bittencourt et al., 2014) possess a dorsally arching neural spine where the anterior and posterior terminations are sub-equal in height. In *Te. rhadinus*~~*Teleocrater*~~, the posterodorsal ~~extent~~

edge of the neural arch is mediolaterally thick and overhangs a deep postspinal fossa that is framed by the neural spine and the postzygapophyses, as is common in the axes of other archosauromorphs.

Two anterior cervical vertebrae (NMT RB505; NMT RB506; Fig. 5; Table 3) are referred to *T. rhadinus* ~~*Teleocrater*~~ and their morphology closely matches that of the holotype vertebra 'CeA'. As in 'CeA', the two referred specimens have exceptionally elongate centra with minimum length/posterior height ratio of approximately 3.2 (NMT RB505) and 3.0 (NMT RB506). Both have a posterior articular surface that is positioned ventral to the anterior articular surface. ~~Centrum elongation and the presence of a ventrally offset posterior centrum articular surface also occur in dinosauriforms (e.g., *Marasuchus lilloensis*, Sereno and Arcucci, 1994a; *Eoraptor lunensis*, Sereno et al., 2013) among avemetatarsalians, in some pseudosuchians (e.g., *Qianosuchus mixtus*, Li et al., 2006), and in allokotosaurians (Nesbitt et al., 2015) and tanystropheids (Wild, 1973) among non-archosauriform archosauromorphs.~~ The ventral surface of the centrum has two pairs of low ridges paralleling the long axis, with a weakly developed ridge on the midline and paramedian ridges at the lateral sides of the ventral surface, as with the anterior cervical vertebra of the holotype ('CeA'). The parapophysis sits on the anteroventral edge of the centrum and has a slightly concave articular surface. A deep fossa lies between the parapophyses on the ventral surface. The diapophysis and parapophysis touch anteriorly and a deep cleft separates ~~the their articular faces posteriorly~~them, as in 'CeA'. A weakly developed posterior centrodiapophyseal lamina extends posteriorly from the oval diapophysis; this lamina terminates well anterior of the posterior articular surface of the centrum. The posterior centrodiapophyseal laminae in

both NMT RB505 and NMT RB506 are not as laterally ~~extensive~~ expanded as in 'CeA' and the development of the laminae differs on the left and right sides of NMT RB505. Ventral to the posterior centrodiapophyseal lamina, there is a laterally opening fossa that is bound ventrally by another low ridge, resembling the condition of an anterior postaxial cervical of ~~*Silesaurus*~~ *Si. opolensis* (ZPAL Ab III/411/7). The anterior articular face of the centrum is concave, but not as deeply concave as the posterior articular face.

Anteriorly, the neural canal aperature is oval in outline with the long axis oriented mediolaterally, and is larger than the ~~neural canal in~~ posterior ~~view~~ aperature (Fig. 5). The prezygapophyses extend well anterior of the centrum, are angled at 45 degrees to the horizontal in anterior view, and, in dorsal view, diverge anterolaterally at ~30 degrees from the midline. A thin interprezygapophyseal lamina connects the prezygapophyses and a deep prespinal fossa excavates the base of the neural spine.

At the posterior end of the lateral surface, in lateral view, a weakly developed postzygodiapophyseal lamina and the posterior portion of the posterior centrodiapophyseal lamina frame a shallow, triangular postzygapophyseal centrodiapophyeal fossa as in other non-theropod archosaurs (Langer and Benton, 2006). A shallow fossa is present dorsal to the anterior part of the postzygodiapophyseal lamina at the base of the neural spine, resembling the condition in several other Permo-Triassic archosauromorphs (Ezcurra, 2016). The postzygodiapophyseal lamina is gently rounded where it meets the lateral surface of the postzygapophysis. Just dorsal to this ridge, the bone surface is rugose and extends posteriorly to form a posteriorly directed epipophysis, as occurs in dinosauriforms and a variety of other archosauromorphs (Langer and Benton, 2006; Nesbitt, 2011; Ezcurra, 2016). The articular facets of the postzygapophyses are

angled at 45 degrees to the horizontal in posterior view. A deep postspinal fossa is present between the postzygapophyses and excavates the posterior base of the neural spine.

In both of the referred anterior cervical vertebrae (NMT RB505; NMT RB506; Fig. 5), the neural spine is completely preserved. The blade-like anterior edge slopes anterodorsally and the posterior edge slopes posterodorsally. This results in a greatly expanded distal end of the neural spine in lateral view, similar to the condition in the anterior post-axial cervical vertebrae of several early non-archosauriform archosauromorphs (e.g., *Macrocnemus bassanii*, PIMUZ T4822; *Prolacerta broomi*, BP/1/2675) and *Yarasuchus Y. deccanensis* (Sen, 2005). The neural spine is similar in mediolateral thickness throughout its height, except for near its apex where it expands laterally to form a rounded, rugose surface. This rugose surface expands anteriorly and posteriorly to form small apices that overhang the neural spine, and this feature is also present in *Yarasuchus Y. deccanensis* (Sen, 2005) and the erythrosuchid *Guchengosuchus shiguaiensis* (IVPP V8808-10). The lateromedial expansion of the The most apical-most part of the neural spine, however, does is thin and is not expanded into form the flat, concave, or gently convex surfaces seen in some archosauriforms (e.g., *Sarmatosuchus otschevi*, PIN 2865/68-20; *Euparkeria E. capensis*, SAM-PK-K5867) and pseudosuchians (e.g., *Batrachotomus B. kupferzellensis*, Gower and Schoch, 2009).

The referred material includes two middle cervical vertebrae (NMT RB511; NMT RB512: Fig. 6; Table 3), representing a portion of the presacral series that is not present in the holotype. We interpret these vertebrae as middle cervical vertebrae, as they have intermediate morphologies between the anterior and posterior cervical

Formatted: Font: (Default) Times New Roman, 12 pt

Formatted: Font: (Default) Times New Roman, 12 pt

vertebrae, but their exact positions within the series are not known. NMT RB511 is similar in size to the holotype whereas NMT RB512 is significantly larger than the holotype. The centra have offset articular surfaces and are elongate, with a minimum length/posterior height ratio of approximately of 2.5 (NMT RB512) and 2.4 (NMT RB511), closely resembling the proportions of the middle cervical centra in ~~*Spondylosoma* *Sp.*~~ *absconditum* (ratio approximately 2.3, GPIT 479/30/1) and ~~*Yarasuchus* *Y.*~~ *deccanensis* (ratio approximately 2.5−2.6, ISI R334). The ventral surfaces of both middle cervical vertebrae ~~s~~ bear ~~ridges on the~~a midline ridge~~:~~ that ~~in NMT RB512~~ is much more pronounced ~~than of NMT RB511~~in NMT RB512. ~~These~~ Midline ridges are also present on the middle cervical vertebrae ~~s~~ of ~~*Yarasuchus* *Y.*~~ *deccanensis* (ISI R334) and several other archosauriforms (e.g., ~~*Euparkeria* *E.*~~ *capensis*, SAM-PK-5867; ~~*Chanaresuchus* *C.*~~ *bonapartei*, MCZ 4037; ~~*Gracilisuchus* *G.*~~ *stipanicicorum*, PULR 08). The ~~lateral~~ sides of the centra immediately dorsal to the ventral surface are rounded and grade dorsally into a deep fossa roofed by the ventrolaterally ~~arching~~ expanding posterior centrodiapophyseal lamina, which arches dorsally in lateral view. As in the anterior postaxial cervical vertebrae ~~s~~, this lateral fossa extends anteriorly to divide the diapophysis from the parapophysis. The posterior portion of the centrum expands laterally and is distinctly convex around the rim. The posterior articular surface of the centrum is deeply concave, whereas the anterior ~~articular surface~~ is concave but much shallower. The oval parapophysis sits on the ~~anterolateral~~ ventrolateral edge of the anterior portion of the centrum, but the deep ventral fossa that is present between the parapophyses ~~on the ventral surface~~ in the anterior cervical vertebrae is absent. In both of the middle cervical vertebrae~~s~~, the oval diapophysis is posteriorly separated from the

parapophysis in lateral view, rather than being in partial contact with it as in the anterior cervical vertebrae ~~s~~.

The neural arches of the middle cervical vertebrae ~~s~~ bear more pronounced laminae than the anterior cervical vertebrae~~s~~. In lateral view, a rounded, but distinct, postzygodiapophyseal lamina and the posterior portion of the posterior centrodiapophyseal lamina form a distinct, triangular postzygapophyseal centrodiapophyeal fossa that is deeper anteriorly than posteriorly. This deep fossa also occurs in ~~*Spondylosoma*~~ *Sp.* *absconditum* (GPIT 479/30/1), ~~*Silesaurus*~~ *Si.* *opolensis* (Piechowski and Dzik, 2010), and dinosaurs (Langer and Benton, 2006), whereas the feature is rare outside Avemetatarsalia. A weakly developed lamina extends from the dorsal portion of the prezygapophyses and terminates in the anteroposterior middle of the neural arch, just ventral to a fossa at the base of the neural spine, resembling the condition in some early archosauriforms (e.g., *Chasmatosuchus rossicus*; Ezcurra, 2016). In NMT RB511, a prezygodiapophyseal lamina connects the lateral side of the prezygapophysis with the diapophysis and this lamina creates a deep anteriorly opening prezygapophyseal centrodiapophyseal fossa (sensu Wilson et al., 2011). As in the anterior cervical vertebrae, the articular surfaces of the prezygapophyses are angled at 45 degrees to the horizontal in anterior view and they extend anterior to the centrum. The prezygapophyses are connected medially by a thin interprezygapophyseal lamina. A prespinal fossa is located at the base of the neural spine. The postzygapophyses taper posterolaterally and their articular surfaces are shifted slightly dorsally from the ~~do not include the~~ interpostzygapophyseal lamina. ~~; this lamina is shifted slightly ventrally from the articulation surface.~~ Dorsal to the postzygapophyses, posteriorly projecting

Formatted: Font: (Default) Times New Roman, 12 pt

epipophyses are present and the apices of these small processes continue anterodorsally along the spinopostzygapophyseal laminae, as also occurs in the middle cervical vertebraes of ~~*Yarasuchus*~~ *Y. deccanensis* (ISI R334). The presence of epipophyses in the middle cervical vertebrae s ~~of~~ ~~*Spondylosoma*~~ *Sp. absconditum* is equivocal because ~~these~~ some specimens have been lost since the original description by Huene (1942). Galton (2000) reported the absence of these structures, but Langer (2004) considered them as present. The postspinal fossae are exceptionally deep in the middle cervical vertebraes. ~~The~~ The anterior neural canal opening ~~neural canal~~ is oval with a mediolateral long axis ~~anteriorly~~, whereas the posterior opening~~posteriorly the neural canal~~ is nearly square.

The neural spine of NMT RB512 (Fig. 6) is like that of the anterior cervical vertebrae in that the spine expands more strongly anterodorsally than posterodorsally in lateral view. The anterior margin of NMT RB511 is slanted anterodorsally, but is more vertical than that of NMT RB512 and the anterior cervical vertebrae, and closely resembles the condition in the middle cervical vertebrae ~~s~~ of ~~*Spondylosoma*~~ *Sp. absconditum* (Huene, 1942:pl. 30) and ~~*Yarasuchus*~~ *Y. deccanensis* (ISI R334). The apices of the neural spines are blade-like and their lateral portions expand like those of the anterior cervical vertebrae (see above) and those present in ~~*Yarasuchus*~~ *Y. deccanensis* (ISI R 334; Sen, 2005). The lateral rugosities are much less pronounced and the dorsal margin is anteroposteriorly more convex in NMT RB511 than in NMT RB512.

A very well -preserved posterior cervical vertebra (NMT RB514; Fig. 7; Table 3) is referred to *T. rhadinus* ~~*Teleocrater*~~ and closely matches the morphology of vertebra 'DB' in the holotype. The parapophysis is connected with an accessory rib articular surface as evidenced by a change of slope on the left side of the centrum, supporting the

Formatted: Font: (Default) Times New Roman, 12 pt

Formatted: Font: (Default) Times New Roman, 12 pt

inference of three-headed ribs in the posterior cervical region. All of the laminae and associated deep fossae present in vertebra 'DB' are complete on at least one side of NMT RB514. The diapophysis extends from the centrum laterally with a small posterior component and has a rounded articular surface. The prezygapophyses and postzygapophyses are connected to their antimeres at the midline by thin interprezygapophyseal and interpostzygapophyseal laminae and deep prespinal and postspinal fossae excavate the neural spine. The neural spine is complete and extends dorsally from the neural arch, being proportionally taller than in more anterior vertebrae. The neural spine is approximately twice the height of the centrum, resembling the condition present in the anterior ~~dorsals~~ trunk vertebrae of ~~*Yarasuchus*~~ *Y. deccanensis* (ISI R334). By contrast, the posterior cervical vertebrae possess proportionally shorter neural spines in most non-archosaur eucrocopodans (e.g., ~~*Euparkeria*~~ *E. capensis*, SAM-PK-K5867; ~~*Chanaresuchus*~~ *C. bonapartei*, MCZ 4037), early pseudosuchians (e.g., ~~*Gracilisuchus*~~ *G. stipanicicorum*, PULR 08), and early dinosauriforms (e.g., ~~*Silesaurus*~~ *Si. opolensis*, Piechowski and Dzik, 2010; ~~*Lewisuchus*~~ *L. admixtus*, ~~:~~ Bittencourt et al., 2014; ~~*Herrerasaurus*~~ *H. ischigualastensis*~~:~~, Sereno and Novas, 1994). The thin anterior edge of the neural spine in *T. rhadinus* ~~*Teleocrater*~~ is angled slightly anterodorsally in lateral view whereas the thicker posterior edge is angled slightly posterodorsally: as a result, the neural spine increases in anteroposterior width towards its ~~distal~~ apex in lateral view. In lateral view the distal surface is convex anteroposteriorly and the ~~lateral~~ sides of the ~~spine~~ apex are slightly rugose as in the more anterior vertebrae.

Trunk Vertebrae (Holotype)—All of the trunk centra are longer than they are tall. In 'DC–DG' (Figs. 3, 8; Table 1), the centrum is conspicuously elongate with

length/posterior height ratios ranging from 1.70–2.23. By contrast, the centra of 'DH–DI' (Fig. 8) are less elongate with length/posterior height ratios of 1.28–1.57. As a result, the range of ratios observed in the trunk vertebrae of *Teleocrater rhadinus* overlaps that of *Yarasuchus deccanensis* (ISI R334) and *Spondylosoma absconditum* (GPIT 479/30). In most other respects, the trunk centra are similar, however, with lateral surfaces that are longitudinally concave and dorsoventrally convex, with a concave ventral margin in lateral view. None of the centra exhibit any pneumatic openings or nutrient foramina. The lateral and ventral surfaces merge around a smooth continuous curve without any distinct break in slope. None of the trunk vertebrae possess ventral midline keels, grooves, or concavities, which are also absent from the middle and posterior trunk centra of ~~*Yarasuchus*~~ *Y. deccanensis*, but the anterior trunk vertebrae of the latter species possess a low median keel (ISI R334). All of the centra of *T. rhadinus* ~~*Teleocrater*~~ have a constricted, spool-shaped outline in ventral view. The anterior and posterior articular surfaces are more elliptical in outline in DC–DI (slightly wider than tall) than in the posterior cervical vertebrae~~s~~. A prominent parapophysis migrates dorsally through this series: it has an elliptical outline, with its long axis oriented dorsoventrally to slightly posterodorsally, and a shallowly concave articular surface. In DD–DI the parapophysis is situated on the neural arch (see below). Laterally prominent parapophyses are also present in ~~*Yarasuchus*~~ *Y. deccanensis* (ISI R334) and *Silesaurus opolensis* (Piechowski and Dzik, 2010).

None of the neural arches are complete, so most of the following description is based upon 'DD', which has the most complete arch, supplemented with details from other vertebrae where possible. The anterior neural canal openings are sub-elliptical in

outline with the long axes ~~of these ellipses~~ oriented mediolaterally. They are larger in diameter than the posterior neural canal openings, which have elliptical outlines whose long axis is dorsoventrally oriented. This difference in anterior/posterior neural canal shape is present in all trunk vertebrae with preserved neural arches ('DD', 'DE', 'DG', 'DH'), but contrasts with ~~*Yarasuchus*~~ *Y.* *deccanensis* (ISI R334), in which the openings of the neural canal are similar in shape and size anteriorly and posteriorly, with most of them being transversely broader than tall. All of the preserved prezygapophyses have sub-triangular transverse cross-sections and possess flat articular facets with oval outlines that face dorsomedially at an angle of approximately 45 degrees to the horizontal. In dorsal view, the prezygapophyses diverge at an angle of approximately 45 degrees. The bases of the prezygapophyses are connected by an intraprezygapophyseal lamina, which forms a short shelf anterior to the neural spine. This shelf is not as extensive as that seen in the cervical vertebrae and resembles the condition of the anterior trunk vertebrae of ~~*Yarasuchus*~~ *Y.* *deccanensis* (ISI R334) and ~~*Spondylosoma*~~ *Sp.* *absconditum* (GPIT 479/30/4). This shelf is absent in ~~*Silesaurus*~~ *Si.* *opolensis* (Piechowski and Dzik, 2010). Well-developed spinoprezygapophyseal laminae extend from the bases of the prezygapophyses to the anterior margin of the neural spine, forming the medial margins of a small, triangular prespinal fossa. In 'DD' and 'DE' a weak prezygoparapophyseal lamina is present, but its presence/absence is equivocal in the remaining trunk vertebrae. A prezygoparapophyseal lamina is absent in the preserved trunk vertebrae of ~~*Yarasuchus*~~ *Y.* *deccanensis* (ISI R334) and ~~*Spondylosoma*~~ *Sp.* *absconditum* (GPIT 479/30/3, 4). 'DD' and 'DE' possess distinct prezygodiapophyseal laminae (although it is reduced in length

and prominence in 'DE'), but it appears that this lamina is lost in 'DI', although poor preservation makes this difficult to confirm.

In 'DD' and 'DE', the parapophysis forms a stalk-like process at the anteroventral corner of the neural arch: in the remaining trunk vertebrae it migrates posteriorly and dorsally to a position adjacent to the diapophysis (in 'DG' and 'DH') and it probably merged with the diapophysis in some other trunk vertebrae ('DI'). Parapophyses forming stalk-like processes are also present in some of the anterior trunk vertebrae of ~~*Yarasuchus*~~ *Y. deccanensis* (ISI R334) and ~~*Silesaurus*~~ *Si. opolensis* (Piechowski and Dzik, 2010). A clear paradiapophyseal lamina is present in 'DC–DE', but is obliterated by the ~~fusion~~merging of the ~~two structures~~~~fusion with the diapophysis~~parapophysis with the diapophysis in the other trunk vertebrae. The paradiapophyseal and prezygodiapophyseal laminae frame a deep triangular and anteriorly opening prezygapophyseal paradiapophyseal fossa in 'DC–DE'. A very short centroparapophyseal lamina arises from the ventral margin of the parapophysis in 'DD' and 'DE'. Almost all of the diapophyses are missing and those that are present are incomplete. Where present they are laterally projecting, anteroposteriorly narrow flanges with flattened sub-elliptical cross-sections (e.g., 'DD', 'DE'). In all trunk vertebrae, the posteroventral margin of the diapophysis supports a prominent posterior centrodiapophyseal lamina that extends posteroventrally to merge with the posterodorsal margin of the centrum. The paradiapophyseal and posterior centrodiapophyseal laminae frame a deep, triangular, and ventrally opening centrodiapophyseal fossa in all of the trunk vertebrae preserving this region, with the exception of 'DK', which lacks this feature and bears only a shallow depression in this region. 'DD' and 'DE' possess well-developed postzygodiapophyseal

Formatted: Font: (Default) Times New Roman, 12 pt

Formatted: Font: (Default) Times New Roman, 12 pt

laminae, which form the dorsal borders of large posteriorly opening postzygapophyseal centrodiapophyseal fossae, but both the lamina and fossa appear to be lost in 'DG', 'DH', and other posterior vertebrae.

In vertebra 'DD' a very short accessory lamina branches ventrally from the postzygodiapophyseal lamina, at a point approximately halfway along its length, and extends posteroventrally to merge with the posterior margin of the neural arch, subdividing the postzygapophyseal centrodiapophyseal fossa into dorsal and ventral portions. However, this lamina cannot be seen in any of the other trunk vertebrae because this area is damaged in all other examples. This accessory lamina is also present in ~~*Spondylosoma*~~ *Sp. absconditum* (GPIT 479/30/3), ~~*Silesaurus*~~ *Si. opolensis* (Piechowski and Dzik, 2010), and some early saurischian dinosaurs (e.g., *Guaibasaurus candelariensis*, MCN-PV 2355). Nevertheless, the accessory lamina is vertical or slightly anteroventrally oriented in *Silesaurus* and dinosaurs. The presence or absence of this lamina cannot be determined confidently in ~~*Yarasuchus*~~ *Y. deccanensis* because the area is not well preserved in the available trunk vertebrae. Anteriorly, in vertebra 'DD' there is a large gap between the prezygapophyses that is consistent with the morphology of the hypantrum in dinosaurs (e.g., theropods; Rauhut, 2003). Referred specimens confirm the presence of hyposphene-hypantrum articulations (see below), as in saurischian dinosaurs (Gauthier, 1986) and several other Triassic archosauriforms. None of the preserved neural spines are complete, but those portions that are preserved indicate that its base formed a mediolaterally-compressed sheet that extended for almost the full length of the neural arch.

Trunk Vertebrae (Referred)—Three trunk vertebrae can be referred to

Teleocrater rhadinus, an anterior trunk vertebra (NMT RB500) and two posterior trunk vertebrae (NMT RB516; NHMUK PV R6796; Fig. 9; Table 3). The anterior and posterior trunk vertebrae preserve nearly all of the features present in the trunk vertebrae of the holotype and do not need to be described in detail here. However, NMT RB500 and NMT RB516 do have clear hyposphene-hypantrum accessory intervertebral articulations. Posteriorly, the hypantrum forms a rectangular structure that is more complicated than the simple, mediolaterally thin, and vertical lamina present on the midline in *Spondylosoma absconditum* (GPIT 479/30/3), some dinosauriforms (e.g., *Silesaurus opolensis*, Piechowski and Dzik, 2010; *Guaibasaurus candelariensis,* Langer et al., 2011), and pseudosuchians (e.g., *Batrachotomus kupferzellensis*, SMNS 80305; *Aetobarbakinoides brasiliensis*, Desojo et al., 2012). *Yarasuchus deccanensis* apparently lacks hyposphene-hypantrum articulations in its preserved trunk vertebrae (ISI R334), but this condition should be re-examined in the future if new, better preserved specimens are found. In NMT RB500 and NMT RB516, a deep anteroposteriorly-oriented groove lies at the medial surface of thosee articular facets ~~of the postzygapophysis~~. The groove continues anteriorly and marks the anterior-most extent of the articular surface of the postzygapophysis. In posterior view, the hyposphene is constricted dorsally and is slightly expanded laterally at its ventral margin. The ventral surface of the hyposphene is flat. In dorsal view, there is a clear gap between the prezygapophyses. The rounded medial edges of the prezygapophyses are straight in dorsal view for much of their length and then converge just posterior to the articular facets. The rounded medial edges fit into the grooves at the medial margins of the postzygapophyses and the hyposphene structure fits perfectly within the hypantrum.

Sacral Vertebra (Referred)—No sacral vertebrae are present in the holotype, but we refer a sacral vertebra (NMT RB519; Fig. 10; Table 3) to *Teleocrater rhadinus* based on its size, which is similar to that of other *T. rhadinus* ~~*Teleocrater*~~ material recovered from the same locality (Z183), and on its similarity to the sacral vertebrae of *Yarasuchus deccanensis*. We identify NMT RB519 as a second sacral vertebra based on its robust sacral rib, which extends from the anteroposterior middle of the centrum, and on its close similarity to the second sacral of *Asilisaurus kongwe* (NMT RB159) and the primordial second sacral vertebra of dinosaurs (e.g., *Saturnalia tupinquim*, MCP 3844-PV). NMT RB519 is nearly complete, missing only parts of the neural arch and its sacral rib. The centrum ~~has~~ is amphicoelous ~~articular facets~~ and the ventral surface lacks any groove or ridge; the ventral surface of the centrum is similarly smooth in ~~*Yarasuchus*~~ *Y. deccanensis* (ISI R334) and *Spondylosoma absconditum* (GPIT 479/30/7). Laterally, the sacral rib is completely co-ossified to the centrum, although a raised ridge marks the contact between ~~the sacral rib and the centrum~~these elements. The prezygapophyses are anteriorly short, angled at ~60 degrees to the horizontal in anterior view, and are well separated by a gap in dorsal view. A circular prespinal fossa is present at the anterior base of the neural spine. Just lateral to the prezygapophyses, a prezygodiapophyseal lamina extends from the prezygapophysis to the sacral rib, and a deep fossa is present anterior to this lamina, as is also the case in ~~*Yarasuchus*~~ *Y. deccanensis* (ISI R334). A shallow dorsolaterally open fossa is present between the prezygapophyses and postzygapophyses at the base of the neural spine. The small postzygapophyses are angled at ~60 degrees to the horizontal, complementing the orientation of the prezygapophyses. A dorsoventrally tall postspinal fossa separates the postzygapophyses in posterior view.

Formatted: Font: Italic

The sacral rib extends laterally from its junction with the centrum and neural arch. Laterally, the rib splits into two components, a smaller, dorsoventrally thinner process that extends posteriorly and more dorsally that the other portion, and a larger, more robust portion that extends anteroventrally (Fig. 10). The more posterior process occurs only within avemetatarsalians and is present in ~~*Yarasuchus*~~ *Y. deccanensis* (ISI R334), ~~*Spondylosoma*~~ *Sp. absconditum* (GPIT 479/30/7), ~~*Asilisaurus*~~ *As. kongwe* (NMT RB159), and in dinosaurs (e.g., *Saturnalia tupinquim*, MCP 3844-PV). The more robust anteroventral portion of the sacral rib is similar to that of ~~*Yarasuchus*~~ *Y. deccanensis* (ISI R334) and ~~*Asilisaurus*~~ *As. kongwe* (NMT RB159) in that ~~they both taper~~it tapers anteroventrally to a rounded termination with a distinct facet for articulation with the previous sacral rib, the articulation with the ilium is nearly vertical, and the posterior portion tapers posterodorsally. The sacral rib is restricted to this vertebra, contrasting with the condition in *Silesaurus opolensis* (ZPAL Ab III/362), in which the sacral ribs are shared between consecutive sacral vertebrae.

Caudal Vertebrae (Holotype)—With the exception of vertebra 'DK', we accept all of Charig's (1956) identifications of caudal vertebra position (Figs. 8, 11; Table 1). We identify vertebra 'DK' (Fig. 8L) as an anterior caudal vertebra rather than a posterior trunk vertebra. 'DK' possesses no centrodiapophyseal laminae, has a ~~unique~~ single ventral keel, and dorsoventrally compressed, anteroposteriorly elongated processes that we identify as caudal ribs, but it lacks chevron facets. These features place this vertebra close to the beginning of the caudal series. The anterior and posterior articular surfaces of the centrum are slightly ~~amphicoelous~~concave, like ~~the~~ in the other trunk and caudal vertebrae, and have sub-equal heights and lengths. The ventral centrum surface is

transversely concave as also occurs in *Yarasuchus deccanensis* (ISI R334). The vertebra has anteriorly short prezygapophyses and laminae that occur lateral to the prezygapophyses and likely continued onto the postzygapophyses. The base of the neural spine suggests that the structure was anteroposteriorly restricted, thus probably contrasting with the anteroposteriorly extensive neural spine bases deep bases of the neural spines of the anterior caudal vertebrae in ~~*Yarasuchus*~~ *Y. deccanensis* (ISI R334).

All of the middle to distal caudal centra are mildly amphicoelous and longer than they are tall, with length/posterior height ratios of 1.92–3.58, with this ratio increasing in the more distal caudals within the series (Figs. 8, 11). The range of this ratio partially overlaps with that of the middle to distal caudals of ~~*Yarasuchus*~~ *Y. deccanensis*, but the latter taxon possesses some caudal vertebrae that are proportionally shorter than those of *T. rhadinus* ~~*Teleocrater*~~ (ratio = 1.68, ISI R334/45). The lateral surfaces of all of the caudal vertebrae are gently concave longitudinally and lack pneumatic or nutrient foramina. In most cases the lateral and ventral surfaces merge smoothly into each other without distinct breaks in slope, producing a spool-like morphology with a convex ventral surface. However, in a small number of caudal vertebrae ('CaE', 'CaI–CaK'), the lateral and ventral surfaces are separated by a more angular break in slope, creating a more distinctive ventral surface that bears a shallow midline groove. Similar morphological variation is observed in the middle–distal caudal vertebrae~~s~~ of ~~*Yarasuchus*~~ *Y. deccanensis* (ISI R334) and *Silesaurus opolensis* (ZPAL Ab III/361/3, 362/8, 1975). Both the anterior and posterior articular surfaces of the centra are shield-shaped in outline with rounded ventral margins and slightly straighter lateral margins. Distinct anterior chevron facets are not present on any of the preserved caudal vertebrae, but small

posterior facets are visible in 'CaA–CaK' (but absent in 'CaL–CaO'). The posterior chevron facets in the larger vertebrae have a notched ventral margin and a 'W'-shaped outline, whereas in smaller vertebrae they become harder to distinguish from the rest of the posterior articular surface and have a crescentic outline.

The neural canal openings are elliptical in both anterior and posterior views, with the long axis of the ellipse directed mediolaterally. 'CaA–CaJ' lack complete prezygapophyses, but several of these vertebrae possess spinoprezygapophyseal laminae (e.g., 'CaC–CaD'), which were connected medially by a sheet-like interprezygapophyseal lamina. The prespinal fossa is absent in 'CaA–CaB' (the only vertebrae to preserve this region). In 'CaK–CaN', the prezygapophyses are short, stub-like processes that are oriented at around 15 degrees to the horizontal in lateral view and that do no project far beyond the ends of their respective centra, as also occurs in ~~*Yarasuchus*~~ *Y. deccanensis* (ISI R334). By contrast, the prezygapophyses of the distal caudal vertebrae of ~~*Silesaurus*~~ *Si. opolensis* (ZPAL Ab III/1975) and some early saurischians (e.g., *Herrerasaurus ischigualastensis*, Novas, 1994) overlap anteriorly at least one-third of the preceding vertebra. The prezygapophyses are conjoined medially for most of their length, except for their anterior tips, which are bluntly rounded. Spinoprezygapophyseal laminae are present in 'CaK–CaL', but are absent in the more distal caudal vertebrae~~s~~. None of the preserved caudal vertebrae possesses a prezygodiapophyseal lamina or any of its accompanying fossae.

None of the caudal ribs are preserved completely, but their broken bases indicate that they were thin, dorsoventrally compressed plates that extended laterally for approximately half of the length of the neural arch. Caudal ribs appear to have been

present on ‘CaA–CaK’, but lost from ‘CaL’ onwards. There is no indication of an anterior centrodiapophyseal lamina in any of the caudals, but ‘CaA–CaJ’ each possesses a short, weakly ~~-~~expressed posterior centrodiapophyseal lamina and, where the postzygapophyses are preserved, a weak postzygodiapophyseal lamina. Distinct neural arch fossae associated with these laminae are absent from all of the preserved caudal vertebrae. The postzygapophyses are reduced in size to small, rounded processes that are oriented at approximately 30 degrees to the horizontal in ‘CaB’ and around 15 degrees to the horizontal in ‘CaM–CaN’. They do not extend, or only slightly extend, beyond the posterior margin of the centrum in any of the caudal vertebrae in which they are preserved, contrasting with the more posteriorly projecting postzygapophyses of the middle–distal caudal vertebrae of ~~*Yarasuchus* *Y.*~~ *deccanensis* (ISI R334). The postzygapophyses have sub-elliptical cross-sections in ‘CaB’ and ‘CaK’, but merge into a single, midline compound process in ‘CaM–CaN’. ‘CaB’ lacks a postspinal fossa and spinopostzygapophyseal laminae are absent from all of the preserved vertebrae.

In ‘CaB’, the neural spine is as tall as the centrum, but in more posterior vertebrae it is reduced in height (e.g., ‘CaH’, ‘CaK’) and it is further reduced to a ridge in ‘CaM’ and lost in ‘CaN’–‘CaO’. Where preserved, it is a laterally compressed, anteroposteriorly narrow, and posterodorsally inclined sheet. The neural spines of the middle caudal vertebrae of ~~*Yarasuchus* *Y.*~~ *deccanensis* (ISI R334), and to a lesser degree ~~*Silesaurus* *S.*~~ *opolensis* (ZPAL Ab III/361/3, 1975), are distinctly taller than in ‘CaB’.

Cervical Rib (Holotype)—A partial cervical rib was found with the holotype (Fig. 12), but was excluded from it by Charig (1956). However, ~~the~~ its size and shape is consistent with ~~the size~~~~those~~the other cervical ribs in~~of~~ the holotype and we ~~consider~~

refer this element ~~as part of the holotypeit~~to this specimen. The cervical rib is missing the tip of the anterior process and most of the thin posterior process. The capitulum and tuberculum are nearly touching and separated by only a thin margin (though this area is partially obscured by matrix). The tuberculum (dorsal portion) has a larger articular surface area than the capitulum. The anterior process is elongated and slightly curved anterodorsally at its tip. Dorsally, this curvature results in a concave surface. The posterior process tapers and is highly compressed mediolaterally.

Trunk Rib (Holotype)—The proximal end of a single trunk rib is preserved (Fig. 12). The tuberculum forms an elongate process that extends dorsal to the capitulum and terminates in a sub-elliptical articular facet. It has an oval transverse cross-section and narrows mediolaterally as it merges with the capitulum and rib shaft ventrally. The articular surface for the capitulum is damaged and its outline cannot be determined. A prominent flange of bone arises from the proximal end of the shaft at the same level as the capitulum giving the rib a sub-triangular cross-section. Deep grooves separate this flange from both the capitulum and tuberculum.

Pectoral Girdle

Scapula (Holotype and Referred)—A partial right scapula (Fig. 13) missing the anterior margin and distal blade was assembled from pieces collected with the rest of the holotype, but for unknown reasons was separated from the rest of the holotype by Charig (1956). The size and preservation of the element suggests that it belongs to the holotype, and it possesses a distinct longitudinal ridge on the posterior edge of the blade that is shared only by avemetatarsalians (see below). As further support, a nearly complete,

slightly smaller, right scapula (NMT RB480; Fig. 13; Table 4) is assigned to *Teleocrater rhadinus* and both share identical morphology.

Proximally, the glenoid has a rounded rim and is directed more posteriorly than posterolaterally, as in *Spondylosoma absconditum* (GPIT 479/30/10), *Yarasuchus deccanensis* (ISI R334/49), and dinosauriforms (e.g., *Silesaurus opolensis*, Dzik, 2003; *Eoraptor lunensis*, Sereno et al., 2013). The preserved portion of the articular surface with the coracoid is triangular and tapers anteriorly. A weakly defined scar in the form of a shallow pit just distal to the lateral margin of the glenoid is interpreted to be the attachment site of the M. anconaeus scapularis lateralis externus, as in crocodylians (Brochu, 1992). By contrast, the inferred attachment of this muscle in several other early archosaurs, such as ~~*Yarasuchus*~~ *Y. deccanensis* (ISI R334/49), ~~*Silesaurus*~~ *Si. opolensis* (ZPAL Ab III/2534), and ~~*Turfanosuchus*~~ *T. dabanensis* (IVPP V3237), is developed as a low, prominent tuberosity (Nesbitt, 2011). ~~Anteriorly~~The anterior part of ~~,~~ the proximal margin that articulates with the coracoid is not complete in either specimen and is very thin (Fig. 13). The referred specimen (NMT RB480) preserves a weakly developed acromion that is laterally ~~distinct~~ raised from the rest of the surface of the proximal end, as in most archosaurs (Nesbitt, 2011) and in proterochampsids (e.g., *Chanaresuchus bonapartei*, PVL 4575; Ezcurra, 2016). A shallow fossa is present between the glenoid and the acromion. Compared to the distal end, the proximal end is more strongly expanded anteroposteriorly, as also occurs in ~~*Silesaurus*~~ *Si. opolensis* (ZPAL Ab III/1930).

A shallow proximodistally-oriented groove is present just distal to the glenoid on the posterior surface. At a distance of 30 mm distally (~from the posterior edge of the

glenoid; 47% the preserved length), a thin ridge that is 10 mm in proximodistal length demarcates the posterior edge of the blade. This ridge is present in ~~*Spondylosoma*~~ *Sp. absconditum* (GPIT 479/30/10), *Asilisaurus kongwe* (NMT RB159), ~~*Silesaurus*~~ *Si. opolensis* (ZPAL Ab III/2534), and *Lewisuchus admixtus* (PULR 01), but absent in dinosaurs. A finished edge on part of the anterior edge of the holotype scapula blade indicates that 1) the scapula is narrow throughout its midshaft (~1.5 cm width at its narrowest point) and 2) that the distal end of the scapula blade expands anteriorly and posteriorly. This is confirmed by the referred specimen (NMT RB480), in which the distal end of the blade is more strongly expanded anteriorly than posteriorly, resembling the condition in ~~*Silesaurus*~~ *Si. opolensis* (ZPAL Ab III/2534) and ~~*Lewisuchus*~~ *L. admixtus* (PULR 01). Distally, the anterior edge thickens mediolaterally and bears a ridge that parallels the anterior margin. The distal end is thicker posteriorly in distal view than it is anteriorly. The distal surface is rugose and nearly flat.

Coracoid (Holotype)—A possible left coracoid was preserved with the holotype (Fig. 13). The size corresponds well with that of the holotype scapula and the preservation is also similar. However, the articular surface with the scapula is slightly different from that expected for a typical coracoid; it is directed at an unusual angle and is either poorly preserved or over-prepared. The posterior orientation of the glenoid confirms that the glenoid formed by the scapula and coracoid was directed posteroventrally like that of *Yarasuchus deccanensis* (ISI R334/49) and dinosauriforms. There is a clear notch ventral to the posterior portion of the glenoid and the surface ventral to the notch is mediolaterally thick, but it is unclear if there was a tuber here as present in proterochampsids (Ezcurra, 2016) and nearly all archosaurs (Nesbitt, 2011). A

coracoid foramen appears to be present on the anterior margin of the preserved portion.

Forelimb

Humerus (Referred)—No humerus was found directly with the holotype, but the distal half of a left humerus (NHMUK PV R6796; Fig. 15) was found nearby (Charig, 1956) and two well-preserved left humeri (NMT RB476; NMT RB477; Fig. 14; Table 4) are also referred to the taxon. In general, the proximal and distal ends of the humerus are greatly expanded compared to the midshaft as in some non-archosaurian archosauriforms (e.g., *Erythrosuchus africanus*; Gower, 2003), *Yarasuchus deccanensis* (Sen, 2005), and sauropodomorph dinosaurs (Langer and Benton, 2006). The proximal half bears a robust and anterolaterally directed deltopectoral crest that is distally elongated. The anterolateral apex of the deltopectoral crest extends greater than 30% the length of the humerus in *Teleocrater rhadinus* (Table 4), as also occurs in ~~*Yarasuchus*~~ *Y. deccanensis* (Sen, 2005), dinosaurs (Langer and Benton, 2006), and probably *Nyasasaurus parringtoni* (Nesbitt et al., 2013a). The deltopectoral crest of *T. rhadinus* ~~*Teleocrater*~~ does not flare laterally and does not possess the small ventral notch seen in ~~*Nyasasaurus*~~ *N. parringtoni* (Nesbitt et al., 2013a). Connected with the rest of the proximal surface, the deltopectoral crest has a nearly straight anterolateral margin with a small concave surface between the proximal surface and the apex of the crest, as also occurs in ~~*Yarasuchus*~~ *Y. deccanensis* (ISI R334/53). A proximodistally-oriented faint ridge, the supinator ridge, is present on the posterolateral surface of the deltopectoral crest and extends distally to the midshaft, resembling the condition in other archosauriforms (e.g., *Aetosauroides scagliai*, PVL 2073).

The proximal surface has two proximally extended peaks, one proximal to the deltopectoral crest and one that represents the humeral head, which closely resembles the condition in ~~*Yarasuchus* *Y.* *deccanensis*~~ (ISI R334/53), but not that of other archosauriforms. The humeral head, like the rest of the proximal surface, is poorly ossified. In NMT RB476 and NMT RB477, a groove is present on the proximal surface lateral to the humeral head. The medial tuberosity is distally shifted from the humeral head, but is not separated from it, and this is similar to other early archosauriforms (e.g., *Euparkeria capensis*, SAM-PK-K5867; ~~*Yarasuchus* *Y.* *deccanensis*~~, ISI R334/53; *Silesaurus opolensis*, ZPAL Ab III/452; *Parasuchus hislopi*, ISI R42). The anteroventral surface of the proximal portion is broadly concave and the posterodorsal surface is broadly convex and bears two proximodistally-oriented fossae separated by a low convex surface.

This midshaft is sub-circular in cross-section and the long axis of the proximal surface is twisted at an angle of ~45 degrees to the long axis of the distal end, resembling the condition in ~~*Euparkeria* *Eu.* *capensis*~~ (SAM-PK-K5867) and some pseudosuchians (e.g., ~~*Parasuchus* *P.* *hislopi*~~, ISI R42; ~~*Aetosauroides* *A.* *scagliai*~~, PVL 2073). By contrast, the torsion between the proximal and distal ends is approximately 10 degrees in ~~*Yarasuchus* *Y.* *deccanensis*~~ (ISI R334/53), *Marasuchus lilloensis* (PVL 3871), ~~*Silesaurus* *Si.* *opolensis*~~ (ZPAL Ab III/452), and early dinosaurs (e.g., ~~*Herrerasaurus ischigualastensis*~~*Tawa hallae*, ~~PVSJ~~ GR ~~373~~242). The lateral and medial edges of the distal end gradually diverge to form a broadly triangular distal end in anterior view. Posterodorsally, a broadly concave surface divides the rounded epicondyles~~entepicondyle (medial) and ectepicondyle (lateral) of the distal end~~. Likewise, a concave surface

Formatted: Font: (Default) Times New Roman, 12 pt

(=radial fossa) separates the entepicondyle and ectepicondyle anteromedially. Across the three humeri, there is variation in the breadth and depth of this fossa. In the largest example, NMT RB476, the concave surface is broad and the shallowest of the three. The depth is greater in NMT RB477 and the fossa is deepest and most mediolaterally restricted in NHMUK PV R6796. The distal development of the entepicondylar and ectepicondylar sides also varies across the three specimens. In the smallest ~~of the three~~ (NMT RB477), the condyles are approximately equal in distal extent whereas in the ~~other~~ two larger specimens (NMT RB476 and NHMUK PV R6796), the entepicondyle is much more extended distally, as also occurs in the preserved humerus of ~~*Yarasuchus*~~ *Y. deccanensis* (ISI R334/53). The lateral side of the ectepicondyle ~~of the ectepicondylar side~~ has a clear supinator process, but this ~~process~~ is poorly developed and does not expand far laterally with respect to the rest of the ectepicondylar lateral surface. A groove lies adjacent and parallel to the supinator process. The presence of a supinator process and accompanying groove occurs in most archosauriforms (e.g., ~~*Erythrosuchus*~~ *Er. africanus*; Gower, 2003; *Batrachotomus kupferzellensis*, Gower and Schoch, 2009; ~~*Aetosauroides*~~ *A. scagliai*, PVL 2073; ~~*Yarasuchus*~~ *Y. deccanensis*, ISI R334/53) and in some dinosauriforms (e.g., *Asilisaurus kongwe*, NMT RB159), but is lost in ~~*Silesaurus*~~ *Si. opolensis* (ZPAL Ab III/452), *Lewisuchus admixtus* (CRILAR-Pv 552), and early dinosaurs (e.g., *Herrerasaurus ischigualastensis*; Sereno, 1994). The distal surface has a deep groove that parallels the surface's long axis.

Radius (Holotype)—A complete, but poorly preserved right radius (Fig. 16; Table 2) and the distal one-third of the left radius is present in the holotype (NHMUK PV R6795; Fig. 17). The proximal surface is concave in anterior view, resembling the

Formatted: Font: (Default) Times New Roman, 12 pt

condition in *Euparkeria capensis* (SAM-PK-K5867), and asymmetrical with the lateral margin ~~of the proximal end~~ extending further proximally than the medial ~~margin~~. A sharp intermuscular line is present on the anterior surface, beginning around 20 mm distal to the proximal surface (~22% the length of the element), but this fails to reach the midshaft. A second intermuscular line on the posterolateral surface originates just proximal to midshaft and extends to the distal margin. ~~In distal view,~~ T~~t~~he distal surface is concave with a circular outline.

Ulna (Holotype and Referred)—A complete, well-preserved right ulna is present in the holotype (NHMUK PV R6795; Fig. 16; Table 2), but it is heavily fractured throughout its length. Two other well-preserved left ulnae (NMT RB486; NMT RB485) are referred to *Teleocrater rhadinus* and are identical to that of the holotype. The shaft of the ulna is rather robust compared to those of dinosauriforms (e.g., *Marasuchus lilloensis*, PVL 3871; *Silesaurus opolensis*, Dzik, 2003) and is nearly straight, closely resembling that of *Yarasuchus deccanensis* (ISI R334). The long axis of the proximal surface is mediolaterally oriented and is offset from the anteromedially oriented long axis of the distal surface by ~45 degrees, as also occurs in ~~*Yarasuchus*~~ *Y. deccanensis* (ISI R334) and several other early archosaurs (e.g., *Aetosauroides scagliai*, PVL 2073; ~~*Silesaurus*~~ *S. opolensis*, ZPAL Ab III/404/7). Proximally, an olecranon process is present but poorly expanded relative to the rest of the proximal surface, as also occurs in *Yarasuchus deccanensis* (ISI R 334) and a referred specimen of *Dongusuchus efremovi* (PIN 952/84-2; Niedźwiedzki et al., 2016). The proximal surface is concave, and poorly preserved in the holotype. Anterolaterally, the surface is bowed, and a short, poorly defined, and proximodistally oriented ridge is present that is homologous with the lateral (=radial)

tuber of other archosaurs. This weakly developed expansion is also present in ~~*Yarasuchus*~~ *Y. deccanensis* (ISI R334). A muscle scar is present anterolateral to the lateral tuber, forming a shallow depression that is also present in *Asilisaurus kongwe* (NMT RB159). A rugose surface on the anterolateral surface of the ulna of *T. rhadinus* ~~*Teleocrater*~~ is also present in ~~*Yarasuchus*~~ *Y. deccanensis* (ISI R334), ~~*Asilisaurus*~~ *A. kongwe* (NMT RB159), *Lewisuchus admixtus* (CRILAR-Pv 552), and the sauropodomorph *Saturnalia tupiniquim* (Langer et al., 2007a). The anterolateral portion of the proximal surface tapers in proximal view. Sharp ridges define the anterior and posterior edges of the shaft whereas the lateral and medial surfaces are gently rounded. The distal end is moderately expanded relative to the midshaft, as also occurs in several archosauriforms (e.g., *Euparkeria capensis*, SAM-PK-K5867; *Parasuchus hislopi*, ISI R42; ~~*Lewisuchus*~~ *L. admixtus*, CRILAR-Pv 552). A shallow fossa is present on the posteromedial surface of the distal end. The elliptical distal surface is concave, as in ~~*Yarasuchus*~~ *Y. deccanensis* (ISI R334) and ~~*Lewisuchus*~~ *L. admixtus* (CRILAR-Pv 552).

Metacarpal (Referred)—A single metacarpal (NMT RB484; Table 4) was recovered from locality Z183 (Fig. 18). The assignment of the metacarpal to *Teleocrater rhadinus* is tentative and cannot be confirmed ~~at this time~~ because no metacarpal is present in the holotype or in ~~*Yarasuchus*~~ *Y. deccanensis* for comparison. However, ~~the~~ its size ~~of the metacarpal~~ is consistent with ~~the size~~that of the other material referred to ~~*Teleocrater*~~ *T. rhadinus* from the same locality. We identify NMT RB484 as a right metacarpal II based on its similarity to that of *Azendohsaurus madagaskarensis* (Nesbitt et al., 2015), and the anterolateral cant of its proximal end. The metacarpal has a proximal portion that is expanded relative to the narrow midshaft. The convex proximal

surface is trapezoidal with an acute anterolateral corner and a long axis that is nearly anteroposteriorly oriented. The proximal portions lack distinct articular surfaces, in contrast to the deep facets present in some dinosaurs (e.g., *Herrerasaurus ischigualstensis*, Sereno, 1994; *Tawa hallae*, Nesbitt et al., 2009a) and in contrast to the clear facets present in ~~*Azendohsaurus*~~ *A. madagaskarensis* (Nesbitt et al., 2015). The posteromedial ~~portion~~ surface of the proximal portion is rugose and bears numerous proximodistally-oriented striations. The medial side of the proximal portion is nearly flat, and ~~this surface~~ likely represents the articular surface for metacarpal I. The distal end is asymmetrically expanded, being expanded more strongly laterally than medially ~~in anterior view~~. In distal view, the articular surface is rectangular with a mediolaterally-oriented long axis; the posterior side tapers both medially and laterally. The anterior surface bears a deep extensor pit, although this is not as deep as those of neotheropods (e.g., *Coelophysis bauri*, Colbert, 1989). Medially, the distal end is nearly flat whereas the lateral surface bears a deep ligament pit.

Pelvic Girdle

Ilium (Holotype and Referred)—The partial left ilium of the holotype (NHMUK PV R6795; Fig. 19) is largely complete but is missing the postacetabular process; a slightly larger, referred left ilium (NMT RB489; Fig. 19) consists mostly of the acetabular region but lacks the supra-acetabular crest and postacetabular process. Overall, the ilium has a deep acetabulum framed by a laterally (or ventrolaterally) directed supra-acetabular crest. The supra-acetabular crest is well defined and forms a thin ridge; small radiating ridges ornament its ventral surface. The supra-acetabular crest extends to the

contact with the pubis anteriorly and fades out dorsal to the posterior end of the ischial peduncle posteriorly. The pubic articular surface of the ilium is shorter than that for the ischium. Both the pubic and ischial peduncles meet in the anterior half of the acetabulum at an angle of nearly 90 degrees. A similar condition is present in dinosauriforms (e.g., *Asilisaurus kongwe*, NMT RB159) and poposauroids (e.g., *Arizonasaurus babbitti,* MSM 4590). A small notch at the ventral margin of the ischial ~~peduncle~~ articulation indicates that the acetabulum might be partially open (see below). A notch positioned halfway between the iliac articulation with the pubis and the posterior extent of the ischial peduncle is also present in *Yarasuchus deccanensis* (ISI R334/56), some dinosauriforms (e.g., ~~*Asilisaurus*~~ *As. kongwe*, NMT RB159; *Silesaurus opolensis*, ZPAL Ab III/404/1), and poposauroid pseudosuchians (e.g., ~~*Arizonasaurus*~~ *Ar. babbitti*, MSM P4590). By contrast, the articular margin of the ischial peduncle is straight in most archosauriforms, including the dinosauriform *Marasuchus lilloensis* (PVL 3871). The articular surface of the pubic peduncle is nearly flat whereas that of the ischial peduncle is slightly concave in the holotype. However, these surfaces are better preserved in NMT RB489 and in this specimen the contact surface with the pubis is rugose and slightly angled anterolaterally, whereas the rugose surface of the ischial peduncle is distinctly convex mediolaterally. An antitrochanter on the lateral surface of the ischial peduncle within the acetabulum is absent in both specimens, contrasting with ~~the~~ its presence ~~of this feature~~ in *Lagerpeton chanarensis* (PVL 4619) and some dinosaurs (e.g., *Herrerasaurus ischigualastensis*, MCZ 4381). Within the acetabulum of NMT RB489, a small ridge separates the fibrous surface texture on the anterior half of the acetabulum from the smoother bone texture

Formatted: Font: Italic

present on the posterior half of the ilium (Fig. 19). The holotype also appears to show this transition, but poor preparation within the acetabulum obscures these details.

The anterior (=preacetabular) process is separated from the rest of the ilium by a well-defined vertical ridge that originates from the dorsal surface of the supra-acetabular crest. The anterior-most portion of the anterior process arcs medially; this curvature results in a distinct pocket medial to the lateral surface of the anterior process and the well-defined vertical ridge. The vertical ridge is confluent with the anterior process, as in dinosauriforms (~~*Asilisaurus*~~ *As. kongwe* NMT RB159), and a similar vertical crest is also present in poposauroids (e.g., ctenosauriscids, Nesbitt, 2005a, b; Butler et al., 2011), *Batrachotomus kupferzellensis* (Gower and Schoch, 2009), and early crocodylomorphs (Nesbitt, 2011). The dorsal surface of the crest bears deep grooves and sharp ridges and these ridges continue onto the anterior process.

Much of the surface medial to the acetabulum is relatively smooth and featureless. Two distinct sacral rib scars are present, one anterior and medial to the level of the supra-acetabular crest and the other more posterior and medial to the ischial peduncle. The articular surface for the first sacral rib is rounded and a small piece of the dorsal portion of the scar appears to contact the medially curved anterior process as in some poposauroids (~~*Arizonasaurus*~~ *Ar. babbitti*, MSM P4590; Nesbitt, 2005a, 2007, 2011). The scar for the second sacral rib lies ventral to a well-defined medial ridge; the posterior portion of this scar is present on a thin flange at the posterior margin of the ischial peduncle.

Ischium (Referred)—A complete left ischium (NMT RB479; Fig. 20) is referred to *Teleocrater rhadinus* based on its similarity to that of *Yarasuchus deccanensis* and its

size, which is consistent with the other ~~*Teleocrater* *T. rhadinus*~~ material identified from the same bonebed. The ~~left~~ ischium exhibits a widened articular surface for the ilium and a long shaft that extends posteroventrally. ~~The~~ Its proximal portion ~~of the ischium~~ articulates with the ischial peduncle of the ilium anterodorsally and the pubis anteriorly and these articular surfaces are continuous, as in most archosauriforms (Nesbitt, 2011), including ~~*Yarasuchus* *Y. deccanensis*~~ (ISI R334), and in contrast to those of dinosauriforms (e.g., *Silesaurus opolensis*, Dzik, 2003; *Marasuchus lilloensis*, PVL 3870) in which the two surfaces are separated. The articular surfaces for the ischial peduncle of the ilium ~~ilium~~ and the posteroventral rim of the acetabular margin~~um~~ of the ilium are continuous and ~~they~~ do not form two distinct surfaces. The acetabular rim of the ischium is a simply, rounded ridge, contrasting with the raised lip that is present in dinosauromorphs with a pelvic antitrochanter (e.g., *Lagerpeton chanarensis*, PVL 4619; *Herrerasaurus ischigualastensis*, MCZ 4381). The articular surface for ~~the ischial peduncle of~~ the ilium is nearly straight, suggesting that the notch in the ventral portion of the ilium (Fig. 19) was not in-filled by bone when the ischium and ilium were in articulation, and that this represents a small opening in the acetabulum; the same feature can be inferred for ~~*Yarasuchus* *Y. deccanensis*~~ (ISI R334). The articulation with the pubis is straight and indicates that the contact between the two elements was more restricted than in *Euparkeria capensis* (SAM-PK-K5867), other non-archosaurian archosauriforms (e.g., *Tropidosuchus romeri*, PVL 4601), and ~~*Lagerpeton* *L. chanarensis*~~ (PVL 4619). Dorsally, just posterior to the acetabular rim, a long groove is positioned on the ischial shaft. This groove, which is present in a wide variety of diapsids (Ezcurra, 2016), occupies about half of the length of the dorsal shaft surface. The ventral edge of the

Formatted: Font: Italic

Formatted: Font: (Default) Times New Roman, 12 pt

ischium tapers, resulting in a triangular shaft cross-section for nearly its entire length. The ~~tapered~~ ventral edge is also tapered in *Asilisaurus kongwe* (NMT RB159), but this contrasts with the more rounded ventral ~~end~~margin ~~of~~seen in dinosaurs (e.g., *Eoraptor lunensis*; Sereno et al., 2013). Posteriorly, as in ~~*Yarasuchus*~~ *Y. deccanensis* (ISI R334; the ischium was originally reported as absent: see Sen, 2005), the shaft subtly expands ventrally, as also occurs in a variety of archosaurs, including poposauroids (*Arizonasaurus babbitti*, MSM P4590) and dinosauriforms (e.g., *Asilisaurus kongwe*, NMT RB135; *Eoraptor lunensis*; Sereno et al., 2013). Proximodistally oriented ~~Parallel thin~~ striations are present on the dorsal and lateral surfaces just anterior to the distal surface. The distal end is generally rounded in posterior and lateral views.

Medially, the proximal portion bears a broad fossa that is framed by its articulations with the ilium anterodorsally, the pubis anteriorly, and its contact with the other ischium (Fig. 20). A flat, striated surface forms the articular surface for the other ischium and, proximally, this articulation approaches, but does reach, the articular facet for the pubis. Nevertheless, this proximal extension indicates that the two ischia contacted each other over nearly their entire lengths, as also occurs in silesaurids (e.g., *Silesaurus opolensis*, ZPAL Ab III/404/1), early dinosaurs (*Eoraptor lunensis*, Sereno et al., 2013), and paracrocodylomorphs (e.g., ~~*Arizonasaurus*~~ *A. babbitti*, MSM P4590; *Postosuchus kirkpatricki*, TTUP 9000, Weinbaum, 2013). This is in contrast to the condition in *L. chanarensis* (PVL 4619) and other stem archosaurs (e.g., *E. capensis*, Ewer, 1965) where the ischia meet ~~on~~along their medial edges. The medial surface of the shaft of *T. rhadinus* is flat and bears many minute ridges and grooves that parallel ~~the~~ its dorsal and ventral margins ~~of the shaft~~bone.

Formatted: Font: Italic

Formatted: Font: Italic

Hindlimb

Femora (Holotype and Referred)—The left and right femora of the holotype (NHMUK PV R6795; Figs. 21, 23; Table 2) are complete, three-dimensionally undistorted, and have surfaces that are well preserved (although fractured in some places). We also refer another well preserved, but smaller, right femur (NMT RB498; Figs. 22, 23; Table 4) to *Teleocrater rhadinus*. The femur lies in the parasagittal plane when in articulation with the ilium (as in other eucrocopods) and, therefore, the following description will orient the long axis of the bone vertically. The shaft is sigmoidal in anterolateral and posteromedial views ~~view~~ and the proximal half arcs medially in posterior view. The long axis of the proximal surface is anteromedially to posterolaterally ~~anteromedially~~ orientated and is offset from the mediolaterally oriented long axis of the distal surface by ~45 degrees ~~°~~ as in most archosaurs and eucrocopodan archosauriforms (e.g., *Euparkeria capensis*, Ewer, 1965; *Chanaresuchus bonapartei*, MCZ 4035).

The proximal head of the femur is directed anteromedially to posterolaterally~~anteromedially~~, and the proximal surface is slanted anteroventrally, as occurs in most eucrocopods (e.g., ~~*Euparkeria*~~ *Eu. capensis*, Ewer, 1965; ~~*Chanaresuchus*~~ *C. bonapartei*, MCZ 4035; *Yarasuchus deccanensis*, ISI R334; *Marasuchus lilloensis*, PVL 3871; *Turfanosuchus dabanensis*, IVPP V3237). The proximal surface exhibits a slight rugosity that surrounds a well defined depression that is straight and oriented parallel to the long axis of the proximal surface (Figs. 21G, ~~–~~22~~: g3~~), resembling the condition in ~~*Yarasuchus*~~ *Y. deccanensis* (ISI R334), *Dongusuchus efremovi* (PIN 952/15-1), some pseudosuchians (e.g., *Arizonasaurus babbitti*, MSM 4596; *Batrachotomus*

Formatted: Font: (Default) Times New Roman, 12 pt

Formatted: Font: (Default) Times New Roman

Formatted: Font: (Default) Times New Roman

kupferzellensis, SMNS 52970), and some dinosauriforms (e.g., *Asilisaurus kongwe*, NMT RB19; *Silesaurus opolensis*, Dzik, 2003). The posterolateral corner of the proximal surface arcs distally gradually whereas the anteromedial portion forms a nearly 90 degree angle with ~~that of~~ the medial surface of the proximal portion. The proximal portion bears a well-defined anterolateral tuber that extends distally 20 mm from the proximal surface (~12% the length of the element). Posteromedially, only a broad posteromedial tuber (Figs. 21–23; pmt) is present with no indication of an anteromedial tuber. This is similar to the femora of ~~*Euparkeria*~~ *Eu. capensis* (Ewer, 1965) and other non-crown archosauriforms (Nesbitt, 2011), but differs from the condition in most archosaurs that possess an anteromedial tuber (Nesbitt, 2011). The anteromedial surface of the proximal end is continuous with the shaft and does not have ~~any bone scars to indicate the presence of the~~ an 'offset femoral head' present in dinosauriforms. The femoral head of the holotype is poorly preserved whereas ~~the head~~that of NMT RB498 is well preserved. An extremely low scar demarcates the femoral head from the rest of the femur. This scar lies just distal to the head (Figs. 21–23C–D; sc) and we suggest that it is homologous, but represents a different condition to the 'ventral emargination' in *Lagerpeton chanaresnsis* and *Dromomeron* (Irmis et al., 2007; Nesbitt et al., 2009b), the surface just distal to the head in ~~*Asilisaurus*~~ *A. kongwe* (Griffin and Nesbitt, 2016), and the ligament sulcus in dinosaurs (e.g., *Saturnalia tupinquim*; Langer, 2003). The anterolateral surface bears a faint muscle scar for the M. iliofemoralis externus at the distal end of the anterolateral tuber (Fig. 23; mie~~: mie~~), as also occurs in *Dongusuchus efremovi* (Niedźwiedzki et al., 2016). This structure~~,~~ ~~which~~ is highly reminiscent of, and here suggested to be homologous with, the low anterior trochanter in ~~*Yarasuchus*~~ *Y. deccanensis* (ISI R334)

and early dinosauromorphs (e.g., *Dromomeron gregorii*, Nesbitt et al., 2009b; ~~*Asilisaurus*~~ *A. kongwe*, Griffin and Nesbitt, 2016). The scar is proximally inclined on the posterolateral portion of the proximal femur, reaches a peak just posterior to the distal margin of the anterolateral tuber, and then extends anteromedially to form the proximal portion of the linea intermuscularis cranialis (Fig. 23; ail). The anterior trochanter also follows this pattern in ~~*Yarasuchus*~~ *Y. deccanensis* (ISI R334) and ~~*Asilisaurus*~~ *A. kongwe* (NMT RB159). The linea intermuscularis cranialis is located on the anterolateral edge of the femur, but disappears at a proximally opening foramen located at a point approximately two-fifths of the length of the femur from the proximal surface. We have looked at a number of well preserved stem archosaurs and pseudosuchians and have not observed a similar scar in the same position as *T. rhadinus* and Y. *decannesis*. Admittely, the scar is subtle in these specimens and requires exceptional surface preservation.

-A small, raised muscle scar (Fig. 23; mic~~: mie~~) located on the posterior half of the anterolateral surface, approximately 50 mm from the proximal surface (~30% the length of the element), likely represents the attachment of the iliofemoralis musculature. Based on its position and inferred muscle attachment this attachment is considered here ~~and is therefore~~ homologous with the trochanteric shelf of dinosauriforms and large lagerpetids (Nesbitt et al., 2009b; Martinez et al., 2016). This scar is located in the same position in *Mandasuchus tanyauchen* (NHMUK PV R6792; Butler et al., 2017) and *Erythrosuchus africanus* (NHMUK PV R3592; Gower, 2003). The ~~division~~ separation of the anterior trochanter and the trochanteric shelf ~~seen~~present in *T. rhadinus* ~~*Teleocrater*~~ is also present in ~~*Yarasuchus*~~ *Y. deccanensis* (ISI R334) and ~~*Dongusuchus*~~ *Do. efremovi* (Sennikov, 1988; Niedźwiedzki et al., 2016). This division suggests that the muscles

Formatted: Font: Italic

Formatted: Font: Italic

Formatted: Indent: First line: 0.5"

attaching to the anterior trochanter (M. iliofemoralis externus: Hutchinson, 2001) and the trochanteric shelf (M. ischiotrochantericus: Hutchinson, 2001) were present as separate units in basal avemetatarsalians and became a single unit in later dinosauromorphs.

The ridge for attachment of the caudofemoralis musculature (= fourth trochanter) is low and proximodistally oriented, resembling the condition in *Yarasuchus deccanensis* (ISI R334) and ~~*Dongusuchus*~~ *Do. efremovi* (PIN 952/15-1). By contrast, the fourth trochanter is far more strongly developed in ~~*Euparkeria*~~ *Eu. capensis* (Ewer, 1965), proterochampsids (e.g., *Tropidosuchus romeri*, PVL 4601; ~~*Chanaresuchus*~~ *C. bonapartei*, MCZ 4035), most pseudosuchians (e.g., *Riojasuchus tenuisceps*, PVL 3827; *Aetosauroides scagliai*, PVL 2073), and dinosauromorphs (e.g., ~~*Lagerpeton*~~ *L. chanarensis*, PVL 4619; ~~*Marasuchus*~~ *M. lilloensis*, PVL 3871; ~~*Silesaurus*~~ *S. opolensis*, Dzik, 2003). Anteromedial to the ridge, a deep depression parallels it along its length. The bone surface within the depression is striated. *Teleocrater rhadinus* lacks the dorsolateral trochanter of dinosauriforms on the anterolateral surface of the proximal portion of the femur, but has a scar that has been interpreted to be associated with this feature on the posterolateral side of the femur (= posterior portion of the dorsolateral trochanter: Griffin and Nesbitt, 2016). Given the lack of a dorsolateral trochanter, however, the morphology present in *T. rhadinus* ~~*Teleocrater*~~ suggests that this scar on the posterior surface may not be associated with the dorsolateral trochanter. Distal to the scar and posterior to the attachment of the caudofemoralis musculature, a clear scar is present and we suggest that this scar is homologous to the attachment location of the M. caudofemoralis brevis in crocodylians (see Hutchinson, 2001). A similar scar is present in ~~*Asilisaurus*~~ *A. kongwe* (Griffin and Nesbitt, 2016).

The posterolateral edge of the femur is well rounded proximally, then forms a sharp ridge that starts at the midshaft and extends distally, but becomes rounded again 40 mm (~76% the length of the element) from the distal surface. From the midshaft, the femur gradually expands, with the expansion of the distal end being similar in magnitude to that of the proximal end, resembling the condition in several eucrocopods (e.g., ~~*Euparkeria* *Eu.*~~ *capensis*, Ewer, 1965; ~~*Chanaresuchus* *C.*~~ *bonapartei*, MCZ 4035; ~~*Yarasuchus* *Y.*~~ *deccanensis*, ISI R334; ~~*Dongusuchus* *Do.*~~ *efremovi*, PIN 952/15-1; ~~*Marasuchus* *M.*~~ *lilloensis*, PVL 3871; ~~*Turfanosuchus* *T.*~~ *dabanensis*, IVPP V3237). The distal condyles are poorly differentiated from the shaft and are separated on the posterior surface by a shallow depression. This depression separates the condyles for at least 35 mm proximally from the distal surface (~2~~8~~0% the length of the element). About 15 mm from the distal surface (~9~~1~~% the length of the element), a bone scar is present in the intercondylar depression in posterior view. This bone scar is also present in ~~*Asilisaurus* *A.*~~ *kongwe* (NMT RB159), but absent in ~~*Mandasuchus* *AM.*~~ *tanyauchen* (Butler et al., 2017) and ~~*Erythrosuchus* *Er.*~~ *africanus* (NHMUK PV R3592). The posterior edges of the distal condyles are gently rounded and the crista tibiofibularis is poorly differentiated from the lateral condyle. A well-developed bone scar is present on the posterior surface of the medial condyle. The scar is 30 mm long, 7 mm at its widest, and terminates 5 mm from the distal surface. This scar is present in *Asilisaurus kongwe* (NMT RB159), ~~*Dongusuchus* *Do.*~~ *efremovi* (PIN 952/15-1), ~~*Dromomeron* *Dr.*~~ *gregorii* (TMM 31100-1306), ~~*Dromomeron* *Dr.*~~ *romeri* (GR 216), and dinosaurs (*Tawa hallae*, GR 244; *Saturnalia tupiniquim,* MCP 3944-PV) in a similar form, but is absent in ~~*Mandasuchus* *M.*~~ *tanyauchen* (Butler et al., 2017). A similar scar is present in ~~*Erythrosuchus* *Er.*~~

africanus (NHMUK PV R3592), but is far deeper and proportionally much smaller/shorter. Anteriorly, a shallow fossa oriented proximodistally separates the medial and lateral condyles. The distal surface is rounded with a central depression oriented parallel to the long axis of the surface.

Tibiae (Holotype and Referred)—Both tibiae are present in the holotype (Fig. 24) and a left tibia (NMT RB481) is referred to ~~*the taxon*~~*Teleocrater rhadinus*. The right side is much better preserved than the left in the holotype. The tibiae are shorter than the femora (~85% of their length). ~~In~~ The proximal ~~view~~outline ~~, the proximal surface of the tibia~~ is triangular with rounded edges, because the tibial condyles are well separated and the cnemial crest is basically absent, resembling the condition in *Dorosuchus neoetus* (PIN 1579/61), *Euparkeria capensis* (SAM-PK-K6047B), *Dongusuchus efremovi* (PIN 952/84-5), *Yarasuchus deccanensis* (ISI R334), and pseudosuchians (e.g., Nesbitt, 2011; Ezcurra, 2016). By contrast, the tibia of proterochampsids (e.g., *Tropidosuchus romeri*, PVL 4601; *Chanaresuchus bonapartei*, MCZ 4035) and dinosauromorphs (Novas, 1996) possesses a well developed, anteriorly projecting cnemial crest. The tibial condyles are separated by a slight gap, and are poorly offset from rest of the proximal end, as also occurs in ~~*Dongusuchus*~~ *D. efremovi* (PIN 952/84-4, 5), but the gap between the condyles is deeper in ~~*Yarasuchus*~~ *Y. deccanensis* (ISI R334). The proximal surface is largely convex with a few grooves ornamenting the surface. The proximal end bears several well defined muscle scars, one located near the posteromedial edge as a deep depression located on the medial surface bounded anteriorly by a distinct ridge, which is interpreted as the attachment of the M. puboischiadictibialis (=M. flexor tibialis interior of Brochu, 1992); a scar proximoposteriorly to the aforementioned scar on the medial surface and in

Formatted: Font: Italic

the form of a slightly raised surface interpreted as the attachment of the internal lateral ligament (Brochu, 1992); a scar located on the medial crest that extends onto the anterior surface in the form of a striated surface, which is interpreted as the attachment of the M. tibialis anterior (Brochu, 1992); and a scar distal to the more lateral tibial condyle in the form of a slightly raised and striated surface. A small proximally opening foramen is present on the lateral surface, 40 mm distal to the proximal surface (~30% the length of the element).

At midshaft, the tibia is elliptical with an anteroposteriorly oriented long axis. On the distal one-third of the bone, a proximodistally-oriented ridge is present on the anteromedial edge but fails to reach the distal end. In distal view, the tibia is sub-oval in outline and tapers slightly to its anterolateral edge, resembling the condition in ~~*Euparkeria* *E.*~~ *capensis* (SAM-PK-K6047B) and ~~*Yarasuchus* *Y.*~~ *deccanensis* (ISI R334). The lateral surface of the distal end of the tibia of ~~*Teleocrater* *T.*~~ *rhadinus*, ~~*Yarasuchus* *Y.*~~ *deccanensis* (ISI R334), and ~~*Dongusuchus* *D.*~~ *efremovi* (PIN 952/84-4, 5) is homogenously convex and lacks the lateral longitudinal groove present in proterochampsids and dinosauriforms (Nesbitt, 2011; Ezcurra, 2016). The distal surface is nearly flat without any indication of any divisions of the surface for articulation with the astragalus. The distal surface of the bone is concave in *Yarasuchus deccanensis* (ISI R334) and ~~*Dongusuchus* *D.*~~ *efremovi* (PIN 952/84-4, 5). There is no facet for the reception of ~~the~~ an ascending process of the astragalus and there is no posterolateral process on the distal end of the tibia of *T. rhadinus*~~*Teleocrater rhadinus*~~, ~~*Yarasuchus* *Y.*~~ *deccanensis* (ISI R334), and ~~*Dongusuchus* *D.*~~ *efremovi* (PIN 952/84-4, 5; contra Niedźwiedzki et al., 2016), contrasting with dinosauriforms (Novas, 1996).

Fibula (Holotype and Referred)—The left fibula of the holotype (Fig. 25; Table 2) is complete and very well preserved and two additional right fibulae are referred to *Teleocrater rhadinus* (NMT RB482; NMT RB488; Table 4). Overall, the shaft of the fibula is weakly sigmoidal in lateral view. The long axis of the proximal surface is anteroposteriorly oriented, and is set at approximately 30 degrees to the anteromedially to posterolaterally ~~anteromedially~~ oriented long axis of the distal surface. The proximal surface ~~is anteroposteriorly elongated with~~has a broader posterior edge compared to the tapered anterior end. The anterior-most corner of the proximal end slightly curls anteromedially, as in dinosauriforms (e.g., *Asilisaurus kongwe*, NMT RB159). In lateral view the anterior margin of the proximal end is straight and vertical, whereas the posterior edge is straight but slanted ~~posterodorsally~~proximally. A distinct muscle scar is present on the anterior edge of the lateral surface around 10 mm from the proximal surface (~7% the length of the element). Another muscle scar, represented by proximodistally-oriented striations, is present on the posterior edge of the lateral surface immediately distal to the proximal surface. Also, immediately distal to the proximal surface, ~~Medially,~~ the proximal end of the fibula bears a small scar on its posterior surface ~~immediately distal to the proximal surface~~. More anteriorly a proximodistally oriented and well-defined ridge forms the anterior margin of the fibula. Proximally, this ridge arcs posteriorly and frames a slight depression located in the middle of the medial surface of the proximal surface of the fibula.

A well-developed iliofibularis crest originates on the anterior ~~edge~~ margin of the fibula ~30 mm from the proximal surface (~21% the length of the element), crosses the lateral surface ~~of the fibula~~, and reaches the posterior ~~edge~~ margin of the element ~55

Formatted: Indent: First line: 0", No widow/orphan control, Don't adjust space between Latin and Asian text, Don't adjust space between Asian text and numbers, Tab stops: 0.39", Left + 0.78", Left + 1.17", Left + 1.56", Left + 1.94", Left + 2.33", Left + 2.72", Left + 3.11", Left + 3.5", Left + 3.89", Left + 4.28", Left + 4.67", Left

Formatted: Font: (Default) Times New Roman

Formatted: Font: (Default) Times New Roman

Formatted: Font color: Black, (Asian) Japanese

mm from the proximal surface (~38% the length of the element). The crest has a nearly equal lateral expansion for its entire length. This is in contrast to the more proximally restricted scar in *Mandasuchus tanyauchen* (Butler et al., 2017), aetosaurs, and phytosaurs (Nesbitt, 2011). The iliofibularis crest is restricted to the anterolateral edge of the bone in dinosauriforms (e.g., *Lewisuchus admixtus*, CRILAR-Pv 552; *Silesaurus opolensis*, ZPAL Ab III/3284). The posterior edge of the fibula has a poorly -defined ridge that extends for the entire length of the element, whereas the anterior edge of the fibula bears a sharp ridge that originates at the iliofibularis crest and terminates at the distal end.

The distal end of the fibula extends further distally at its posterior margin than it does anteriorly, resulting in an asymmetrical distal end resembling the condition in *Marasuchus lilloensis* and several pseudosuchians (Nesbitt, 2011). A shallow depression representing a muscle scar is present on the posterior side of the distal end. Another scar is present in the middle of the lateral surface immediately proximal to the distal surface. The distal surface is ellipsoid with its long axis trending slightly medially with respect to the anteroposterior plane. A shallow depression is present on the distal surface.

Calcaneum (Referred)—The only ankle element recovered from *Teleocrater rhadinus* is a referred, well-preserved right calcaneum (NMT RB490; Fig. 26) that was found among the scattered remains of the taxon (Nesbitt et al. 2017b). This nearly complete calcaneum is missing only a small chip from the posteromedial side of the calcaneum tuber. Several calcanea were collected with the holotype of *Yarasuchus deccanensis*, but were never described (see Sen, 2005). These calcanea appear to be identical to that of *T. rhadinus*~~*Teleocrater*~~.

Proximally, the calcaneum of *T. rhadinus* ~~*Teleocrater*~~ has a convex, triangular surface that articulated with the fibula. This articular surface has the same shape as that of the dinosauriform *Asilisaurus kongwe* (NMT RB159) and the non-archosaur archosauriform *Euparkeria capensis* (UMCZ T692). A groove lies on the posteromedial surface of the proximal portion separating the fibular facet from the rest of the calcaneum, resembling the condition in ~~*Euparkeria*~~ *E. capensis* (UMCZ T692). Anteriorly, the calcaneum of *T. rhadinus* ~~*Teleocrater*~~ possesses a concave facet for articulation with, presumably, the convex surface of the astragalus. This configuration is present in all pseudosuchians and has been termed 'crocodile normal' (Chatterjee, 1978; Cruickshank, 1979; Gauthier, 1986; Benton and Clark, 1988; Sereno, 1991; Parrish, 1993; Juul, 1994; Dyke, 1998; Benton, 2004; Brusatte et al., 2010; Nesbitt, 2011), but is now clearly present in at least some dinosauriforms such as ~~*Asilisaurus*~~ *A. kongwe* (NMT RB159) and *Lewisuchus admixtus* (PVL 4629, holotype of *Pseudolagosuchus major*) (Nesbitt et al., 2010). In contrast, the homologous region in ~~*Euparkeria*~~ *E. capensis* (UMCZ T692) is distinctly convex. Like ~~*Asilisaurus*~~ *A. kongwe* (NMT RB159) and some other archosauriforms (*Nundasuchus songeaensis*, Nesbitt et al., 2014; Nesbitt et al., 2017b), the concave surface for articulation with the astragalus stretches from near the lateral extent to the medial termination. A rim surrounds the proximal and medial portions of the concave surface in *T. rhadinus*~~*Teleocrater*~~.

The fibular facet and the facet for articulation with distal tarsal four nearly contact each other, but are separated by a short non-articular surface, and this condition is also present in an exceptionally well preserved example of ~~*Asilisaurus*~~ *A. kongwe* (NMT RB159). In pseudosuchians (e.g., *Mandasuchus tanyauchen,* Butler et al., 2017;

Revueltosaurus callenderi, PEFO 34561) and ~~*Euparkeria*~~ *E. capensis* (UMCZ T692) these two facets are continuous, whereas in most non-archosaurian archosauriforms (e.g., *Erythrosuchus africanus*, Gower, 1996), these facets are well separated. ~~Distally,~~ T~~t~~he triangular and mildly convex facet for articulation with distal tarsal four occupies much of the distal surface. The lateral surface of the calcaneum of *T. rhadinus* ~~*Teleocrater*~~ is concave, with a slight rim formed from the fibular facet, the calcaneum tuber, and the articulation surface for distal tarsal four. The homologous surface in ~~*Asilisaurus*~~ *A. kongwe* (NMT RB159) is much smaller, not as posteriorly extensive, and bears a cluster of small foramina in its center.

The calcaneum tuber is well developed in *T. rhadinus* ~~*Teleocrater*~~ (Fig. 26). It extends posteriorly and proximally at its posterior extension with no ventral expansion. In cross-section, the shaft of the tuber is ovoid with a longer proximodistal ~~component~~ than mediolateral component. These proportions are similar to those of ~~*Euparkeria*~~ *E. capensis* (UMCZ T692) and ~~*Nundasuchus*~~ *N. songeaensis* (Nesbitt et al., 2014), but contrast with the much taller than wide tubera present in the following non-archosaur archosauriforms: the proterochampsids *Tropidosuchus romeri* (PVL 4601) and *Chanaresuchus bonapartei* (Cruickshank, 1979), *Vancleavea campi* (Nesbitt et al., 2009c), and *Erythrosuchus africanus* (Gower, 1997). The posterior portion of the tuber of *T. rhadinus* ~~*Teleocrater*~~ is gently rounded, as in ~~*Euparkeria*~~ *E. capensis* (UMCZ T692) and ~~*Chanaresuchus*~~ *C. bonapartei* (Cruickshank, 1979), and this morphology is in contrast to the more tapered tuber of ~~*Asilisaurus*~~ *A. kongwe* (NMT RB159), ~~*Lewisuchus*~~ *L. admixtus* (PVL 4629), and *Marasuchus lilloensis* (Sereno and Arcucci, 1994a). The posterior surface of the tuber of *T. rhadinus* ~~*Teleocrater*~~ is rugose and lacks any

dorsoventrally oriented groove.

Metatarsals—Two proximal metatarsals (Fig. 27) were recovered with the holotype, but were not originally thought to pertain to it (Charig, 1956). The metatarsals are consistent in size and preservation with the rest of the hind limb material and we regard them as part of the holotype individual. We assign these ~~one fragment~~ fragments to the third ~~metatarsal~~ (Fig. 27E) ~~and the other to the~~ and fourth metatarsals (Fig. 27D), respectively, based on comparisons with the feet of *Asilisaurus kongwe* (NMT RB159). Specifically, the similar proximal expansion of the third and fourth metatarsals and the rectangular proximal shape of those elements in *A. kongwe* (NMT RB159) matches well with those of *T. rhadinus*. Both metatarsals expand proximally in lateral view and are highly compressed mediolaterally. The broken shafts are circular and suggest that the metatarsals were likely proportionately elongate (~one-third to half of the length of the fibula). The shorter preserved metatarsal (Fig. 27E) was sectioned and described by de Ricqlés et al. (2008), but cannot be located currently (V. de Buffrénil, pers. comm.).

Formatted: Font: Italic

Formatted: Font: Italic

Phalanges (Holotype)—Three complete phalanges are present (Fig. 27), but were excluded from the holotype by Charig (1956). However, the phalanges are consistent in size and preservation with the rest of the hind limb material and we regard them as pertaining to the holotype. An assignment to individual digits is currently impossible. All of the phalanges are elongated relative to their widths (e.g., length = 22 mm, midshaft width = 6 mm), have proximally and distally expanded ends, a concave articular facet on the proximal end, a ~~sconvex~~ addle-shaped distal articular surface, and medial and lateral ligament pits. The smallest phalanx has a deep retractor pit on the dorsal surface of the

distal end and the distal condyles are asymmetrically developed, where either the lateral or medial ~~distal~~ condyle is extended further distally ~~than the other condyle~~.

PHYLOGENETIC RELATIONSHIPS

~~We~~ P~~p~~reviously, we included *Teleocrater rhadinus* in the two most comprehensive phylogenetic datasets of Triassic archosauromorphs compiled to date (Nesbitt, 2011; Ezcurra, 2016) in order to test the relationships of the taxon and to determine its effect on character optimizations and the evolutionary history of the clade (Nesbitt et al., 2017b). We repeat the methods ~~-~~and results here, as this information underpins the subsequent discussion of character evolution (below). Although some of the characters overlap between Nesbitt (2011) and Ezcurra (2016), these datasets are mostly independent. We used the taxon sampling and strategy outlined in Nesbitt et al. (2017b~~in review~~) for both the Nesbitt (2011) and Ezcurra (2016) datasets. Our iteration of the Nesbitt (2011) dataset with modifications by Butler et al. (2014) includes 82 taxa (excluding *Archosaurus rossicus*, *Prestosuchus chiniquensis*, UFRGS 0156 T, UFRGS 152 T, *Lewisuchus admixtus*, *Pseudolagosuchus majori*, *Parringtonia gracilis*, *Erpetosuchus granti*, *Asilisaurus kongwe*, *Asilisaurus kongwe* skeleton, *Teleocrater* holotype, *Teleocrater* 2015 quarry) ~~-~~and 419 characters. Our iteration of the Ezcurra (2016) dataset includes 84 taxa and 605 characters (following Nesbitt et al., 2017b). The following characters were ordered in the Nesbitt (2011) dataset: 32, 52, 121, 137, 139, 156, 168, 188, 223, 247, 258, 269, 271, 291, 297, 328, 356, 399, and 413. The following characters were ordered in the Ezcurra (2016) dataset: 1, 2, 7, 10, 17, 19, 20, 21, 28, 29,

Formatted: Font: Italic
Formatted: Font: Italic
Formatted: Font: Italic
Formatted: Font: Italic
Formatted: Font: Italic
Formatted: Font: Italic
Formatted: Font: Italic
Formatted: Font: Italic
Formatted: Font: Italic
Formatted: Font: Italic

36, 40, 42, 50, 54, 66, 71, 75, 76, 122, 127, 146, 153, 156, 157, 171, 176, 177, 187, 202, 221, 227, 263, 266, 279, 283, 324, 327, 331, 337, 345, 351, 352, 354, 361, 365, 370, 377, 379, 398, 410, 424, 430, 435, 446, 448, 454, 458, 460, 463, 472, 478, 482, 483, 489, 490, 504, 510, 516, 529, 537, 546, 552, 556, 557, 567, 569, 571, 574, 581, 582, and 588.

Both matrices were analyzed under equally weighted parsimony using TNT 1.5 (Goloboff et al., 2008; Goloboff and Catalano, 2016). A heuristic search with 100 replicates of Wagner trees (with a random addition sequence) followed by TBR branch-swapping (holding 10 trees per replicate) was performed. The best trees obtained from the replicates were subjected to a final round of TBR branch swapping. Zero length branches in any of the recovered MPTs were collapsed. Decay indices (=Bremer support values) were calculated and a bootstrap resampling analysis, using 10,000 pseudoreplicates, was performed reporting both absolute and GC (i.e., difference between the frequencies of recovery in pseudoreplicates of the original group and the most frequently recovered contradictory group) frequencies.

Analysis of the Nesbitt (2011) dataset with modifications of Butler et al. (2014) resulted in 36 most parsimonious trees (MPTs) with lengths of 1374 steps (Consistency Index [CI] = 0.356; Retention Index [RI] = 0.764) (Fig. 28). Analysis of the Ezcurra (2016) dataset resulted in two most parsimonious trees (MPTs) with lengths of 2671 steps (CI = 0.297; RI = 0.616) (Fig. 28). In both cases we recover *Teleocrater rhadinus* in a clade with *Spondylosoma absconditum*, *Dongusuchus efremovi*, and *Yarasuchus deccanensis*. This clade, ~~Silendasauria~~Aphanosauria, is the sister taxon of Ornithodira (Nesbitt et al. 2017b).

DISCUSSION

Relationships of *Teleocrater rhadinus* Within Archosauria

The description of well-preserved, three-dimensional remains of *Teleocrater rhadinus* revolutionizes our ability to assess homologies and evaluate character support at the base of Archosauria, Avemetatarsalia, and Ornithodira. Prior to the discovery of the silesaurid clade just outside Dinosauria (Ezcurra, 2006; Irmis et al., 2007; Nesbitt et al., 2010; Baron et al., 2017; but see Langer and Ferigolo, 2013), the majority of non-dinosaurian avemetatarsalians were represented by either partial skeletons missing key parts of the skeleton (e.g., lagerpetids), specimens embedded in slabs (e.g., most pterosaurs), or poorly-preserved natural molds (e.g., *Scleromochlus taylori*). Moreover, the small size and fragile ~~nature~~ condition of many non-dinosaurian avemetatarsalians also precluded additional preparation in many cases. These factors prevented full sampling of the anatomical variation present among basal members of Avemetatarsalia. However, the new data available from ~~*Teleocrater*~~ *T. rhadinus* and other members of the newly recognized clade ~~Silendasauria~~ Aphanosauria now mitigate some of these issues, enabling us to examine character state optimizations and the evolution of avemetatarsalian anatomy in greater detail than before. Nevertheless, although we present the following character state support for these basal clades, the study of this part of the archosaur tree is still in its infancy and additional specimens and characters are needed to tease apart the events occurring during basal divergences within the clade. Here, we also identify and discuss several other character states that are not present in either dataset or optimized unambiguously at a particular node in order to broaden this discussion.

We utilize optimizations from both the Nesbitt (2011: designated as 'N, character number-state') and Ezcurra (2016: designated as 'E, character number-state') datasets. Some of the character state optimizations in the two analyses agree and in these cases both character states are listed. In many cases, the optimizations are not perfectly consistent because of: 1) differences in taxon sampling; 2) differences in included characters; and 3) disagreement over the closest relatives of Archosauria (e.g., the position of *Euparkeria capensis* versus proterochampsids, the position of Phytosauria within Pseudosuchia or outside Archosauria). Nevertheless, both datasets obtain the same relative phylogenetic positions for all of the taxa that they share within Avemetatarsalia.

Teleocrater rhadinus is critical to the position of ~~Silendasauria~~ Aphanosauria within Archosauria. For example, without the inclusion of *T. rhadinus*~~*Teleocrater*~~, the phylogenetic positions of *Yarasuchus deccanensis* and *Dongusuchus efremovi* were most recently found to lie outside Archosauria (Ezcurra, 2016). Character support at the base of Archosauria, however, has always been weak, with variable topologies occurring due to differences in taxon inclusion (Nesbitt et al., 2014). This is the also case in the two datasets used here, given that the closest relatives of Archosauria in each case are found to differ, with Phytosauria recovered as the sister taxon to Archosauria using the Nesbitt (2011) dataset, whereas phytosaurs are recovered within Pseudosuchia with Proterochampsia as the sister taxon of Archosauria using the Ezcurra (2016) dataset. *Teleocrater rhadinus* is recovered as an archosaur based on the presence of the following unambiguous character states: palatal processes that meet on the midline (N32-2); an antorbital fossa on the dorsal process and dorsal portion of the posterior process of the maxilla (N137-2; E54-2); acromion of the scapula distinct (N220-1); lateral tuber of the

ulna present (N237-1); articulation between astragalus and calcaneum concavoconvex with concavity on the calcaneum (E532-1); and articular surfaces for fibula and distal tarsal 4 continuous (E555-1).

Teleocrater rhadinus is also important for establishing the ~~silendasaur~~ aphanosaur clade at the base of Avemetatarsalia, as character states that previously supported Ornithodira, Dinosauriformes, and even Dinosauria in previous phylogenetic analyses (Gauthier, 1986; Benton and Clark, 1988; Juul, 1994; Benton, 1999, 2004; Brusatte et al., 2010a; Nesbitt, 2011) are now found to support more basal divergences within Avemetatarsalia. *Teleocrater rhadinus* is supported as an avemetatarsalian on the basis of both cranial and postcranial characters, including: a supratemporal fossa on the posterior portion of the frontal (N144-1); greatly elongated cervical vertebrae (N181-1); anterior cervical vertebrae longer than the axis (N183-1); crest dorsal to the supraacetabular crest/rim confluent with anterior extent of the anterior (= preacetabular) process of the ilium (N265-2; E462-2); and proximal end of the fibula mediolaterally compressed (N341-1). By themselves, none of these character states are unique to avemetatarsalians within Archosauria, but their ~~. However, the~~ combination ~~of theses states~~ is unique to avemetatarsalians.

Newly added characters in the Nesbitt (2011; characters 414–418) and Ezcurra (2016; characters 601–605) datasets also support the recovery of *T. rhadinus* ~~*Teleocrater rhadinus*~~ and other ~~silendasaurs~~ aphanosaurs as avemetatarsalians. All five of these characters have states that optimize ambiguously or unambiguously at the node including *T. rhadinus* ~~*Teleocrater*~~ + bird-line archosaurs in both datasets. The presence of a posterolateral projection of the second sacral vertebra (N416-1; E601-1) and the presence

of a well defined proximodistally oriented scar extending proximally from the posterior portion of the medial condyle of the distal end of the femur (N417-1; E604-1) both unambiguously support ~~silendasaurs~~ aphanosaurs as avemetatarsalians in both datasets. In addition, the following characters also support this position: a distinct notch (= dorsal concavity) between the posterior and anterior ends of the ischial peduncle of the ilium (N414-1 ambiguous; E603-1 ambiguous); sharp ridge on the posterior edge of the fibula (N415-1; E605-1 ambiguous); and a distinct, longitudinal sharp ridge on the posterior edge of the scapular blade, immediately dorsal to the glenoid region (N418-1 ambiguous; E602-1 ambiguous).

~~Silendasaurs~~ Aphanosaurs lack a number of synampomorphies present in Ornithodira in both analyses. Aphanosaurs ~~Silendasaurs~~ lack an elongated tibia relative to the length of the femur, which is present in early pterosaurs, *Scleromochlus taylori*, and in the dinosauriform *Marasuchus lilloensis* (N299-1). The proximal portion of the aphanosaur~~s~~ ~~silendasaur~~ femur lacks the distinct posteromedial condyle (or medial head) that is present in all ornithodirans (N301-1). Moreover, the bone wall thickness of aphanosaurs ~~silendasaurs~~ is much thicker than that of the thin-walled femora of pterosaurs, lagerpetids, and silesaurids (E508-1; N323-1 ambiguous). The ilium of aphanosaurs ~~silendasaurs~~ lacks a clear antitrochanter as in ornithodirans (E457-1) and the calcaneum tuber of all ornithordirans is either lost (e.g., pterosaurs, lagerpetids) or highly reduced (e.g., ~~*Marasuchus*~~ *M. lilloensis*, *Asilisaurus kongwe*). We do note that the branch support for Ornithodira is weak (i.e., Bremer support and resampling frequencies) largely because of the same problems that previous authors have experienced, namely 1) the earliest dinosauromorphs (e.g., *Dromomeron*, *Lagerpeton chanarensis*) are only known

from parts of the postcranial skeleton and 2) pterosaurs are difficult to score because their morphology is highly ~~derived~~ modified and many of the characters cannot be scored because they are not visible or preserved.

Character Support for Aphanosauria~~Silendasauria~~

Character states that unite Aphanosauria ~~Silendasauria~~ occur in several distinct parts of the postcranial skeleton. Unsurprisingly, the clade lacks diagnostic cranial character states because *Teleocrater rhadinus* is the only taxon with cranial remains, and this is further complicated by the crushed skull material available for early diverging pterosaurs, the poorly known ~~absence of~~ cranial ~~material~~ morphology in lagerpetids (but see the newly described *Ixalerpeton polesinensis*; Cabreira et al., 2016), and the limited cranial material preserved in non-dinosaurian dinosauriforms (e.g., *Marasuchus lilloensis*). The cervical vertebrae of aphanosaurs ~~silendasaurs~~ are greatly elongated, more so than in any other non-dinosaurian avemetatarsalian from the Triassic Period, with the possible exception of *Nyasasaurus parringtoni* (Nesbitt et al., 2013a, 2017b~~in review~~). Ventrally, the centra~~um~~ of the anterior cervical vertebrae of *Teleocrater rhadinus* and *Yarasuchus deccanensis* have paramedian ridges and lack a midline ridge, which results in a sub-rectangular cross-section. The cervical vertebrae~~s~~ bear posteriorly directed epipophyses on at least the anterior and middle cervical vertebrae (N186-1; E336-1). The neural spines of aphanosaurs ~~silendasaurs~~ appear to be unique within Archosauria in bearing steeply inclined anterior neural spine margins (N419-1; E343-1) with rugose bony expansions at the distal end of the neural spines adjacent to a blade-like distal margin (N191-3). The posterior cervical vertebrae of *T. rhadinus* ~~*Teleocrater rhadinus*~~

Formatted: Font: Bold

Formatted: Widow/Orphan control

Formatted: Font: 12 pt, Italic

Formatted: Font: 12 pt

and *Yarasuchus deccanensis* bear accessory articular facets just dorsal to the parapophysis and this additional facet articulates with a distinct third articular facet on the respective rib (N193-1; E314-1). *Yarasuchus deccanensis* is currently the only aphanosaur ~~silendasaur~~ that preserves a three-headed rib, whereas *T. rhadinus* ~~*Teleocrater rhadinus*~~ possesses the three articular facets on a posterior cervical vertebra that should have received a three-headed rib. This accessory articulation on the posterior cervical vertebrae also occurs in poposauroids among archosaurs (see above), so this character cannot be used to diagnose aphanosaurs ~~silendasaurs~~ in isolation. The aphanosaur ~~silendasaur~~ trunk centra are elongate and much longer proportionally than those of other non-dinosaurian avemetatarsalians. The proportions of the trunk vertebrae are similar to those of neotheropods and *Eodromaeus murphi* (Martinez et al., 2011).

Formatted: Font: (Default) Optima

The humeri of ~~*Yarasuchus*~~ *Y. deccanensis* and *T. rhadinus* ~~*Teleocrater rhadinus*~~ are robust and more like those of sauropodomorph dinosaurs and *Nyasasaurus parringtoni* (see Nesbitt et al., 2017b ~~in review~~) than any other archosauriform. Aphanosauria ~~Silendasaurs~~ share an elongated deltopectoral crest (N230-1) with dinosaurs and ~~*Nyasasaurus*~~ *N. parringtoni* and this is significant because an elongated deltopectoral crest has been an important character for diagnosing Dinosauria (Bakker and Galton, 1974; Brusatte et al., 2010b; Langer et al., 2010; Nesbitt et al., 2013a; Baron et al., 2017). Currently, the presence of an elongated deltopectoral crest in aphanosaurs ~~silendasaurs~~ and dinosaurs optimizes as convergent. The distal end of the humerus of ~~*Yarasuchus*~~ *Y. deccanensis* and *T. rhadinus*~~*Teleocrater rhadinus*~~ is wide relative to its length (N235-1), as in sauropodomorph dinosaurs (Langer and Benton, 2006).

Several ischial character states of aphanosaurs ~~silendasaurs~~ support their

monophyly (Nesbitt et al., 2017b~~in review~~). However, the ischial morphology of ~~*Yarasuchus*~~ *Y. deccanensis* and *T. rhadinus* ~~*Teleocrater rhadinus*~~ is much more similar to that of poposauroids and silesaurids + early dinosaurs than to that of other avemetatasalians. For example, the ischia of ~~*Yarasuchus*~~ *Y. deccanensis* and ~~*Teleocrater*~~ *T. rhadinus* have extensive contact along the midline for much of their length (E485-1; N191-1, but ambiguous), a character state that is present in silesaurids, dinosaurs, and poposauroids. By contrast, the ischia of pterosaurs (e.g., *Dorygnathus banthensis*; Padian, 2008), *Lagerpeton chanarensis*, and ~~*Marasuchus*~~ *M. lilloensis* have much more plate-like ischia and these elements meet at a short contact at the midline (Sereno and Arcucci, 1994a, b). Furthermore, the ischia of aphanosaurs ~~silendasaurs~~ terminate in rounded, nearly triangular distal ends in posterior view with closely appressed left and right elements, a morphology more typical of dinosaurs (Langer and Benton, 2006) and poposauroids (Nesbitt, 2007, 2011) than other early ornithodirans.

As with most archosauriform clades, the femur helps diagnose Aphanosauria~~Silendasauria~~. The femora of ~~*Yarasuchus*~~ *Y. deccanensis, Dongusuchus efremovi*, and *T. rhadinus* ~~*Teleocrater rhadinus*~~ share many features including a straight transverse groove on their proximal surface ~~of the femur bone~~ (N314-1; E495-1), a concave articular surface on its~~f~~ ~~the~~ distal end ~~of the femur~~ (E512-2), the absence of an anteromedial tuber ~~of the femur~~;~~,~~ and the presence of a weakly developed ridge (= fourth trochanter) for attachment of the M. caudofemoralis ~~musculature~~. The femur attributed to *Spondylosoma absconditum* lacks the ventral surface depression and the absence of this character state suggests that the taxon may lie within Aphanosauria ~~Silendasauria~~ but outside of a clade including ~~*Yarasuchus*~~ *Y. deccanensis,* ~~*Dongusuchus*~~ *Do. efremovi*, and

~~*Teleocrater* *T.* *rhadinus*~~, as found in our analyses. One of the most intriguing features of ~~the~~ aphanosaur femora ~~of aphanosaurs silendasaurs~~ is the presence of a structure on the anterolateral side of the proximal portion of the femur in a homologous position to the anterior trochanter of dinosauriforms (Novas, 1994, 1996) and likely all dinosauromorphs (see Nesbitt et al., 2009b). As discussed by Niedźwiedzki et al. (2016), this structure is particularly similar in shape and location to the anterior trochanter of dinosauromorphs. Here, we agree with their homology assesment, but find in both of our phylogenetic analyses that the 'anterior trochanter' of aphanosaurs ~~silendasaurs~~ is a character state that diagnoses this clade but not a more inclusive clade including all avemetatarsalians; this is because of the absence of an anterior trochanter in *Lagerpeton chanarensis* and pterosaurs. However, it is possible that either early pterosaurs had the structure, but that it is hard to recognize given the difficulty of assessing muscle scars in the small and crushed pterosaur specimens from the early Mesozoic, and/or that there is a strong ontogenetic component to the early appearance of the anterior trochanter. In support of the latter hypothesis, the anterior trochanter is present only in the largest specimens of *Dromomeron gregorii* (Nesbitt et al., 2009b) and absent in the smallest specimens of the silesaurid *Asilisaurus kongwe* (Griffin and Nesbitt, 2016). This may explain why some small avemetatarsalians appear to lack the feature.

Aphanosaurs ~~Silendasaurs~~ appear to be the only group of avemetatarsalians that have an anterior trochanter ~~but lack~~and a trochanteric shelf that~~, but these~~ are not ~~in an~~ adjoining positions and that are separated from one another by a smooth area of bone surface. In ~~*Dromomeron*~~ *Dr.* *gregorii* (Nesbitt et al., 2009b), the silesaurid *Asilisaurus kongwe*, and many early dinosaurs (e.g., coelophysids), the anterior trochanter and the

trochanteric shelf are always connected when both structures are present. In aphanosaurs~~silendasaurs~~, the structure homologous with the trochanteric shelf is located well ventral to the anterior trochanteric structure and is situated in the plesiomorphic position found in other early archosaurs (see Nesbitt, 2011).

Aphanosaurs ~~Silendasaurs~~ have a crocodile-normal ankle in that it has a concave articular socket on the calcaneum that receives a convex articular surface from the astragalus; a convex articular surface on the calcaneum for the reception of the fibula; and a distinct, posteriorly directed calcaneal tuber. The calcaneal tuber of *T. rhadinus* ~~*Teleocrater rhadinus*~~ and ~~*Yarasuchus*~~ *Y. deccanensis* is reduced in size relative to those of pseudosuchians, but remains better developed than that of the dinosauriforms ~~*Marasuchus*~~ *M. lilloensis*, *Lewisuchus admixtus* (probable senior synonym of *Pseudolagosuchus major*; Arcucci, 1998; Nesbitt et al., 2010), and ~~*Asilisaurus*~~ *A. kongwe*. The shaft of the tuber in aphanosaurs ~~silendasaurs~~ is slightly taller than wide (N376-0) and this is plesiomorphic for Archosauria.

Aphanosauria~~Silendasauria~~-Poposauroidea Convergence?

Formatted: Font: Bold

Surprisingly, the basal-most diverging and stratigraphically earliest bird-line archosaurs, the aphanosaurs~~silendasaurs~~, seem to be partially convergent with the earliest appearing, but not the basal-most, pseudosuchians – the poposauroids. Indeed, *Yarasuchus deccanensis* was recovered as a basally diverging poposauroid when it was first included in a numerical cladistic analysis (Brusatte et al., 2010a). Other than one clear character state that is present in some poposauriods and Aphanosauria~~Silendasauria~~, the presence of an accessory articulation facet just dorsal to the parapophysis in the

posterior cervical vertebrae (N193-1; E314-1), these two clades do not appear to share any synapomorphies that are not present in more inclusive clades. For example, both poposauroids and aphanosaurs ~~silendasaurs~~ share the presence of a concave ventral surface of the ischial peduncle of the ilium (N414-1; E603-1). However, this character state is not exclusive to these two clades but occurs in many avemetatarsalians. Additionally, other similarities between some poposauroids and aphanosaurs~~silendasaurs~~, such as the lack of osteoderms, are highly homoplastic within Archosauria. In the Nesbitt (2011) phylogenetic dataset, poposauroids are firmly established as suchians and possess the synapomorphies of that clade (e.g., a calcaneum with a well-developed tuber; hemicylindrical articulation with the fibula; medially opening fossa for articulation with the 'peg' of the astragalus: Nesbitt, 2007, 2011). The apparent convergence between poposauroids and aphanosaurs ~~silendasaurs~~ is part of a larger trend of evolutionary convergences between the early poposauroid to shuvosaurid lineage and the early avemetatarsalian to coelurosaurian theropod lineage (Nesbitt, 2007). This further illustrates the common convergence present in body plans in early Archosauromorpha (Stocker et al., 2016).

The convergence between some of the character states present in poposauroids (including those taxa once referred to as 'rauisuchians' or 'rauisuchids') and aphanosaurs ~~silendasaurs~~ does, however, make it remarkably difficult to assign isolated skeletal elements from the Early–Middle Triassic to either of those clades. For example, isolated elongated cervical vertebrae from the Early–Middle Triassic of Russia (e.g., *Vjushkovisaurus berjanenesis*, Ochev, 1982; '*Tsylmosuchus donensis*', Sennikov, 1990) may not be assignable to either poposauroids, aphanosaurs~~silendasaurs~~, and non-

eucrocopod archosauriforms, as there is little way to distinguish them given that both taxa have elongated necks with some of the same morphology (see above). Ilia are also potentially difficult to tell apart, as both poposauroids and aphanosaurs ~~silendasaurs~~ have a vertical crest dorsal to the supra-acetabular rim, a short anteromedially directed process, and a partially concave ischial peduncle. This set of character states call into question the taxonomic assignment of an ilium referred to *Bystrowisuchus flerovi* (PIN 1043/831; Sennikov, 2012) to a ctenosauriscid; alternatively, this specimen could also be interpreted as that of an aphanosaur~~silendasaur~~. This ilium is from the same locality as '*Tsylmosuchus*' spp. (Gower and Sennikov, 2000) and all of this material could pertain to a single taxon. The same ~~comments~~ also apply to the ilium of *Vyschegdosuchus zheshartensis* (PIN 3361/134; Sennikov, 1988). Furthermore, an ilium (UCMP 36233; Welles, 1947:fig. 28) from the Moenkopi Formation, previously assigned to an indeterminate reptile, may pertain to a third poposauroid in the Holbrook Member (see Nesbitt, 2003, 2005), or possibly a aphanosaur~~silendasaur~~.

In the same vein, some 'rauisuchians' or non-eucrocopod archosauriforms likely represent members of Aphanosauria~~Silendasauria~~. For example, *Jaikosuchus magnus*, from the late Olenekian Yarenskian Gorizont, is represented by a complete anterior or middle cervical vertebra (Sennikov, 1990). The holotype bears two aphanosaur ~~silendasaur~~ synapomorphies, an anteriorly overhanging neural spine and a laterally rugose distal end of the neural spine. Furthermore, the greatly elongated cervical vertebra appears to possess epipophyses, a character state present in (but not exclusive to) aphanosaurs~~silendasaurs~~. However, we also note that some early diverging archosauriforms could have some of these features (e.g., *Guchengosuchus shiguaiensis*,

IVPP V8808-10) and that the early members of these clades do overlap with aphanosaurs ~~silendasaurs~~ and poposaurioids in time and geographic range.

In summary, we urge caution when assigning isolated elements or even partial skeletons from the Early to Middle Triassic to any archosaurian clade, as elements once though to be diagnosable to poposauroids or 'rauisuchians' may be indistinguishable from those of aphanosaurs~~silendasaurs~~.

Biogeography

Teleocrater rhadinus comes from the lower part of the Lifua Member of the Manda Beds (Fig. 29; Nesbitt et al., 2017b). This area was in the mid southern hemisphere during the Middle Triassic, at a paleolatitude of c. 50–55 degrees° South. *Teleocrater rhadinus* is associated with a tetrapod assemblage that includes the stereospondyl '*Stanocephalosaurus*' *pronus* (Howie, 1970), at least one dicynodont (*Dolichuranus*; Smith et al., 2017; Fig. 29), archosauromorphs (an undescribed azendohsaurid allokotosaurian), and the cynodont *Cynognathus crateronotus* (Wynd et al., 2017; Nesbitt et al., 2017b). Based on comparisons with the tetrapod fauna of the *Cynognathus* Subzone B Assemblage Zone of South Africa (Rubidge, 2005), this portion of the Lifua Member is considered to be Middle Triassic in age (Wynd et al., 2017).

Yarasuchus deccanensis comes from the Yerrapalli Formation of Andhra Pradesh, India (Sen, 2005), which was located geographically close to Tanzania in the Middle Triassic, and at a similar paleolatitude in southern Pangea. The associated faunal assemblage includes a capitosauroid temnospondyl (Sengupta, 2003), kannemeyeriiform dicynodonts (Bandyopadhyay, 1988, 1989), the allokotosaurian archosauromorph

Pamelaria dolichotrachela (Sen, 2003; Ezcurra, 2016), the stenaulorhynchine rhynchosaur *Mesodapedon kuttyi* (Chatterjee, 1980; Schultz et al., 2016), and an undescribed erythrosuchid (MDE, pers. obs., 2015). An Anisian age has been assigned to this assemblage on the basis of vertebrate biostratigraphy (e.g., Sen, 2005).

Dongusuchus efremovi comes from the Donguz I site within the Donguz Svita of Orenburg Province, European Russia (Sennikov, 1988; Niedźwiedzki et al., 2016). This region was situated in the mid northern hemisphere in the Middle Triassic, in the northern part of Pangea, at a paleolatitude of c. 30–35 degrees° North. The Donguz Svita is considered to contain the *Eryosuchus* faunal assemblage, one of the four local faunal assemblages (all named after common temnospondyl genera) that have been recognized by Russian workers (Shishkin et al., 2000). Other taxa recovered from the Donguz Svita include capitosauroid and plagiosaurid temnospondyls (Schoch and Milner, 2000, 2014), a procolophonid (Spencer and Benton, 2000), kannemeyeriiform dicynodonts (Fröbisch, 2009), baurioid therocephalians (Battail and Surkov, 2000; Sues and Hopson, 2010), and among archosauromorphs the non-eucrocopod archosauriform *Sarmatosuchus ostchevi* (Gower and Sennikov, 1997; Ezcurra, 2016), the erythrosuchid *Uralosaurus magnus* (Gower and Sennikov, 2000; Ezcurra, 2016), the early eucrocopod archosauriform *Dorosuchus neoetus* (Sookias et al., 2014), and fragmentary archosaur remains ('*Vjushkovisaurus berdjanensis*' and '*Dongusia colorata*'; Gower and Sennikov, 2000).

Palynological data suggests that the Donguz Svita is of early to middle Anisian age (Niedźwiedzki et al., 2016), and this is consistent with the vertebrate fauna, with the presence of an erythrosuchid, kannemeyeriiform dicynodonts, and baurioid

therocephalians suggesting similarities to the *Cynognathus* Assemblage Zone of South Africa.

The holotype of *Spondylosoma absconditum* was collected at the Baum-Sanga locality of Rio Grande do Sul State, southern Brazil. This area was located in the mid southern hemisphere in the Middle Triassic, in the northern part of Pangea, at a paleolatitude of c. 50 degrees~~°~~ South. *Spondylosoma absconditum* comes from the *Dinodontosaurus* Assemblage Zone of the Pinheiros-Chiniquá Sequence (sensu Horn et al., 2014), which has been dated as Ladinian in age (Langer et al., 2007) but may be as young as Carnian (Marsicano et al., 2016). The associated faunal assemblage includes traversodontid and chiniquodontid cynodonts, kannemeyeriiform dicynodonts, the doswelliid *Archeopelta arborensis*, and the loricatan archosaurs *Prestosuchus chiniquensis* and *Decuriasuchus quartacolonia* (Langer at al., 2007; Desojo et al., 2011; França et al., 2011).

Localities for aphanosaurs ~~silendasaurians~~ therefore appear to span much of the Middle and early Late Triassic, with *T. rhadinus*~~*Teleocrater*~~, ~~*Yarasuchu*~~*Y. deccanensis*~~s~~, and ~~*Dongusuchus*~~ *D. efremovi* all apparently of early Middle Triassic age (Anisian), and ~~*Spondylosoma*~~ *S. absconditum* coming from the late Middle or earliest Late Triassic, although there is considerable uncertainty in the dating of individual stratigraphic units. They have been recovered as part of faunal assemblages that are typical for the Middle Triassic, including capitosauroid temnospondyls, kannemeyeriiform dicynodonts, baurioid therocephalians, allokotosaurian archosauromorphs, non-hyperodapedontine rhynchosaurs, erythrosuchids, and early eucrocopods. As yet, evidence for aphanosaurs ~~silendasaurians~~ in ~~Lower~~ Early or ~~younger~~ early Late Triassic strata is absent.

Teleocrater~~,~~ *rhadinus*, *Y. deccanensis*, and ~~*Yarasuchus*, and~~ *S. absconditum* ~~*Spondylosoma*~~ all come from a relatively paleogeographically restricted belt of localities in southern Pangea, clustering around a paleolatitude of 50 degrees~~°~~ South. By contrast, ~~*Dongusuchus*~~ *D. efremovi* comes from a biogeographically distinct and distant locality in the northern hemisphere, suggesting that aphanosaurs ~~silendasaurians~~ had a broad distribution across Pangea. Aphanosaurs ~~Silendasaurians~~ are some of the first crown archosaurs to appear in the fossil record, and their broad early paleogeographic distribution matches the pattern observed for ctenosauriscid poposauroids (Butler et al., 2011) and gracilisuchids (Butler et al., 2014). This provides further support for a broad distribution of archosaurs over much or all of Pangea from the end of the Early Triassic onwards, soon after the earliest evidence for the clade in the late Early Triassic (Butler et al., 2011, 2014; Nesbitt et al., 2011).

ACKNOWLEDGMENTS

Our work has been supported by a National Geographic Society grant 9606-14 (to SJN), NSF EAR-1337569 (to CAS), NSF EAR-1337291 (to KDA and SJN), a Marie Curie Career Integration Grant (PCIG14-GA-2013-630123 to RJB), a National Geographic Society Young Explorers grant 9467-14 (to MDE), and a grant from the Special Funds of the NHM (to PMB). We thank C. Saanane (University of Dar es Salaam) and A. Tibaijuka and L. Nampunju (Antiquities Division, Ministry of Natural Resources and Tourism) for assistance in arranging and carrying out fieldwork. We are grateful to M. Langer and S. Brusatte for their careful reviews. We thank L. Steel and A. C. Milner

(NHMUK) for access to the holotype and comparative specimens, ~~and~~ Matthew Lowe (UMCZ) for access to other material collected at the same locality and for access to F. R. Parrington's field notes, and ~~–~~H. Taylor (NHMUK Image Resources) provided the photographs of the holotype specimen. Scott Hartman provided the skeletal reconstruction in Fig. 1 and Mark Witten provided the full reconstruction provided in Fig. 29.

LITERATURE CITED

Abdala, F., P. J. Hancox, and J. Neveling. 2005. Cynodonts from the uppermost Burgersdorp Formation, South Africa, and their bearing on the biostratigraphy and correlation of the Triassic *Cynognathus* Assemblage Zone. Journal of Vertebrate Paleontology 25:192–199.

Appleby, R. M., A. J. Charig, C. B. Cox, K. A. Kermack, and L. B. H. Tarlo. 1967. Reptilia; pp. 695–731 in W. B. Harland, C. H. Holland, M. R. House, N. F. Hughes, A. B. Reynolds, M. J. S. Rudwick, G. E. Satterthwaite, L. B. H. Tarlo, and E. C. Willey (eds.), The Fossil Record. The Geological Society of London, London.

Arcucci, A. B. 1998. New information about dinosaur precursors from the Triassic Los Chanares fauna, La Rioja, Argentina. Journal of African Earth Sciences 27:9–10.

Bakker, R. T., and P. M. Galton. 1974. Dinosaur monophyly and a new class of vertebrates. Nature 248:168–172.

Bandyopadhyay, S. 1988. A kannemeyeriid dicynodont from the Middle Triassic Yerrapalli Formation. Philosophical Transactions of the Royal Society of London, Series B 320:185–233.

Bandyopadhyay S. 1989. The mammal-like reptile *Rechnisaurus* from the Triassic of India. Palaeontology 32:305–312.

Baron, M. G., D. B. Norman, and P. M. Barrett. 2017. A new hypothesis of dinosaur relationships and early dinosaur evolution. Nature 543:501–506.

Battail, B., and M. V. Surkov. 2000. Mammal-like reptiles from Russia; pp. 86–119 in M. J. Benton, M. A. Shishkin, D. M. Unwin, and E. N. Kurochkin (eds.), The Age of Dinosaurs in Russia and Mongolia. Cambridge University Press, Cambridge.

Benton, M. J. 1983. Dinosaur success in the Triassic; a noncompetitive ecological model. Quarterly Review of Biology 58:29–55.

Benton, M. J. 1999. *Scleromochlus taylori* and the origin of dinosaurs and pterosaurs. Philosophical Transactions of the Royal Society of London, Series B 354:1423–1446.

Benton, M. J. 2004. Origin and relationships of Dinosauria; pp. 7–19 in D. B. Weishampel, P. Dodson, and H. Osmólska (eds.), The Dinosauria, 2nd Edition. University of California Press, Berkeley.

Benton, M. J. 2010. Investigating evolutionary radiations; pp. 10–26 in M. Long, and Z. Zhou (eds.), Darwin's Heritage Today -- Proceedings of the Darwin 200 International Conference. Higher Education Press, Beijing.

Benton, M. J., and J. M. Clark. 1988. Archosaur phylogeny and the relationships of the Crocodylia; pp. 295–338 in M. J. Benton (ed.), The Phylogeny and Classification

Formatted: Font: (Default) Times New Roman

Formatted: Line spacing: Double

Formatted: Font: (Default) Times New Roman

of the Tetrapods, Volume 1: Amphibians, Reptiles, Birds. Clarendon Press, Oxford.

Bittencourt, J. S., A. B. Arcucci, C. A. Marsicano, and M. C. Langer. 2015. Osteology of the Middle Triassic archosaur *Lewisuchus admixtus* Romer (Chañares Formation, Argentina), its inclusivity, and relationships amongst early dinosauromorphs. Journal of Systematic Palaeontology 13:189–219.

Brochu, C. A. 1992. Ontogeny of the postcranium in crocodylomorph archosaurs. Unpublished M.A. thesis, The University of Texas at Austin, Austin, Texas, 340 pp.

Brochu, C. A. 1996. Closure of neurocentral sutures during crocodilian ontogeny: implications for maturity assessment in fossil archosaurs. Journal of Vertebrate Paleontology 16:49–62.

Brusatte, S. L., M. J. Benton, J. B. Desojo, and M. C. Langer. 2010a. The higher-level phylogeny of Archosauria (Tetrapoda: Diapsida). Journal of Systematic Palaeontology 8:3–47.

Brusatte, S. L., M. J. Benton, M. Ruta, and G. T. Lloyd. 2008a. The first 50 myr of dinosaur evolution: macroevolutionary pattern and morphological disparity. Biology Letters 4:733–736.

Brusatte, S. L., M. J. Benton, M. Ruta, and G. T. Lloyd. 2008b. Superiority, competition, and opportunism in the evolutionary radiation of dinosaurs. Science 321:1485–1488.

Brusatte, S. L., S. J. Nesbitt, R. B. Irmis, R. J. Butler, M. J. Benton, and M. A. Norell. 2010b. The origin and early radiation of dinosaurs. Earth-Science Reviews 101:68–100.

Butler, R. J., P. M. Barrett, R. L. Abel, and D. J. Gower. 2009. A possible ctenosauriscid archosaur from the Middle Triassic Manda Beds of Tanzania. Journal of Vertebrate Paleontology 29:1022–1031.

Butler, R. J., S. J. Nesbitt, A. J. Charig, D. J. Gower, and P. M. Barrett. 2017. *Mandasuchus tanyauchen* gen. et sp. nov., a pseudosuchian archosaur from the Manda Beds of Tanzania; pp. xxx-xxx in C. A. Sidor, and S. J. Nesbitt (eds.), Vertebrate and climatic evolution in the Triassic rift basins of Tanzania and Zambia. Society of Vertebrate Paleontology Memoir 17. Journal of Vertebrate Paleontology 37 (6, supplement).

Butler, R. J., S. L. Brusatte, M. Reich, S. J. Nesbitt, R. R. Schoch, and J. J. Hornung. 2011. The sail-backed reptile *Ctenosauriscus* from the latest Early Triassic of Germany and the timing and biogeography of the early archosaur radiation. PLoS One 6:e25693. DOI:10.1371/journal.pone.0025693

Butler, R. J., C. Sullivan, M. D. Ezcurra, J. Liu, A. Lecuona, and R. B. Sookias. 2014. New clade of enigmatic early archosaurs yields insights into early pseudosuchian phylogeny and the biogeography of the archosaur radiation. BMC Evolutionary Biology 14:128. DOI: http://www.biomedcentral.com/1471-2148/14/128

Cabreira, S. F., A. W. A. Kellner, S. Dias-da-Silva, L. R. da Silva, M. Bronzati, J. C. de Almeida Marsola, R. T. Müller, J. de Souza Bittencourt, B. J. A. Batista, and T.

Formatted: Font: (Default) Times New Roman

Raugust. 2016. A unique Late Triassic dinosauromorph assemblage reveals dinosaur ancestral anatomy and diet. Current Biology 26:3090–3095.

Charig, A. J. 1956. New Triassic archosaurs from Tanganyika including *Mandasuchus* and *Teleocrater*. Unpublished PhD dissertation, University of Cambridge, Cambridge, 503 pp. + 53 pls (two volumes).

Charig, A. J., J. Attridge, and A. W. Crompton. 1965. On the origin of the sauropods and the classification of the Saurischia. Proceedings of the Linnean Society of London 176:197–221.

Chatterjee, S. 1978. A primitive parasuchid (Phytosaur) reptile from the Upper Triassic Maleri Formation of India. Palaeontology 21:83–127.

Chatterjee, S. 1980. The evolution of rhynchosaurs. Mémoires de la Société géologique de France, nouvelle série 139:57–65.

Colbert, E. H. 1989. The Triassic dinosaur *Coelophysis*. Bulletin of the Museum of Northern Arizona 57:1–174.

Cope, E. D. 1869. Synopsis of the extinct Batrachia, Reptilia, and Aves of North America. Transactions of the American Philosophical Society 40:1–252.

Cruickshank, A. R. I. 1979. The ankle joint in some early archosaurs. South African Journal of Science 75:168–178.

de Queiroz, K., Gauthier, J. 1990. Phylogeny as a central principle in taxonomy: Phylogenetic definitions of taxon names. Systematic Zoology 39:307–322.

de Ricqlès, A., K. Padian, F. Knoll, and J. R. Horner. 2008. On the origin of high growth rates in archosaurs and their ancient relatives: complementary histological studies

Formatted: Font: (Default) Times New Roman

on Triassic archosauriforms and the problem of a "phylogenetic signal" in bone histology. Annales de Paléontologie 94:57–76.

Desojo, J. B., M. D. Ezcurra, and E. E. Kischlat. 2012. A new aetosaur genus (Archosauria: Pseudosuchia) from the early Late Triassic of southern Brazil. Zootaxa 3166:1–33.

Desojo, J. B., M. D. Ezcurra, and C. L. Schultz. 2011. An unusual new archosauriform from the Middle–Late Triassic of southern Brazil and the monophyly of Doswelliidae. Zoological Journal of the Linnean Society 161:839-871.

Dyke, G. J. 1998. Does archosaur phylogeny hinge on the ankle joint? Journal of Vertebrate Paleontology 18:558–562.

Dzik, J. 2003. A beaked herbivorous archosaur with dinosaur affinities from the early Late Triassic of Poland. Journal of Vertebrate Paleontology 23:556–574.

Ewer, R. F. 1965. The anatomy of the thecodont reptile *Euparkeria capensis* Broom. Philosophical Transactions of the Royal Society of London, Series B 248:379–435.

Ezcurra, M. D. 2006. A review of the systematic position of the dinosauriform archosaur *Eucoelophysis baldwini* Sullivan and Lucas, 1999 from the Upper Triassic of New Mexico, USA. Geodiversitas 28:649-684.

Ezcurra, M. D. 2016. The phylogenetic relationships of basal archosauromorphs, with an emphasis on the systematics of proterosuchian archosauriforms. PeerJ 4:e1778; DOI 10.7717/peerj.1778.

França, M. A. G., J. Ferigolo, and M. C. Langer. 2011. Associated skeletons of a new middle Triassic “Rauisuchia” from Brazil. *Naturwissenschaften* 98:389–395.

Formatted: Spanish (Argentina)

Fraser, N. C. 2006. Dawn of the Dinosaurs: Life in the Triassic. Indiana University Press, Bloomington, 307 pp.

Fröbisch, J. 2009. Composition and similarity of global anomodont-bearing tetrapod faunas. Earth-Science Reviews 95:119–157.

Furin, S., N. Preto, M. Rigo, G. Roghi, P. Gianolla, J. L. Crowley, and S. A. Bowring. 2006. High-precision U-Pb zircon age from the Triassic of Italy: implications for the Triassic time scale and the Carnian origin of calcareous nannoplankton and dinosaurs. Geology 34:1009-1012.

Galton, P. M. 2000. Are *Spondylosoma* and *Staurikosaurus* (Santa Maria Formation, Middle-Upper Triassic, Brazil) the oldest saurischian dinosaurs? Paläontologische Zeitschrift 74:393–423.

Gauthier, J. 1986. Saurischian monophyly and the origin of birds. Memoirs of the California Academy of Sciences 8:1–55.

Gauthier, J., and K. Padian. 1985. Phylogenetic, functional, and aerodynamic analyses of the origin of birds and their flight; pp. 185–197 in M. K. Hecht, J. H. Ostrom, G. Viohl, and P. Wellnhofer (eds.), The Beginning of Birds: Proceedings of the International Archaeopteryx Conference. Freunde des Jura Museums, Eichstätt.

Gauthier, J., and K. De Queiroz. 2001: Feathered dinosaurs, flying dinosaurs, crown dinosaurs, and the name "Aves"; pp. 7–41 in J. Gauthier and L. F. Gall (eds.), New Perspectives on the Origin and Early Evolution of Birds: Proceedings of the International Symposium in Honor of John H. Ostrom. Peabody Museum of Natural History, New Haven.

Goloboff, P. A., and S. A. Catalano. 2016. TNT version 1.5, including a full

Formatted: Indent: Left: 0", Hanging: 0.5", Line spacing: Double, No widow/orphan control, Don't adjust space between Latin and Asian text, Don't adjust space between Asian text and numbers

Formatted: Font: (Default) Times New Roman

Formatted: Widow/Orphan control, Adjust space between Latin and Asian text, Adjust space between Asian text and numbers

Formatted: Font: Times New Roman, 12 pt

Formatted: Font: Times New Roman, 12 pt

Formatted: Font: Times New Roman, 12 pt

Formatted: Font:

implementation of phylogenetic morphometrics. Cladistics 32:221–238.

Goloboff, P., J. Farris, and K. Nixon. 2008. TNT: a free program for phylogenetic analysis. Cladistics 24:774–786.

Gow, C. E. 1970. The palate in *Euparkeria*. Palaeontologia africana 13:61–62.

Gower, D. J. 1996. The tarsus of erythrosuchid archosaurs (Reptilia), and implications for early diapsid phylogeny. Zoological Journal of the Linnean Society 116:347–375.

Gower, D. J. 1997. The braincase of the early archosaurian reptile *Erythrosuchus africanus*. Journal of Zoology 242:557–576.

Gower, D. J. 1999. The cranial and mandibular osteology of a new rauisuchian archosaur from the Middle Triassic of southern Germany. Stuttgarter Beiträge zur Naturkunde, Serie B 280:1–49.

Gower, D. J. 2003. Osteology of the early archosaurian reptile *Erythrosuchus africanus* Broom. Annals of the South African Museum 110:1–84.

Gower, D. J., and R. Schoch. 2009. Postcranial anatomy of the rauisuchian archosaur *Batrachotomus kupferzellensis*. Journal of Vertebrate Paleontology 29:103–122.

Gower, D. J., and A. G. Sennikov. 1997. *Sarmatosuchus* and the early history of the Archosauria. Journal of Vertebrate Paleontology 17:60–73.

Gower, D. J., and A. G. Sennikov 2000. Early archosaurs from Russia; pp. 140–159 in M. J. Benton, M. A. Shishkin, D. M. Unwin, and E. N. Kurochkin (eds.), The Age of Dinosaurs in Russia and Mongolia. Cambridge University Press, Cambridge.

Griffin, C. T., and S. J. Nesbitt. 2016. The femoral ontogeny and long bone histology of the Middle Triassic (?late Anisian) dinosauriform *Asilisaurus kongwe* and

implications for the growth of early dinosaurs. Journal of Vertebrate Paleontology:e1111224. DOI: 10.1080/02724634.2016.1111224

Hancox, P. J. 2000. The Continental Triassic of South Africa. Zentralblatt für Geologie und Paläontologie Teil I, Heft 11–12, 1998:1285–1324.

Hancox, P. J., K. D. Angielczyk, and B. S. Rubidge. 2013. *Angonisaurus* and *Shansiodon*, dicynodonts (Therapsida, Anomodontia) from subzone C of the *Cynognathus* assemblage zone (Middle Triassic) of South Africa. Journal of Vertebrate Paleontology 33:655–676.

Horn, B., T. Melo, C. Schultz, R. Philipp, H. Kloss, and K. Goldberg. 2014. A new third-order sequence stratigraphic framework applied to the Triassic of the Paraná Basin, Rio Grande do Sul, Brazil, based on structural, stratigraphic and paleontological data. Journal of South American Earth Sciences 55:123-132.

Howie, A. A. 1970. A new capitosaurid labyrinthodont from East Africa. Palaentology 13:210–253.

Huene, F. v. 1938. Ein grosser Stagonolepide aus der jüngeren Trias Ostafrikas. Neues Jahrbuch für Geologie und Paläeontologie, Beilage-Bände Abt. B 80:264–278.

Huene, F. v. 1939. Ein kleiner Pseudosuchier und ein Saurischier aus den ostafrikanischen Mandaschichten. Neues Jahrbuch für Geologie und Paläeontologie, Beilage-Bände Abt. B 81:61–69.

Huene, F. v. 1942. Die fossilen Reptilien des südamerikanischen Gondwanalandes: Ergebnisse der Sauriergrabungen in Südbrasilien 1928/29: mit 64 Abbildungen im Text und 38 Tafeln. CH Beck'sche Verlagsbuchhandlung.

Hutchinson, J. R. 2001. The evolution of femoral osteology and soft tissue on the line to extant birds (Neornithes). Zoological Journal of the Linnean Society 131:169–197.

Ikejiri, T. 2012. Histology-based morphology of the neurocentral synchondrosis in *Alligator mississippiensis* (Archosauria, Crocodylia). The Anatomical Record 295:18–31.

Iordansky, N. 1964. The jaw muscles of the crocodiles and some relating structures of the crocodilian skull. Anatomischer Anzeiger 115:256–280.

Irmis, R. B. 2007. Axial skeleton ontogeny in the Parasuchia (Archosauria: Pseudosuchia) and its implications for ontogenetic determination in archosaurs. Journal of Vertebrate Paleontology 27:350–361.

Irmis, R. B., S. J. Nesbitt, K. Padian, N. D. Smith, A. H. Turner, D. Woody, and A. Downs. 2007. A Late Triassic dinosauromorph assemblage from New Mexico and the rise of dinosaurs. Science 317:358–361.

Juul, L. 1994. The phylogeny of basal archosaurs. Palaeontologia africana 31:1–38.

Langer, M. C. 2003. The pelvic and hind limb anatomy of the stem-sauropodomorph *Saturnalia tupiniquim* (Late Triassic, Brazil). PaleoBios 23:1–40.

Langer, M. C. 2004. Basal saurischians; pp. 25–46 in D. B. Weishampel, P. Dodson, and H. Osmólska (eds.), The Dinosauria, 2nd Edition. University of California Press, Berkeley.

Langer, M. C., and M. J. Benton. 2006. Early dinosaurs: A phylogenetic study. Journal of Systematic Palaeontology 4:309–358.

Langer, M. C., and J. Ferigolo. 2013. The Late Triassic dinosauromorph *Sacisaurus agudoensis* (Caturrita Formation; Rio Grande do Sul, Brazil): anatomy and affinities pp. 353–392 in S. J. Nesbitt, J. B. Desojo, and R. B. Irmis (eds.), Anatomy, Phylogeny, and Palaeobiology of Early Archosaurs and their Kin. The Geological Society, London, Special Volume 379.

Langer, M. C., J. S. Bittencourt, and C. L. Schultz. 2011. A reassessment of the basal dinosaur *Guaibasaurus candelariensis*, from the Late Triassic Caturrita Formation of south Brazil. Earth and Environmental Science Transactions of the Royal Society of Edinburgh 101:301–332.

Langer, M. C., M. A. G. França, and S. Gabriel. 2007a. The pectoral girdle and forelimb anatomy of the stem-sauropodomorph *Saturnalia tupiniquim* (Upper Triassic, Brazil). Special Papers in Palaeontology 77:113–137.

Langer, M. C., A. M. Ribeiro, C. L. Schultz, and J. Ferigolo. 2007b. The continental tetrapod-bearing Triassic of south Brazil. New Mexico Museum of History and Science Bulletin 41:201–218.

Langer, M. C., M. D. Ezcurra, J. S. Bittencourt, and F. E. Novas. 2010. The origin and early evolution of dinosaurs. Biological Reviews 85:55–110.

Laurenti, J. N. 1768. Specimen Medicum, Exhibens Synopsin reptilium Emendatam cum Experimentis circa Venena et Antidota Reptilium Austriacorum. 214 pp. J. T. N. de Trattnern, Vienna.

Formatted: Spanish (Argentina)

Laurenti, J. N. 1768. Specimen Medicum, Exhibens Synopsin reptilium Emendatam cum Experimentis circa Venena et Antidota Reptilium Austriacorum. 214 pp. J. T. N. de Trattnern, Vienna.

Formatted: Spanish (Argentina)

Lautenschlager, S., and J. B. Desojo. 2011. Reassessment of the Middle Triassic rauisuchian archosaurs *Ticinosuchus ferox* and *Stagonosuchus nyassicus*. Paläontologische Zeitschrift 85:357–381.

Li, C., X.-C. Wu, Y.-N. Cheng, T. Sato, and L. Wang. 2006. An unusual archosaurian from the marine Triassic of China. Naturwissenschaften 93:200–206.

Linnaeus, C. 1758. Systema Naturae per Raegna Tria Naturae. Volume 1. Regnum Animale. 10th [photographic facsimile] ed. 823 pp. Trustees, British Museum (Natural History), London.

Lucas, S. G. 1998. Global Triassic tetrapod biostratigraphy and biochronology. Palaeogeography, Palaeoclimatology, Palaeoecology 143:347–384.

Madsen, J. H., Jr. 1976. *Allosaurus fragilis*: a revised osteology. Utah Geological Survey Bulletin 109:1–163.

Marsicano, C. A., R. B. Irmis, A. C. Mancuso, R. Mundil, and F. Chemale. 2016. The precise temporal calibration of dinosaur origins. Proceedings of the National Academy of Sciences 113:509–513.

Martínez, R. N., C. Apaldetti, G. A. Correa, and D. Abelín. 2016. A Norian Lagerpetid Dinosauromorph from the Quebrada Del Barro Formation, Northwestern Argentina. Ameghiniana 53:1–13.

Martinez, R. N., P. C. Sereno, O. A. Alcober, C. E. Colombi, P. R. Renne, I. P. Montañez, and B. S. Currie. 2011. A basal dinosaur from the dawn of the dinosaur era in southwestern Pangaea. Science 331:206–210.

Moody, R. T. J., and D. Naish. 2010. Alan Jack Charig (1927–1997): an overview of his academic accomplishments and role in the world of fossil reptile research; pp. 89–

109 in R. T. J. Moody, E. Buffetaut, D. Naish, and D. M. Martill (eds.), Dinosaurs and Other Extinct Saurians: A Historical Perspective. Geological Society, London, Special Publications, 343.

Nesbitt, S. J. 2003. *Arizonasaurus* and its implications for archosaur divergences. . Proceedings of the Royal Society of London, B 270 (Supplement 2):S234–S237.

Nesbitt, S. J. 2005a. The osteology of the Middle Triassic pseudosuchian archosaur *Arizonasaurus babbitti*. Historical Biology 17:19–47.

Nesbitt, S. J. 2005b. A new archosaur from the upper Moenkopi Formation (Middle Triassic) of Arizona and its implications for rauisuchian phylogeny and diversification. Neues Jahrbuch für Geologie und Paläeontologie Monatshefte 2005:332–346.

Nesbitt, S. J. 2007. The anatomy of *Effigia okeeffeae* (Archosauria, Suchia), theropod-like convergence, and the distribution of related taxa. Bulletin of the American Museum of Natural History 302:1–84.

Nesbitt, S. J. 2011. The early evolution of archosaurs: relationships and the origin of major clades. Bulletin of the American Museum of Natural History 352:1–292.

Nesbitt, S. J., and R. J. Butler. 2012. Redescription of the archosaur *Parringtonia gracilis* from the Middle Triassic Manda Beds of Tanzania, and the antiquity of Erpetosuchidae. Geological Magazine 150:225–238.

Nesbitt, S. J., R. J. Butler, and D. J. Gower. 2013b. A new archosauriform (Reptilia: Diapsida) from the Manda beds (Middle Triassic) of southwestern Tanzania. PLoS One:8(9): e72753. doi:10.1371/journal.pone.0072753.

Nesbitt, S. J., J. Liu, and C. Li. 2011. A sail-backed suchian from the Heshanggou Formation (Early Triassic: Olenekian) of China. Earth and Environmental Science Transactions of the Royal Society of Edinburgh 101:271–284.

Nesbitt, S. J., M. R. Stocker, B. J. Small, and A. Downs. 2009c. The osteology and relationships of *Vancleavea campi* (Reptilia: Archosauriformes). Zoological Journal of the Linnean Society 157:814–864.

Nesbitt, S. J., P. M. Barrett, S. Werning, C. A. Sidor, and A. J. Charig. 2013a. The oldest dinosaur? A Middle Triassic dinosauriform from Tanzania. Biology Letters 9:20120949.

Nesbitt, S. J., C. A. Sidor, K. D. Angielczyk, R. M. H. Smith, and L. A. Tsuji. 2014. A new archosaur from the Manda beds (Anisian: Middle Triassic) of southern Tanzania and its implications for character optimizations at Archosauria and Pseudosuchia. Journal of Vertebrate Paleontology 34:1357–1382.

Nesbitt, S. J., J. J. Flynn, A. C. Pritchard, J. M. Parrish, L. Ranivoharimanana, and A. R. Wyss. 2015. Postcranial osteology of *Azendohsaurus madagaskarensis* (?Middle to Upper Triassic, Isalo Group, Madagascar) and its systematic position among stem archosaur reptiles. Bulletin of the American Museum of Natural History 398:1–126.

Nesbitt, S. J., R. B. Irmis, W. G. Parker, N. D. Smith, A. H. Turner, and T. Rowe. 2009b. Hindlimb osteology and distribution of basal dinosauromorphs from the Late Triassic of North America. Journal of Vertebrate Paleontology 29:498–516.

Nesbitt, S. J., C. A. Sidor, R. B. Irmis, K. D. Angielczyk, R. M. H. Smith, and L. A. Tsuji. 2010. Ecologically distinct dinosaurian sister group shows early diversification of Ornithodira. Nature 464:95–98.

Nesbitt, S. J., N. D. Smith, R. B. Irmis, A. H. Turner, A. Downs, and M. A. Norell. 2009a. A complete skeleton of a Late Triassic saurischian and the early evolution of dinosaurs. Science 326:1530–1533.

Nesbitt, S. J., M. R. Stocker, W. G. Parker, T. A. Wood, C. A. Sidor, and K. D. Angielczyk. 2017a. The braincase and endocast of *Parringtonia gracilis*, a Middle Triassic suchian (Archosaur: Pseudosuchia); pp. xxx-xxx in C. A. Sidor, and S. J. Nesbitt (eds.), Vertebrate and climatic evolution in the Triassic rift basins of Tanzania and Zambia. Society of Vertebrate Paleontology Memoir 17. Journal of Vertebrate Paleontology 37 (6, supplement).

Nesbitt, S. J., R. J. Butler, M. D. Ezcurra, P. M. Barrett, M. R. Stocker, K. D. Angielczyk, R. M. H. Smith, C. A. Sidor, G. Niedźwiedzki, A. Sennikov, and A. J. Charig. 2017b~~in press~~. The earliest bird-line archosaurs and the assembly of the dinosaur body plan. Nature.

Niedźwiedzki, G., A. Sennikov, and S. L. Brusatte. 2016. The osteology and systematic position of *Dongusuchus efremovi* Sennikov, 1988 from the Anisian (Middle Triassic) of Russia. Historical Biology 28:550–570, DOI: 10.1080/08912963.2014.992017.

Novas, F. E. 1994. New information on the systematics and postcranial skeleton of *Herrerasaurus ischigualastensis* (Theropoda: Herrerasauridae) from the Ischigualasto Formation (Upper Triassic) of Argentina. Journal of Vertebrate

Formatted: Font: (Default) Times New Roman

Formatted: Font: (Default) Times New Roman

Formatted: Font: (Default) Times New Roman

Paleontology 13:400–423.

Novas, F. E. 1996. Dinosaur monophyly. Journal of Vertebrate Paleontology 16:723–741.

Ochev, V. G. 1982. Pseudosuchia from the Middle Triassic of the southern Ural Forelands. Paleontologicheskii Zhurnal 1982:96–102. [Russian]

Padian, K. 2008. The Early Jurassic pterosaur *Dorygnathus banthensis* (Theodori, 1830) and the Early Jurassic pterosaur *Campylognathoides* Strand, 1928. Special Papers in Palaeontology 80:1–107.

Parrish, J. M. 1993. Phylogeny of the Crocodylotarsi, with reference to archosaurian and crurotarsan monophyly. Journal of Vertebrate Paleontology 13:287–308.

Piechowski, R., and J. Dzik. 2010. The axial skeleton of *Silesaurus opolensis*. Journal of Vertebrate Paleontology 30:1127–1141.

Rauhut, O. W. M. 2003. The interrelationships and evolution of basal theropod dinosaurs. Special Papers in Palaeontology 69:1–213.

Rogers, R. R., C. C. Swisher, III, P. C. Sereno, A. M. Monetta, C. A. Forster, and R. N. Martínez. 1993. The Ischigualasto tetrapod assemblage (Late Triassic, Argentina) and $^{40}Ar/^{39}Ar$ dating of dinosaur origins. Science 260:794-797.

Romer, A. S. 1972. The Chañares (Argentina) Triassic reptile fauna. XIV. *Lewisuchus admixtus*, a further thecodont from the Chañares beds. Breviora 390:1–13.

Rubidge, B. S. 2005. Re-uniting lost continents - fossil reptiles from the ancient Karoo and their wanderlust. South African Journal of Geology 108:135–172.

Schoch, R. R, and A. R. Milner. 2000. Stereospondyli. Handbuch der Paläoherpetologie - Encyclopedia of Paleoherpetology 3B:1–203.

Schoch, R. R., and A. R. Milner. 2014. Temnospondyli I. Handbook of Paleoherpetology 3A2:1–149.

Schultz, C. L., M. C. Langer, and F. C. Montefeltro. A new rhynchosaur from south Brazil (Santa Maria Formation) and rhynchosaur diversity patterns across the Middle-Late Triassic boundary. Paläontologische Zeitschrift:1-17.

Sen, K. 2003. *Pamelaria dolichotrachela*, a new prolacertid reptile from the Middle Triassic of India. Journal of Asian Earth Sciences 21:663–681.

Sen, K. 2005. A new rauisuchian archosaur from the Middle Triassic of India. Palaeontology 48:185–196.

Sengupta, D. S. 2003. Triassic temnospondyls of the Pranhita–Godavari basin, India. Journal of Asian Earth Sciences 21:655–662.

Sennikov, A. 1988. New rauisuchids from the Triassic of European USSR. Palaeontological Journal 22:120–124.

Sennikov, A. G. 1990. New data on the rauisuchids of eastern Europe. Palaeontological Journal 24:1–12.

Sennikov, A. G. 2012. The first ctenosauriscid (Reptilia: Archosauromorpha) from the Lower Triassic of Eastern Europe. Paleontological Journal 46:499–511.

Sereno, P. C. 1991. Basal archosaurs: phylogenetic relationships and functional implications. Society of Vertebrate Paleontology Memoir 2:1–53.

Sereno, P. C. 1994. The pectoral girdle and forelimb of the basal theropod *Herrerasaurus ischigualastensis*. Journal of Vertebrate Paleontology 13:425–450.

Sereno, P. C., and A. B. Arcucci. 1994a. Dinosaurian precursors from the Middle Triassic of Argentina: *Marasuchus lilloensis*, gen. nov. Journal of Vertebrate Paleontology 14:53-73.

Sereno, P. C., and A. B. Arcucci. 1994b. Dinosaurian precursors from the Middle Triassic of Argentina: *Lagerpeton chanarensis*. Journal of Vertebrate Paleontology 13:385–399.

Sereno, P. C., and F. E. Novas. 1994. The skull and neck of the basal theropod *Herrerasaurus ischigualastensis*. Journal of Vertebrate Paleontology 13:451–476.

Sereno, P. C., R. N. Martínez, and O. A. Alcober. 2013. Osteology of Eoraptor lunensis (Dinosauria, Sauropodomorpha). Society of Vertebrate Paleontology Memoir 12:83–179.

Shishkin, M. A., V. G. Ochev, V. R. Lozovskii, and I. V. Novikov. 2000. Tetrapod biostratigraphy of the Triassic of Eastern Europe; pp. 120–139 in M. J. Benton, M. A. Shishkin, D. M. Unwin, and E. N. Kurochkin (eds.), The Age of Dinosaurs in Russia and Mongolia. Cambridge University Press, Cambridge.

Smith, R. M. H., C. A. Sidor, K. D. Angielczyk, S. J. Nesbitt, and N. J. Tabor. 2017. Taphonomy and paleoenvironments of Middle Triassic bone accumulations in the Lifua Member of the Manda Beds, Songea Group (Ruhuhu Basin), Tanzania; pp. xxx-xxx in C. A. Sidor, and S. J. Nesbitt (eds.), Vertebrate and climatic evolution in the Triassic rift basins of Tanzania and Zambia. Society of Vertebrate Paleontology Memoir 17. Journal of Vertebrate Paleontology 37 (6, supplement).

Sookias, R. B., R. J. Butler, and R. B. Benson. 2012. Rise of dinosaurs reveals major body-size transitions are driven by passive processes of trait evolution.

Proceedings of the Royal Society of London B 279:2180–2187. DOI:10.1098/rspb.2011.2441

Sookias, R. B., A. G. Sennikov, D. J. Gower, and R. J. Butler. 2014. The monophyly of Euparkeriidae (Reptilia: Archosauriformes) and the origins of crown Archosauria: a revision of *Dorosuchus neoetus* from the Middle Triassic of Russia. Palaeontology 57:1177–1202.

Spencer, P. S., and M. J. Benton. 2000. Procolophonids from the Permo-Triassic of Russia; pp. 160–176 in M. J. Benton, M. A. Shishkin, D. M. Unwin, and E. N. Kurochkin (eds.), The Age of Dinosaurs in Russia and Mongolia. Cambridge University Press, Cambridge.

Stocker, M. R., S. J. Nesbitt, K. E. Criswell, W. G. Parker, L. M. Witmer, T. B. Rowe, and M. A. Brown. 2016. Iterative convergence across the body plans of archosauromorphs and their dinosaurian descendants. Current Biology. http://dx.doi.org/10.1016/j.cub.2016.07.066

Stockley, G. M. 1932. The geology of the Ruhuhu coalfields, Tanganyika Territory. Quarterly Journal of the Geological Society of London 88:610–622.

Sues, H.-D., and N. C. Fraser. 2010. Triassic Life on Land: The Great Transition. Columbia University Press, New York, 224 pp.

Sues, H.-D., and J. A. Hopson. 2010. Anatomy and phylogenetic relationships of *Boreogomphodon jeffersoni* (Cynodontia: Gomphodontia) from the Upper Triassic of Virginia. Journal of Vertebrate Paleontology 30:1202–1220.

Turner, A. H., and S. J. Nesbitt. 2013. Body size evolution during the Triassic archosauriform radiation; pp. 573–597 in S. J. Nesbitt, J. B. Desojo, and R. B.

Irmis (eds.), Anatomy, Phylogeny, and Palaeobiology of Early Archosaurs and their Kin. The Geological Society, London, Special Volume 379.

Walker, A. D. 1990. A revision of *Sphenosuchus acutus* Haughton, crocodylomorph reptile from the Elliot Formation (Late Triassic or Early Jurassic) of South Africa. Philosophical Transactions of the Royal Society of London, Series B 330:1–120.

Weinbaum, J. C. 2011. The skull of *Postosuchus kirkpatricki* (Archosauria: Paracrocodyliformes) from the Upper Triassic of the United States. PaleoBios 30:18–44.

Weinbaum, J. C. 2013. Postcranial skeleton of *Postosuchus kirkpatricki* (Archosauria: Paracrocodylomorpha), from the Upper Triassic of the United States; pp. 525–553 in S. J. Nesbitt, J. B. Desojo, and R. B. Irmis (eds.), Anatomy, Phylogeny and Palaeobiology of Early Archosaurs and their Kin. The Geological Society, London, Special Volume 379.

Weinbaum, J. C., and A. Hungerbühler. 2007. A revision of *Poposaurus gracilis* (Archosauria: Suchia) based on two new specimens from the Late Triassic of the southwestern U.S.A. Paläontologische Zeitschrift 81:131–145.

Welles, S. P. 1947. Vertebrates from the Upper Moenkopi Formation of the Northern Arizona. University of California Publications in Geological Science 27:241–294.

Wild, R. 1973. Die Triasfauna der Tessiner Kalkalpen XXII. *Tanystropheus longobardicus* (Bassani). Schweizerische Paläontologische Abhandlungen 95:1–162.

Wilson, J. A. 1999. A nomenclature for vertebral laminae in sauropods and other saurischian dinosaurs. Journal of Vertebrate Paleontology 19:639–653.

Wilson, J. A., M. D. D'Emic, T. Ikejiri, E. M. Moacdeih, and J. A. Whitlock. 2011. A nomenclature for vertebral fossae in sauropods and other saurischian dinosaurs. PLoS One 6:e17114. doi:10.1371/journal.pone.0017114.

Wu, X. 1981. The discovery of a new thecodont from north-east Shensi. Vertebrata PalAsiatica 19:122–132. [Chinese]

Wynd, B. M., C. A. Sidor, M. R. Whitney, and B. R. Peecook. 2017. The first occurrence of *Cynognathus* in Tanzania and Zambia, with biostratigraphic implications for the age of Triassic strata in southern Pangea; pp. xxx–xxx in C. A. Sidor and S. J. Nesbitt (eds.), Vertebrate and climatic evolution in the Triassic rift basins of Tanzania and Zambia. Society of Vertebrate Paleontology Memoir 17. Journal of Vertebrate Paleontology 37 (6, supplement).

Submitted October 13, 2016; accepted Month DD, YYYY

FIGURE CAPTIONS

FIGURE 1. Geographic position of the type locality of *Teleocrater rhadinus* (modified from Nesbitt et al., 2014). Reconstruction of skeleton completed by Scott Hartman. Scale bar equals 25 cm. [planned for column width]

FIGURE 2. Cranial elements referred to *Teleocrater rhadinus*. Left maxilla (NMT RB495) in **A**, lateral view; **B**, medial view; **C**, ventral view and close-up of the only

maxillary tooth in **D**, medial view. Right frontal (NMT RB496) in **E**, dorsal view; **F**, ventral view; **G**, lateral view. Left quadrate (NMT RB493) in **H**, medial view, **I**, lateral view; **J**, ventral view; **K**, posterior view; **L**, anterior view. Scale bar equals 1 cm **A–D**, **F–L** and 1 mm in **E**. **Abbreviations**: **a.**, articulates with; **anf**, antorbital fenestra; anfo, antorbital fossa; **cr**, crest; **d**, depression; **fm**, foramen; **fo**, fossa; **lc**, lateral condyle **mc**, medial condyle; **ml**, midline; **na/pmx**, nasal or premaxilla; **ofo**, orbital fossa; **om**, orbital margin; **pa**, parietal; **pal**, palatine; **pf/po**, postfrontal or postorbital; **pp**, palatal process canal; **prf**, prefrontal; **ptp**, pterygoid process; **qf**, quadrate/quadratojugal foramen; **qh**, quadrate head; **qj**, quadratojugal; **stfo**, supratemporal fossa; **t**, tooth. [planned for page width]

FIGURE 3. Selected presacral vertebrae of the holotype of *Teleocrater rhadinus* (NHMUK PV R6795). Anterior cervical vertebra ('CeA') in **A**, left lateral view; **B**, right lateral view; **C**, ventral view; **D**, dorsal view; **E**, posterior view; **F**, anterior view. Middle cervical vertebra ('CeB') in **G**, left lateral view; **H**, right lateral view; **I**, ventral view; **J**, dorsal view; **K**, posterior view; **L**, anterior view. Posterior cervical vertebra ('DB') in **M**, left lateral view; **N**, right lateral view; **O**, ventral view; **P**, dorsal view; **Q**, posterior view; **R**, anterior view. Middle trunk vertebra ('DD') in **S**, left lateral view; **T**, right lateral view; **U**, ventral view; **V**, dorsal view; **W**, posterior view; and **X**, anterior view. Scale bar equals 1 cm. Arrows indicate anterior direction. **Abbreviations**: **dia**, diapophysis; **epi**, epipophysis; **nc**, neural canal; **ns**, neural spine; **par**, parapophysis; **poz**, postzygapophysis; **prz**, prezygapophysis. [planned for page width]

FIGURE 4. Axis (NMT RB504) referred to *Teleocrater rhadinus*. **A**, left lateral view; **B**, right lateral view; **C**, anterior view; **D**, posterior view; **E**, ventral view. Scale bar equals 1 cm. **Abbreviations**: **a.**, articulates with; **atl**, atlas; **axi**, axis intercentrum; **natl**, neural arch of the atlas; **epi**, epipophysis; **nc**, neural canal; **ns**, neural spine; **poz**, postzygapophysis; **prz**, prezygapophysis; **r**, ridge. [planned for column width]

FIGURE 5. Anterior cervical vertebrae referred to *Teleocrater rhadinus*. NMT RB505 in **A**, left lateral view; **B**, right lateral view; **C**, anterior view; **D**, posterior view; **E**, ventral view. NMT RB506 in **F**, right lateral view. Scale bar equals 1 cm. **Abbreviations**: **dia**, diapophysis; **epi**, epipophysis; **ex**, expansion; **nc**, neural canal; **ns**, neural spine; **par**, parapophysis; **poz**, postzygapophysis; **prz**, prezygapophysis. [planned for column width]

FIGURE 6. Middle cervical vertebrae referred to *Teleocrater rhadinus*. NMT RB511 in **A**, left lateral view; **B**, right lateral view; **C**, ventral view; **D**, anterior view; **E**, posterior view. NMT RB512 in **F**, left lateral view; **G**, right lateral view; **H**, ventral view; **I**, anterior view; **J**, posterior view. Scale bars equal 1 cm. **Abbreviations**: **dia**, diapophysis; **epi**, epipophysis; **ex**, expansion; **nc**, neural canal; **ns**, neural spine; **par**, parapophysis; **poz**, postzygapophysis; **prz**, prezygapophysis; **r**, ridge. [planned for column width]

FIGURE 7. Posterior cervical vertebra (NMT RB514) referred to *Teleocrater rhadinus*. **A**, left lateral view; **B**, right lateral view; **C**, ventral view; **D**, anterior view; **E**, posterior view. Scale bar equals 1 cm. **Abbreviations**: **dia**, diapophysis; **ex**, expansion; **fa**, facet;

nc, neural canal; **ns**, neural spine; **par**, parapophysis; **poz**, postzygapophysis; **prz**, prezygapophysis. [planned for column width]

FIGURE 8. The vertebral column of the holotype of *Teleocrater rhadinus* (NHMUK PV R6795). **A–B** cervical vertebrae in left lateral (top) and right lateral (bottom) views; **C–I**, anterior to middle trunk vertebrae in left lateral (top) and right lateral (bottom) views; **J–K**, posterior trunk vertebrae in left lateral (top) and right lateral (bottom) views; **L–M**, anterior caudal vertebrae in left lateral (top) and right lateral (bottom) views; **N–W**, middle to distal caudal vertebrae in left lateral (top) and right lateral (bottom) views. Scale bar equals 1 cm. Arrows indicate anterior direction. [planned for page width]

FIGURE 9. Posterior trunk vertebrae (NMT RB516) referred to *Teleocrater rhadinus*. **A**, left lateral view; **B**, right lateral view; **C**, posterior view; **D**, ventral view; **E**, dorsal view. Scale bar equals 1 cm. **Abbreviations**: **dia**, diapophysis; **hyp**, hypantrum; **hys**, hyposphene; **nc**, neural canal; **ns**, neural spine; **par**, parapophysis; **poz**, postzygapophysis; **prz**, prezygapophysis. [planned for column width]

FIGURE 10. Second sacral vertebra (NMT RB519) referred to *Teleocrater rhadinus*. **A**, anterior view; **B**, posterior view; **C**, ventral view. Scale equals 1 cm. **Abbreviations**: **nc**, neural canal; **ns**, neural spine; **poz**, postzygapophysis; **prz**, prezygapophysis; **sr**, sacral rib; **srp**, sacral rib process. [planned for page width]

FIGURE 11. Distal caudal vertebrae of the holotype of *Teleocrater rhadinus* (NHMUK PV R6795). **A–E**, in left lateral (top) and right lateral (bottom) views. Scale bar equals 1 cm. Arrows indicate anterior direction. [planned for column width]

FIGURE 12. Ribs of the holotype of *Teleocrater rhadinus* (NHMUK PV R6795). Partial trunk rib in **A**, anterior view; **B**, posterior view; **C**, lateral view. Left partial cervical rib in **E**, lateral view; **F**, medial view. **G**, metatarsal in three views. Scale bars equal 1 cm. **Abbreviation**: **ap**, anterior process. [planned for column width]

FIGURE 13. Pectoral girdle elements of *Teleocrater rhadinus*. Partial right scapula (NHMUK PV R6795) in **A**, lateral view; **B**, posterior view; **C**, medial view. Partial right scapula (NMT RB480) in **D**, lateral view; **E**, posterior view; **F**, medial view. Partial left coracoid (NHMUK PV R6795) in **G**, lateral view; **H**, posterior view; **I**, medial view. Scale bars equal 1 cm. **Abbreviations**: **a.**, articulates with; **ac**, acromion; **cf**, coracoid foramen; **co**, coracoid; **gl**, glenoid; **no**, notch; **r**, ridge; **sc**, scapula. [planned for column width]

FIGURE 14. Humeri referred to *Teleocrater rhadinus*. Left humerus (NMT RB476) in **A**, proximal view; **B**, anterior view; **C**, lateral view; **D**, posterior view; **E**, medial view; **F**, distal view. Left humerus (NMT RB477) in **G**, proximal view; **H**, anterior view; **I**, lateral view; **J**, posterior view; **K**, medial view; **L**, distal view. Scale bars equal 1 cm. **Abbreviations**: **dp**, deltopectoral crest; **gr**, groove; **hh**, humeral head; **mtu**, medial tuberocity; **sp**, supinator process. [planned for page width]

FIGURE 15. Distal half of a left humerus (NHMUK PV R6796) referred to *Teleocrater rhadinus*. **A**, posterior view; **B**, anterior view; **C**, distal view. Scale bar equals 1 cm. **Abbreviations**: **gr**, groove; **sp**, supinator process. [planned for column width]

FIGURE 16. Ulna and radius of the holotype of *Teleocrater rhadinus* (NHMUK PV R6795). Right ulna in **A**, proximal view; **B**, posteromedial view; **C**, posterolateral view; **D**, anterolateral view; **E**, anteromedial view; **F**, distal view. Right radius in **G**, proximal view; **H**, posteromedial view; **I**, posterolateral view; **J**, anterolateral view; **K**, anteromedial view; **L**, distal view. Scale bar equals 1 cm. **Abbreviations**: **ol**, olecranon process; **r**, ridge. [planned for column width]

FIGURE 17. Left distal half of the radius of the holotype of *Teleocrater rhadinus* (NHMUK PV R6795). **A**, posteromedial view; **B**, anterolateral view. Scale bar equals 1 cm. **Abbreviation**: **r**, ridge. [planned for column width]

FIGURE 18. Right metacarpal ?II (NMT RB484) referred to *Teleocrater rhadinus*. **A**, dorsal view; **B**, lateral view; **C**, ventral view; **D**, medial view; **E**, proximal view; **F**, distal view. Scale bar equals 1 cm. [planned for column width]

FIGURE 19. Partial left ilium of the holotype of *Teleocrater rhadinus* (NHMUK PV R6795) (**A**–**D**) and a referred partial left ilium (NMT RB489) (**E**–**F**). NHMUK PV R6795 in **A**, dorsal view; **B**, anterior view; **C**, lateral view; **D**, medial view and NMT

RB489 in **E**, lateral view; **F**, medial view. Scale bars equal 1 cm. Arrows indicate anterior direction. **Abbreviations**: **a.**, articulates with; **ace**, acetabulum; **ap**, anterior process; **ip**, ischial peduncle; no, notch; **pp**, pubic peduncle; **sac**, supra-acetabular crest; **sr1**, first sacral rib; **sr2**, second sacral rib; **srv**, rugose subvertical ridge. [planned for column width]

FIGURE 20. Complete left ischium of *Teleocrater rhadinus* (NMT RB479) in **A**, lateral view; **B**, dorsal view; **C**, distal view; **D**, medial view. Scale bar equals 1 cm. **Abbreviations**: **a.**, articulates with; **gr**, groove; **il**, ilium; **is**, ischium; **pu**, pubis. [planned for column width]

FIGURE 21. Femora of the holotype of *Teleocrater rhadinus* (NHMUK PV R6795). Right femur in **A**, proximal view; **B**, anterolateral view; **C**, posterolateral view; **D**, posteromedial view; **E**, anteromedial view; **F**, distal view. Left femur in **G**, proximal view; **H**, anterolateral view; **I**, posterolateral view; **J**, posteromedial view; **K**, anteromedial view; **L**, distal view. Scale bars equal 5 cm. Arrows indicate anterior direction. **Abbreviations**: **alt**, anterolateral tuber; **ctf**, crista tibiofibularis; **d**, depression; **ft**, fourth trochanter; **g**, groove; **mic**, M. iliotrochantericus caudalis scar; **mie**, M. iliofemoralis externus scar; **r**, ridge; **sc,** scar. [planned for page width]

FIGURE 22. Referred right femur (NMT RB498) of *Teleocrater rhadinus* in **A**, proximal view; **B**, anterolateral view; **C**, posterolateral view; **D**, posteromedial view; **E**, anteromedial view; **F**, distal view. Scale bar equals 1 cm. Arrows indicate anterior

direction. **Abbreviations**: **alt**, anterolateral tuber; **cfb**, M. caudofemoralis brevis insertion scar; **ctf**, crista tibiofibularis; **d**, depression; **dltp**, posterior portion of the dorsolateral trochanter; **g**, groove; **mic**, M. iliotrochantericus caudalis scar; **mie**, M. iliofemoralis externus scar; **r**, ridge; **sc,** scar; **ts**, trochanteric shelf. [planned for column width]

FIGURE 23. The femoral scars on the proximal portion of the femur of *Teleocrater rhadinus*. Proximal end of the right femur (NHMUK PV R6795) in posterolateral view **A**, photo; **B**, interpretational drawing. Proximal end of the right femur (NMT RB498) in anteromedial view **C**, photo; **D**, interpretational drawing. Scale bars equal 1 cm. **Abbreviations**: **ail**, anterior intermuscular line; **als**, anterolateral scar; **alt**, anterolateral tuber; **cfb**, M. caudofemoralis brevis insertion scar; **d**, depression; **dltp**, posterior portion of the dorsolateral trochanter; **ft**, fourth trochanter; **mic**, M. iliotrochantericus caudalis scar; **mie**, M. iliofemoralis externus scar; **sc,** scar. [planned for column width]

FIGURE 24. Tibiae of the holotype of *Teleocrater rhadinus* (NHMUK PV R6795). Left tibia in **A**, proximal view; **B**, lateral view; **C**, posterior view; **D**, medial view; **E**, anterior view; **F**, distal view. Right tibia in **G**, proximal view; **H**, lateral view; **I**, posterior view; **J**, anterior view; **K**, distal view; **L**, distal view. Scale bars equal 5 cm. Arrows indicate anterior direction. **Abbreviations**: **cc**, cnemial crest; **ill**, internal lateral ligament; **Mpit**, M. puboischiadictibialis; **Mta**, M. tibialis anterior; **r**, ridge; **sc,** scar. [planned for page width]

Formatted: Font: Not Bold

FIGURE 25. Left fibula of the holotype of *Teleocrater rhadinus* (NHMUK PV R6795). **A**, proximal view; **B**, lateral view; **C**, posterior view; **D**, medial view; **E**, anterior view; **F**, distal view. Scale bar equals 5 cm. **Abbreviations**: d, depression; **ifc**, iliofibularis crest; **r**, ridge. [planned for column width]

FIGURE 26. Referred right calcaneum (NMT RB490) of *Teleocrater rhadinus* in **A**, proximal view; **B**, distal view; **C**, posterior view; **D**, anterior view; **E**, lateral view. Scale bar equals 1 cm. **Abbreviations**: **4t**, fourth tarsal; **a.**, articulates with; **as**, astragalus; **fi**, fibula; **ga**, gap; **tu**, tuber. [planned for column width]

FIGURE 27. Other elements that were found with the holotype of *Teleocrater rhadinus* (NHMUK PV R6795). **A–C**, phalanges in dorsal (top) and ventral (bottom) views. **D**, fourth metatarsal in three views. **E**, third metatarsal in three views. Scale bars equal 1 cm. [planned for column width]

FIGURE 28. Phylogenetic relationships of *Teleocrater rhadinus* among archosauriform reptiles. Strict consensus trees (some taxa collapsed into larger clades) based on the analyses of **A**, Nesbitt (2011) and **B**, the dataset of Ezcurra (2016). Full tree in Nesbitt et al.~~,~~ (2017b)~~in review~~. [planned for column width]

FIGURE 29. Life reconstruction of *Teleocrater rhadinus* feasting on *Cynognathus*. The large dicynodont *Dolichuranus* is seen in the background. Copyright: Mark Witton/Natural History Museum. [planned for page width]

Formatted: Font: Not Bold

Formatted: Font: Italic

Formatted: Left, Widow/Orphan control

Formatted: Font: Italic

Formatted: Font: Italic

Formatted: Font: (Default) Times New Roman, 12 pt

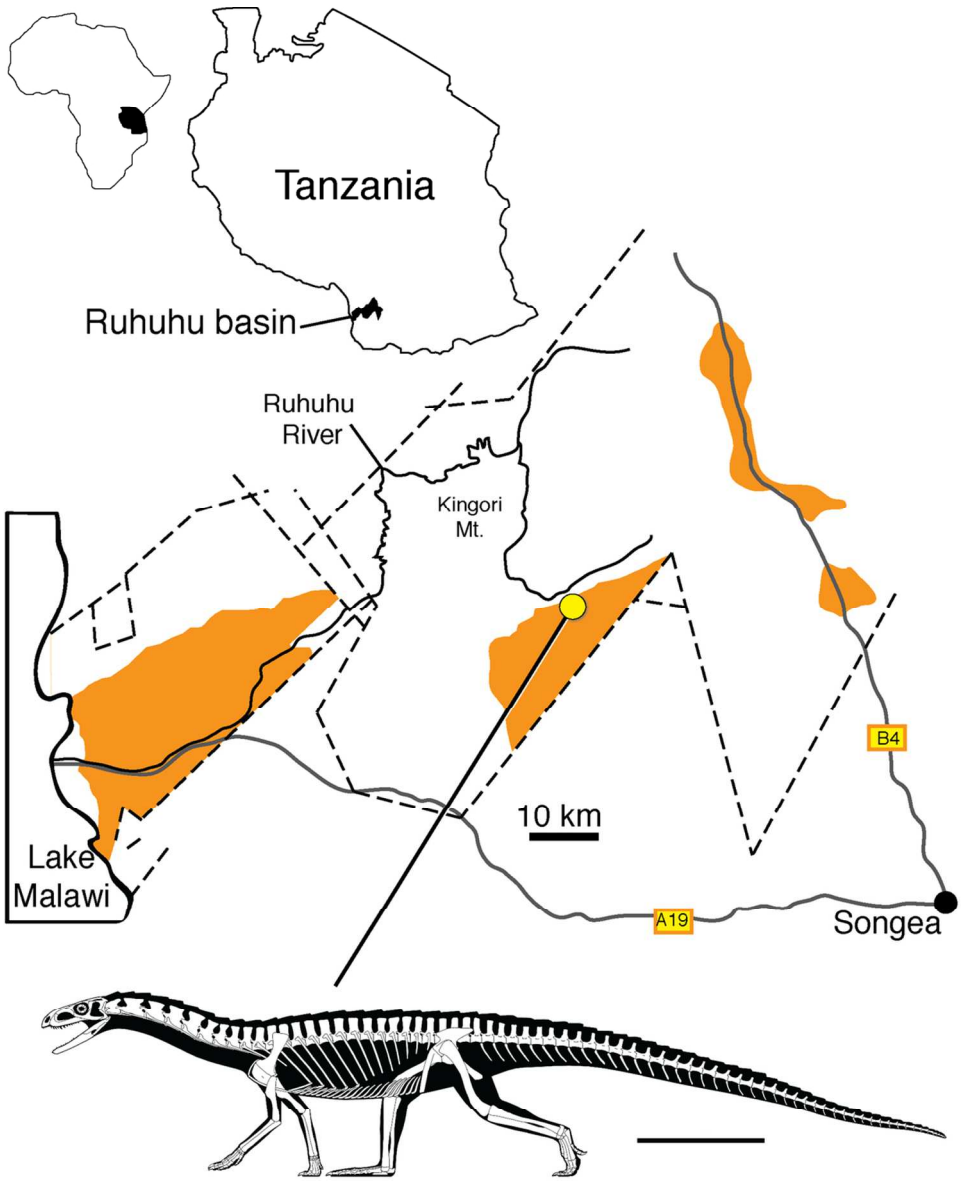

color

108x130mm (300 x 300 DPI)

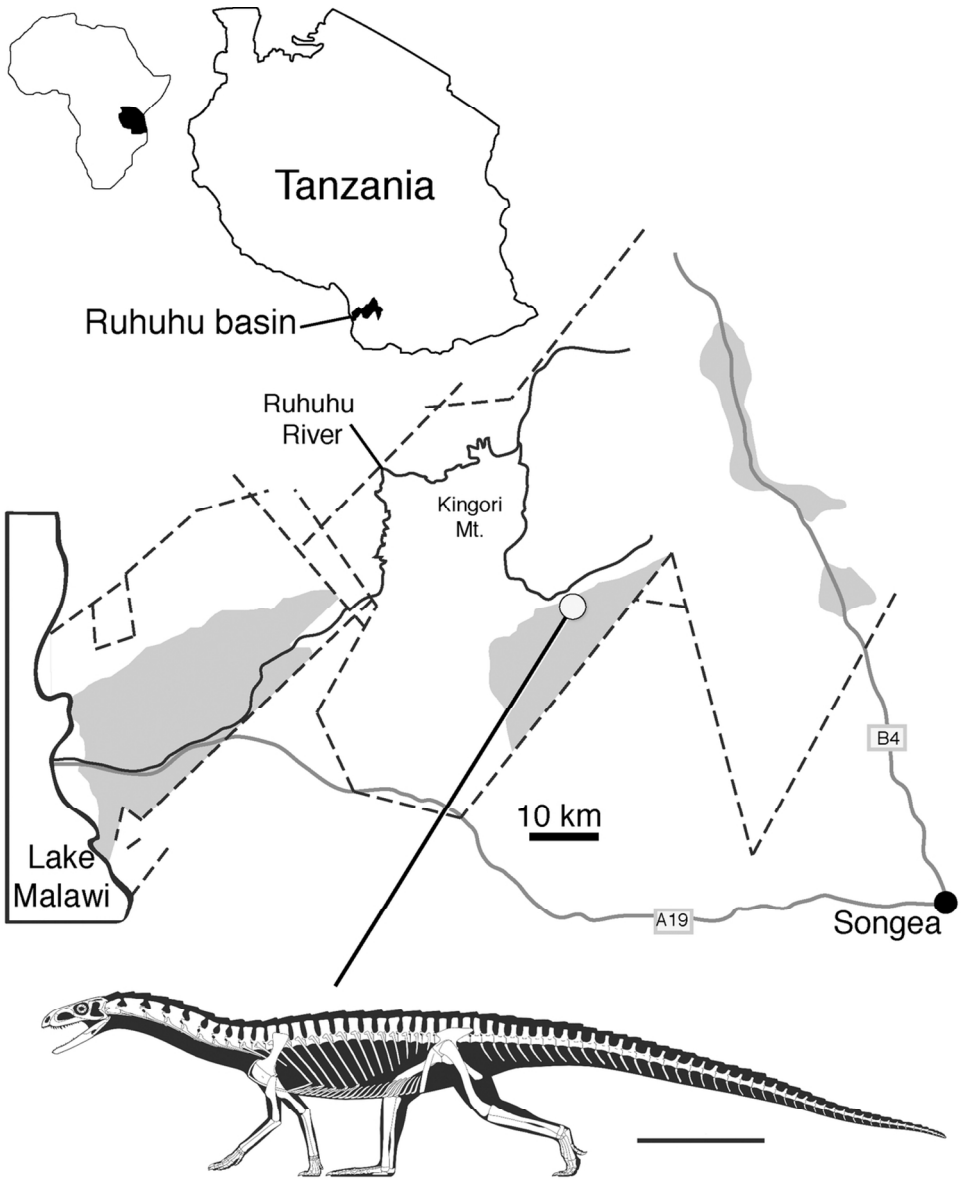

108x130mm (300 x 300 DPI)

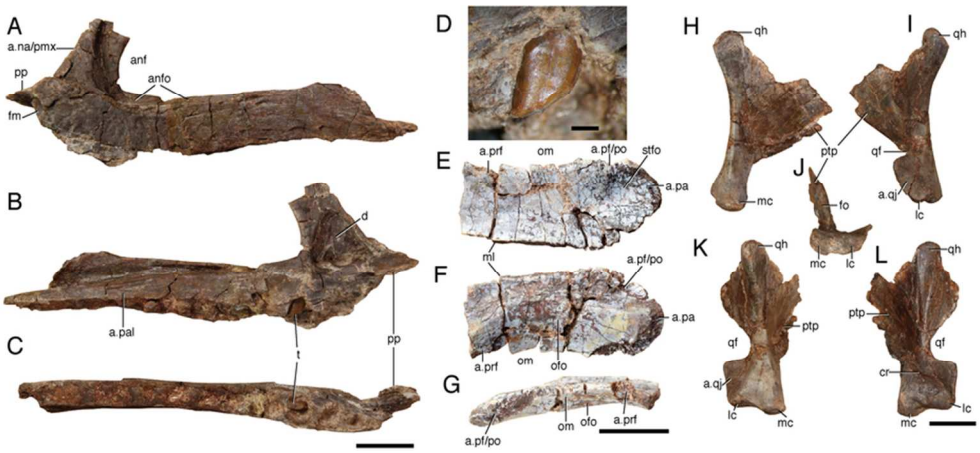

color

80x35mm (300 x 300 DPI)

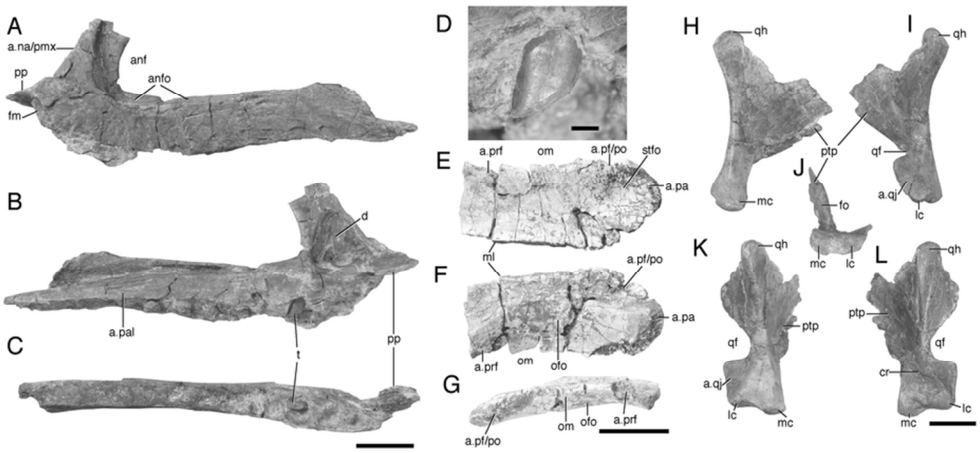

80x35mm (300 x 300 DPI)

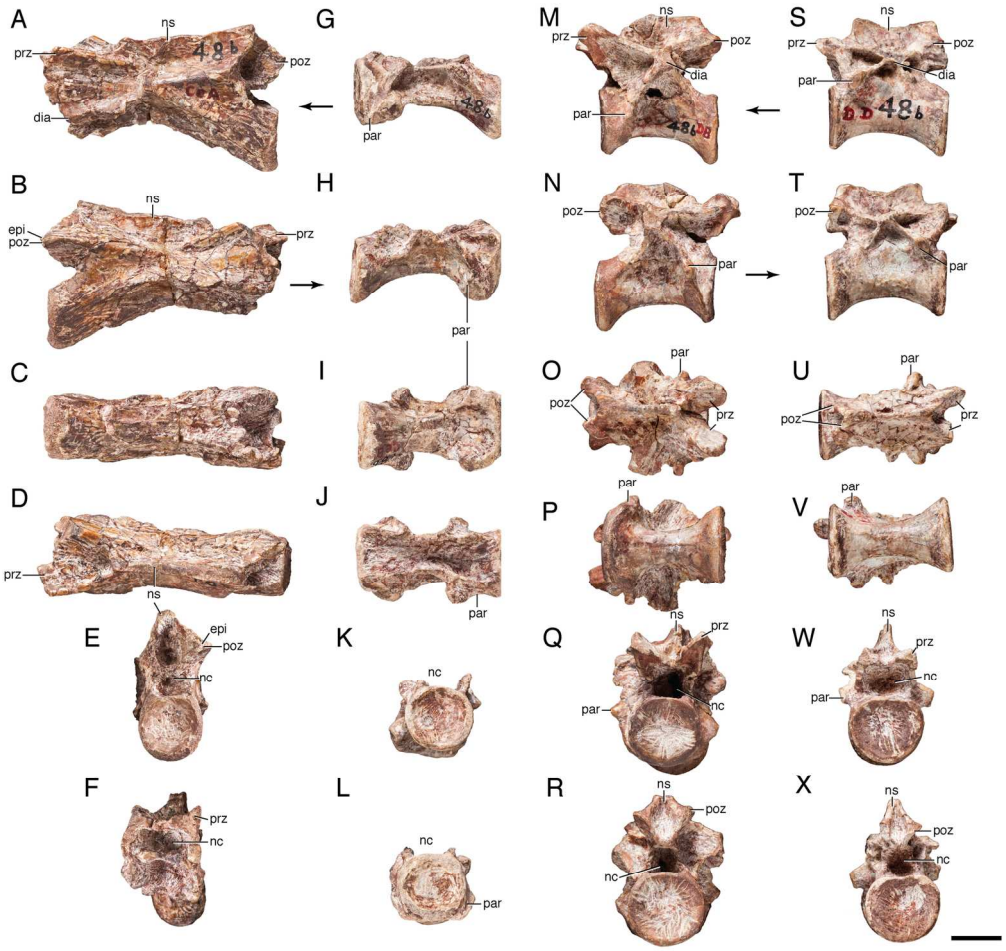

color

160x155mm (300 x 300 DPI)

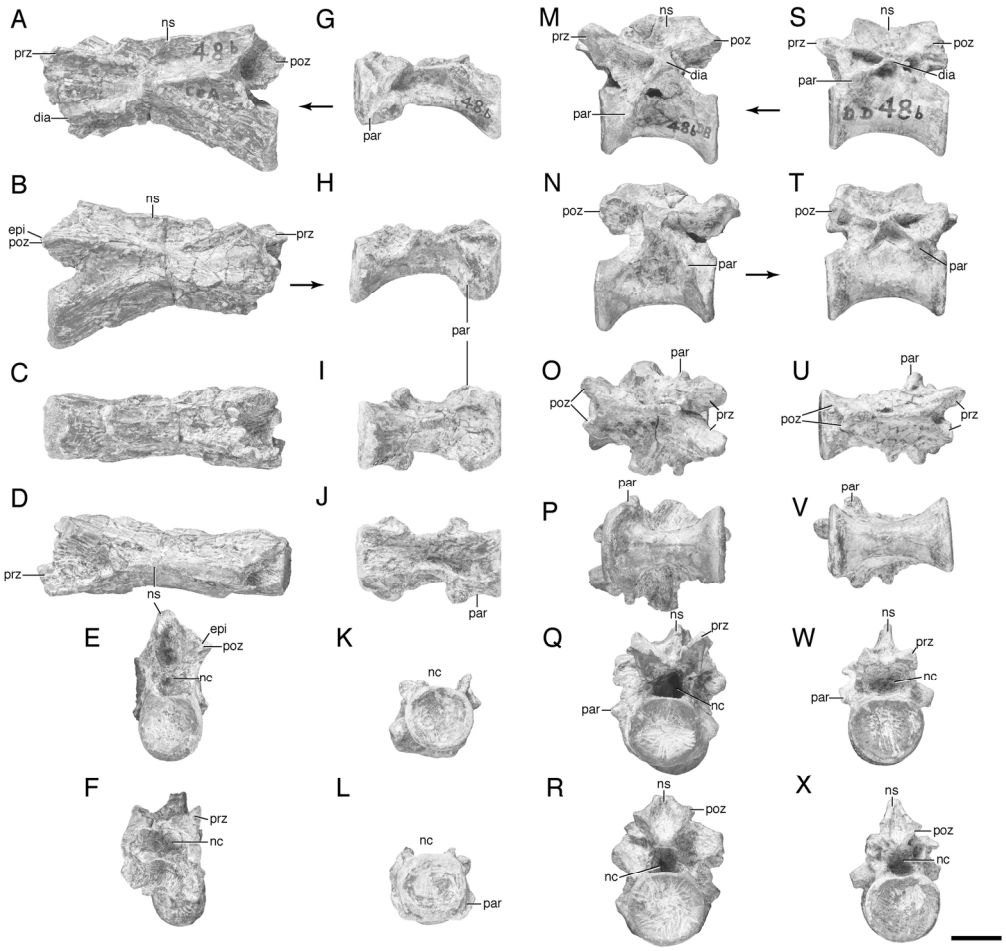

160x155mm (300 x 300 DPI)

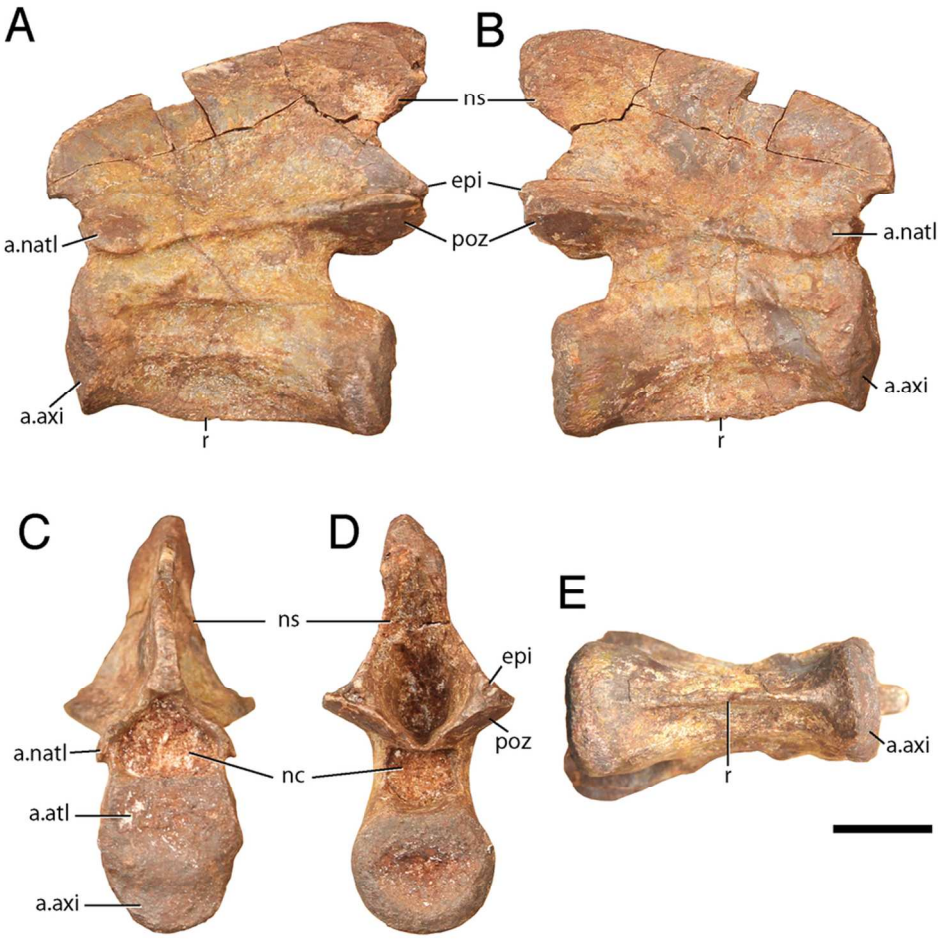

color

88x87mm (300 x 300 DPI)

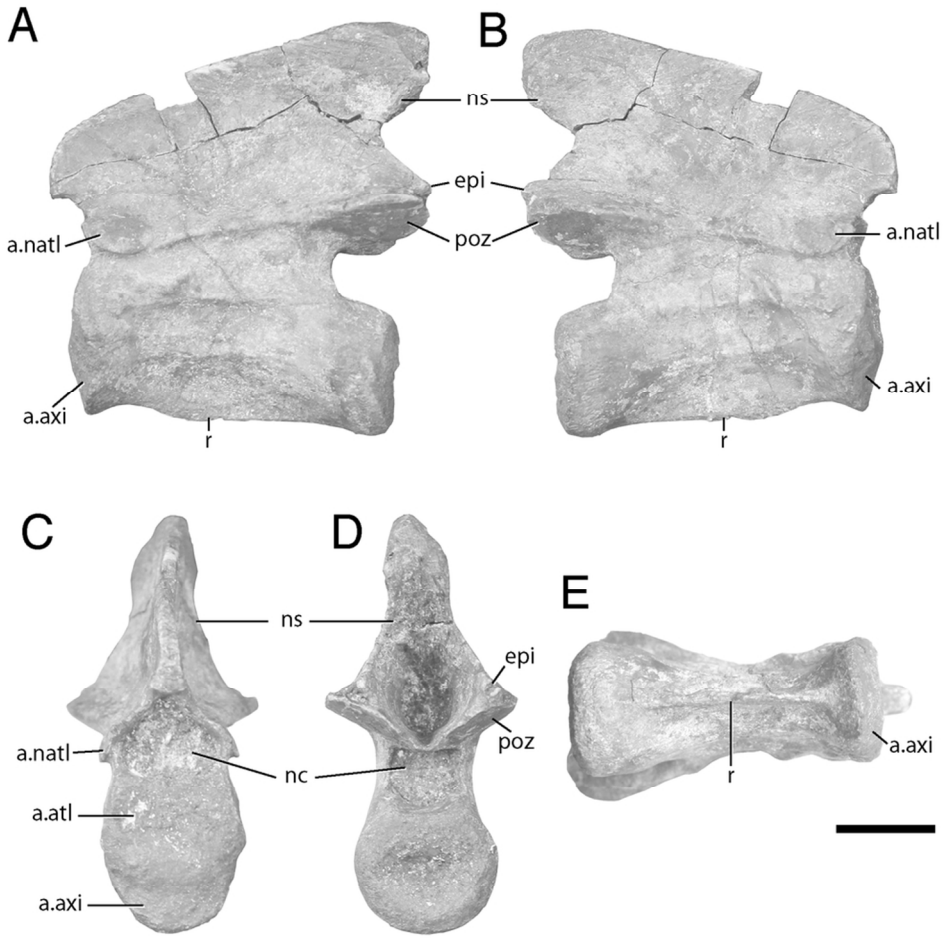

88x87mm (300 x 300 DPI)

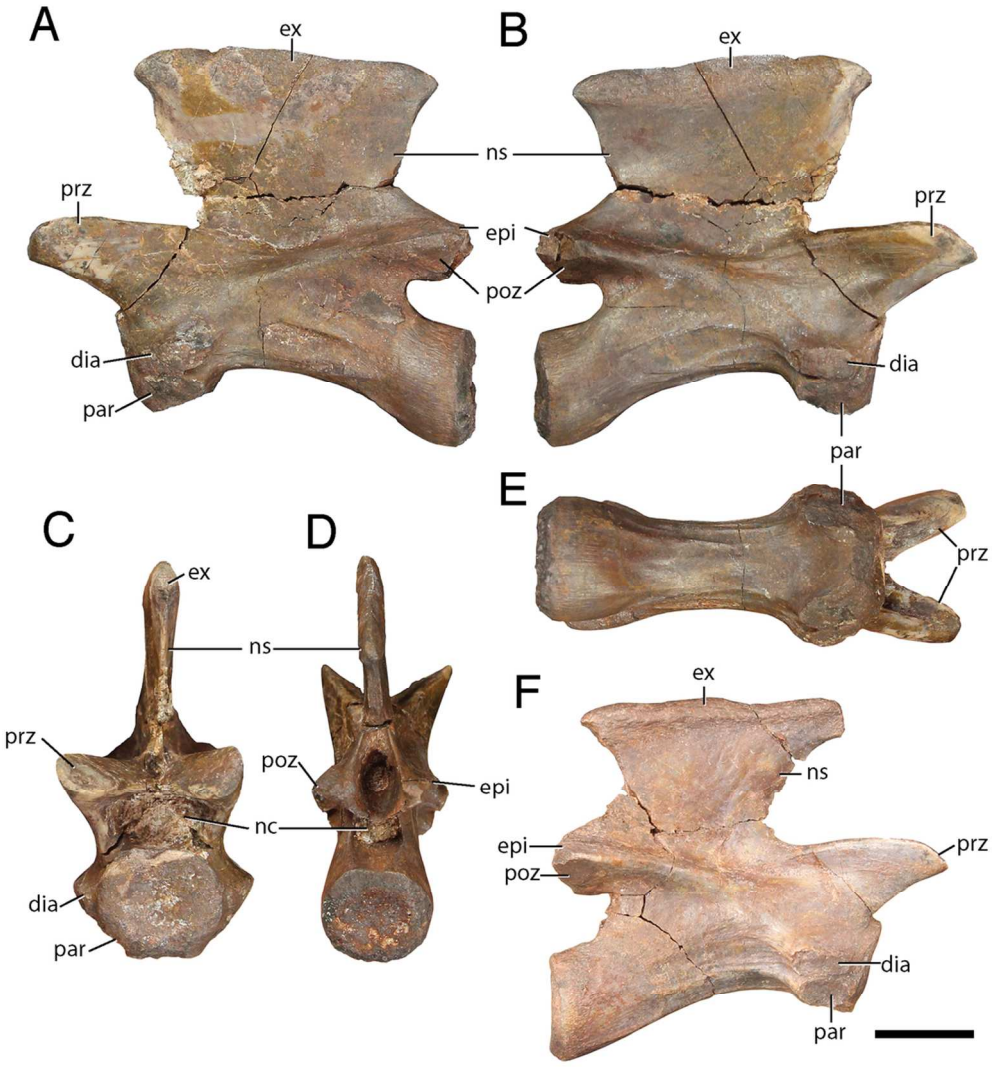

color

101x113mm (300 x 300 DPI)

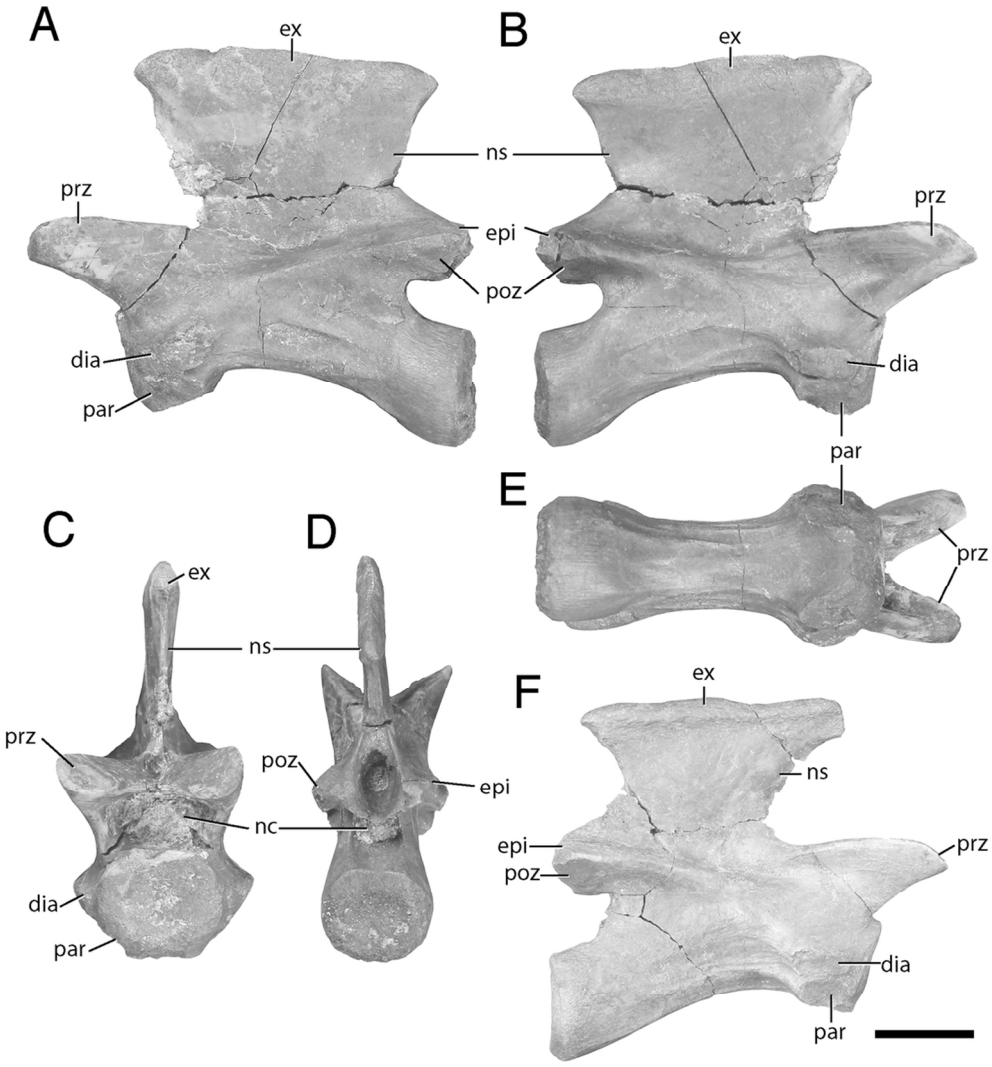

101x113mm (300 x 300 DPI)

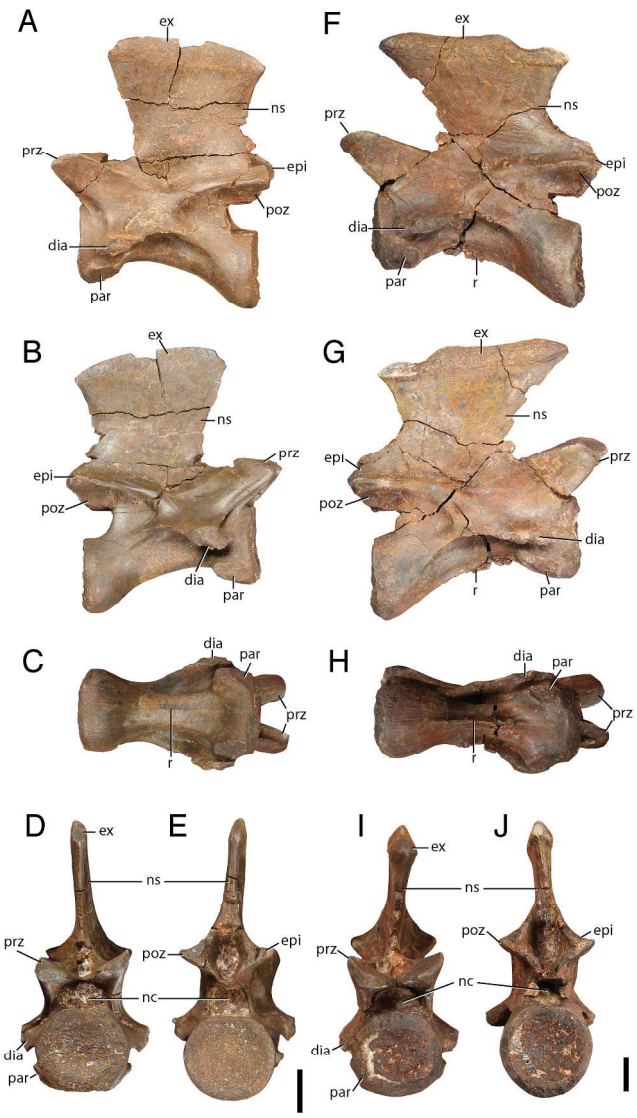

color

165x305mm (300 x 300 DPI)

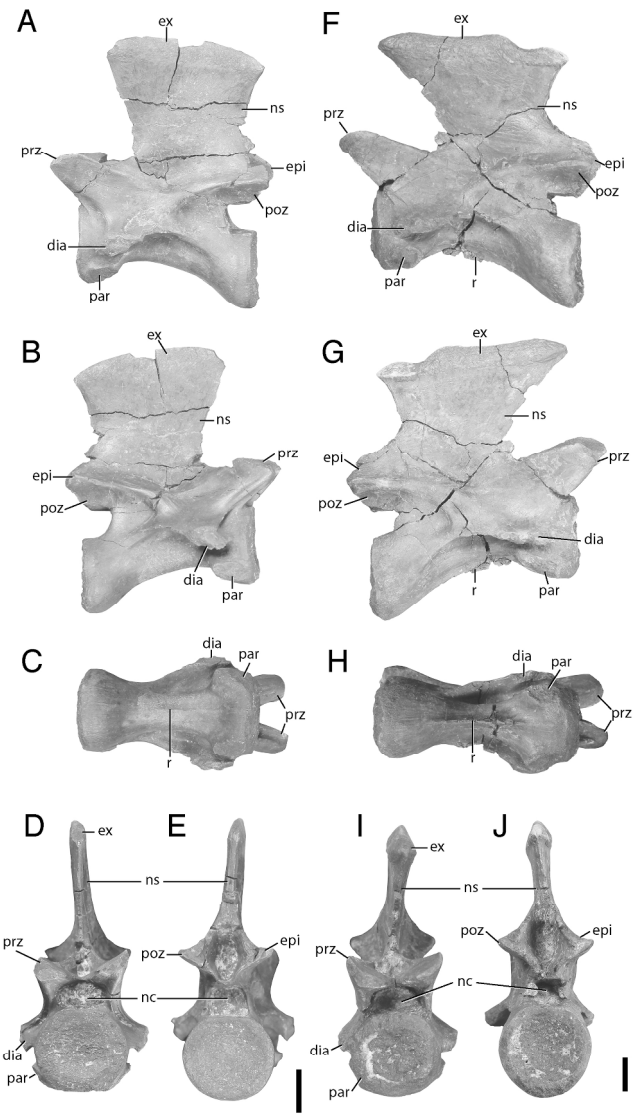

165x305mm (300 x 300 DPI)

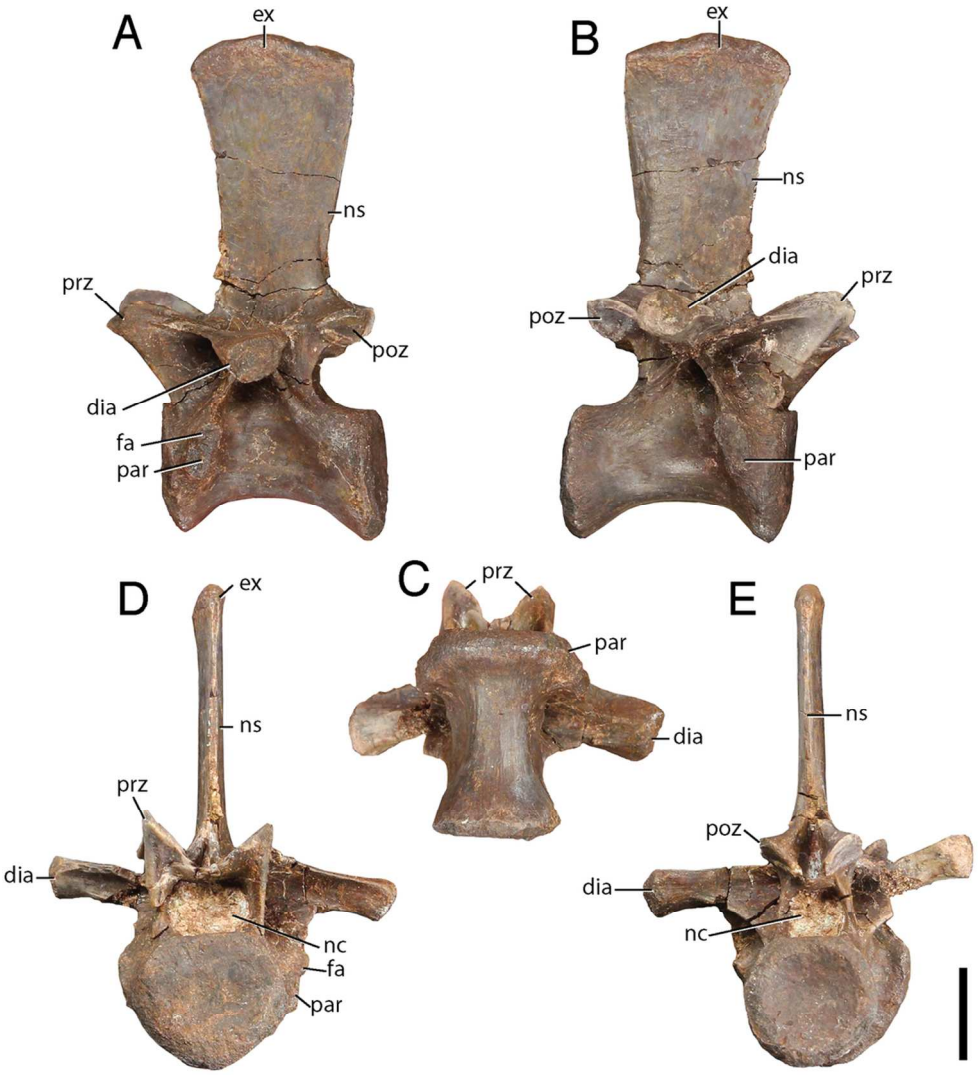

color

100x112mm (300 x 300 DPI)

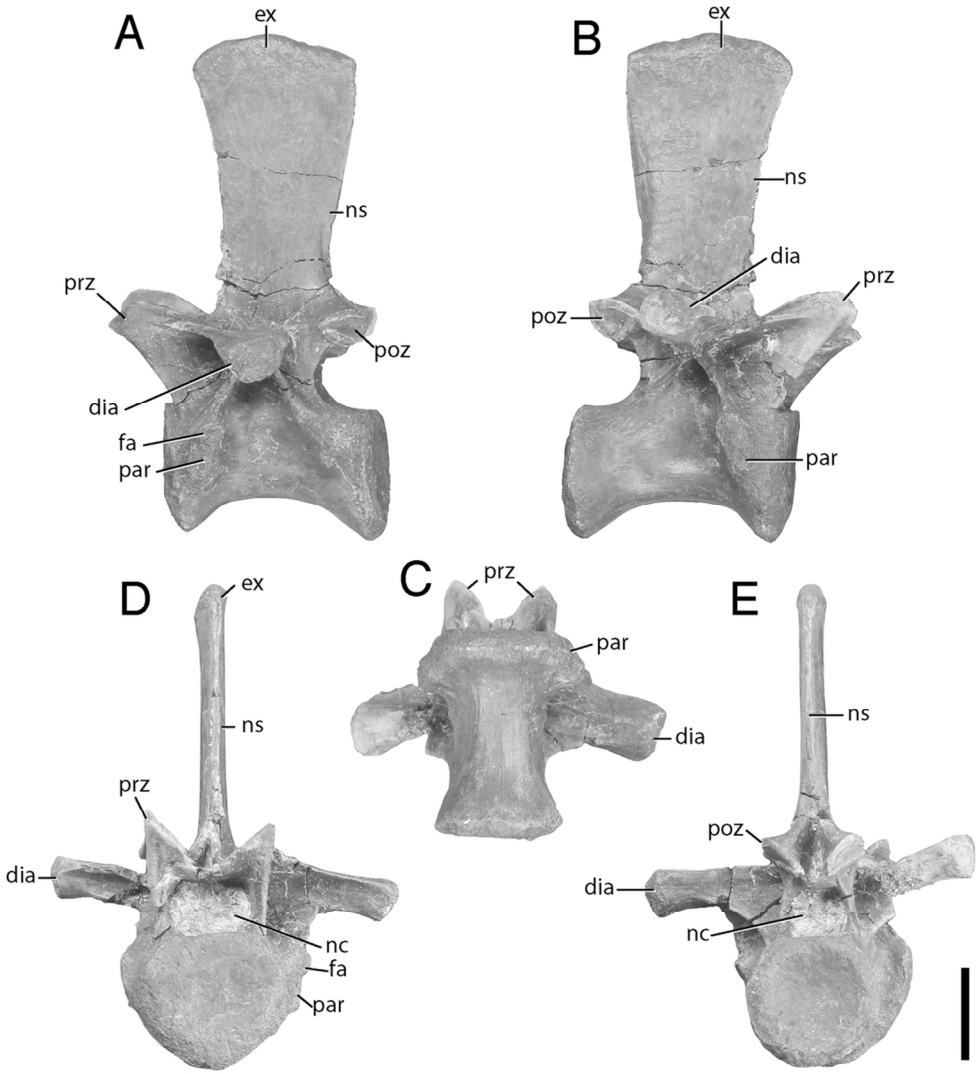

100x112mm (300 x 300 DPI)

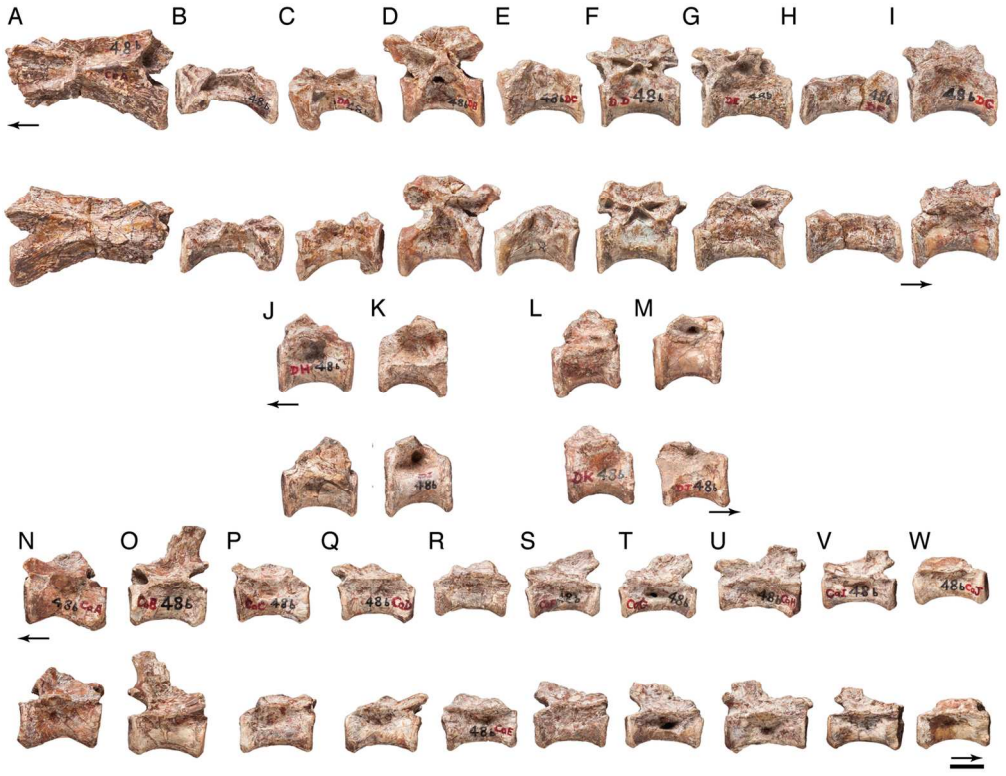

139x108mm (300 x 300 DPI)

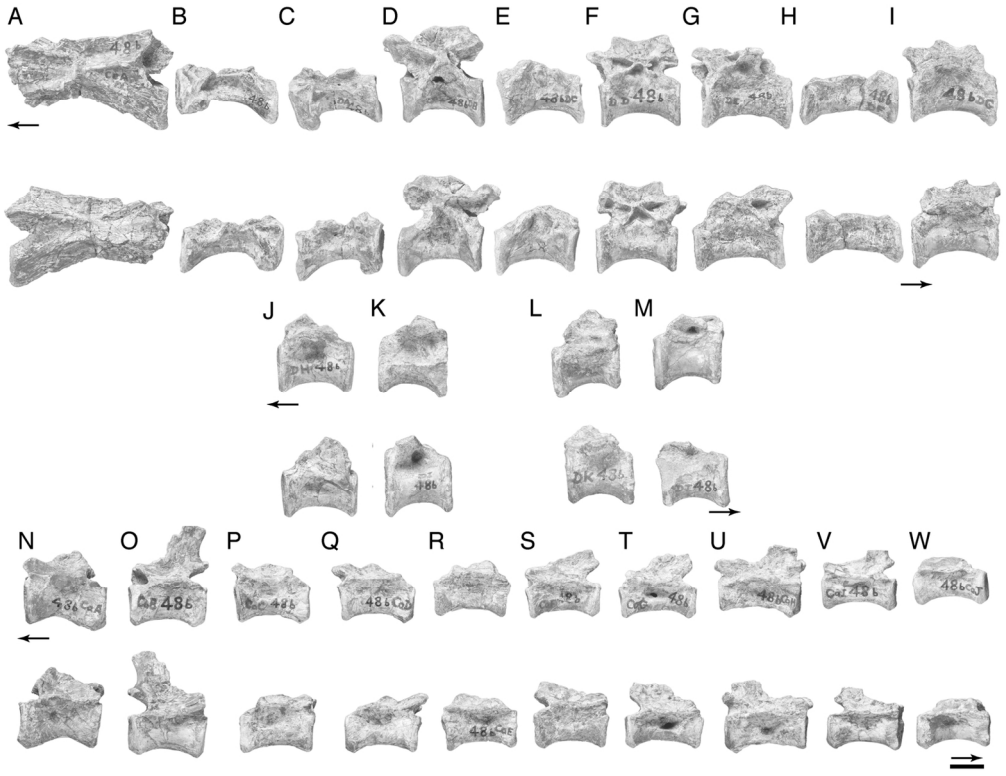

139x108mm (300 x 300 DPI)

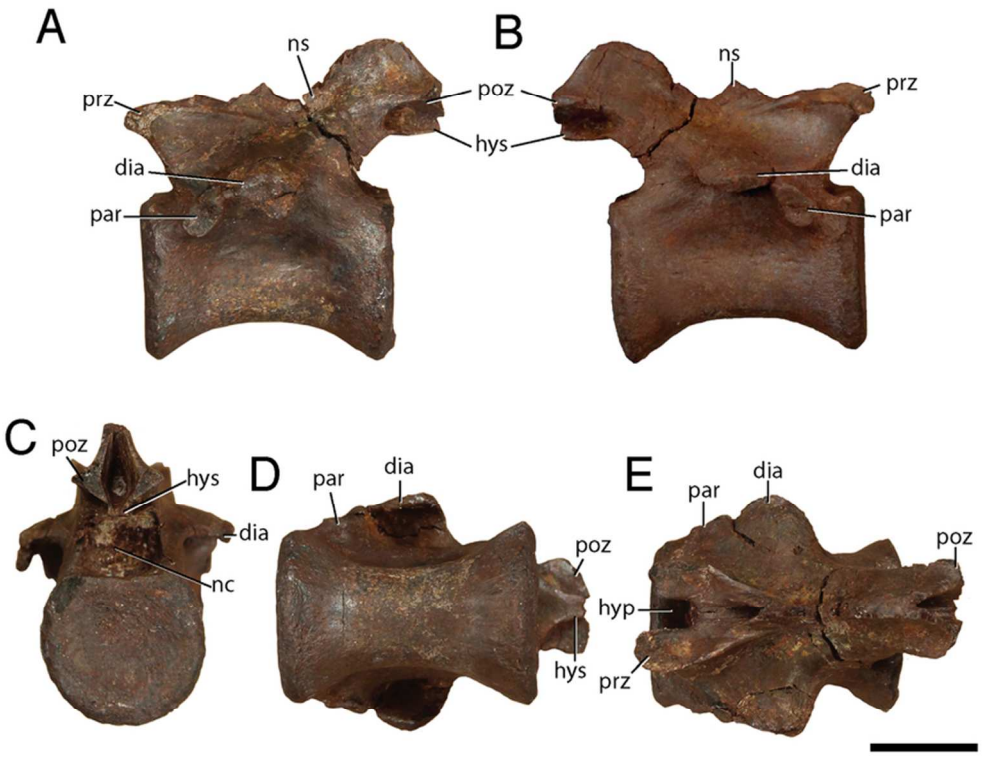

color

73x60mm (300 x 300 DPI)

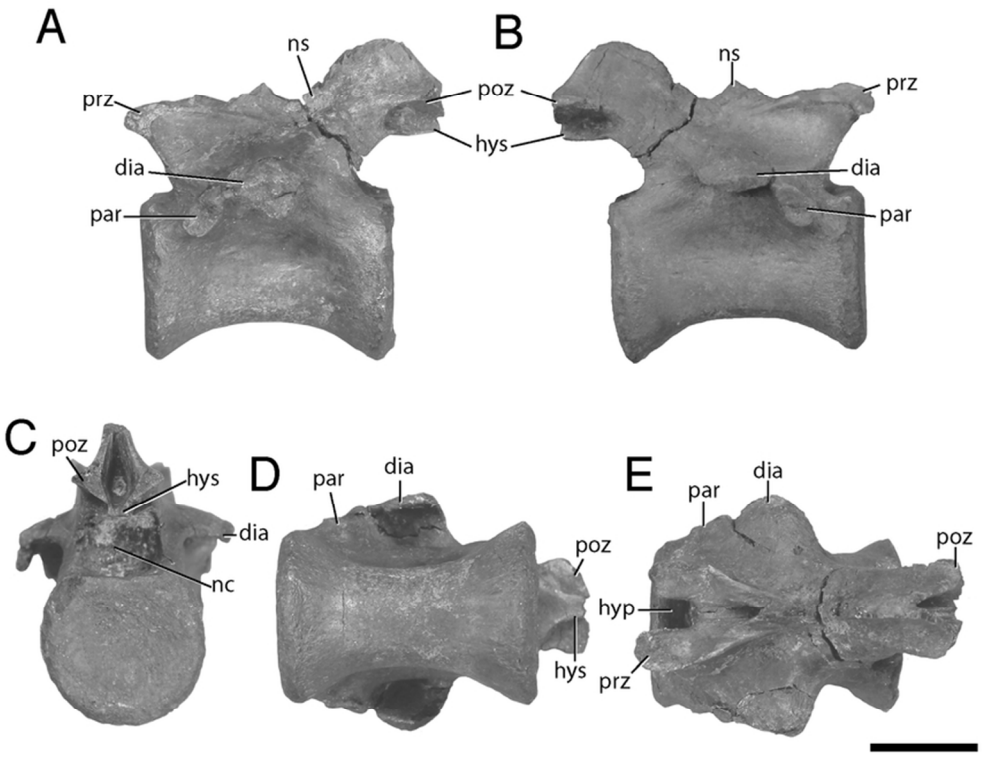

73x60mm (300 x 300 DPI)

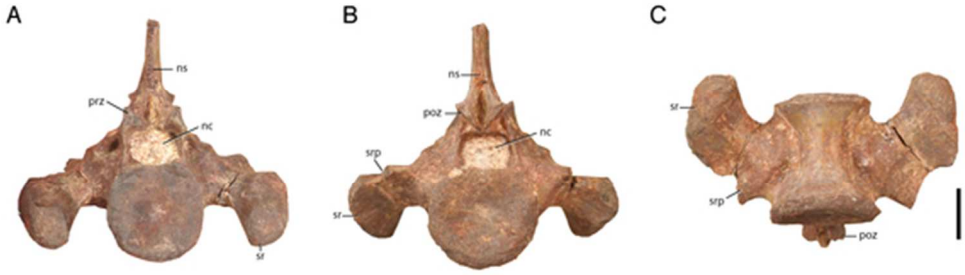

color

49x13mm (300 x 300 DPI)

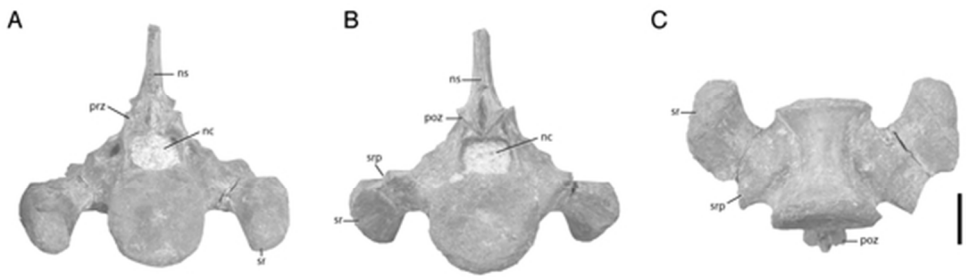

49x13mm (300 x 300 DPI)

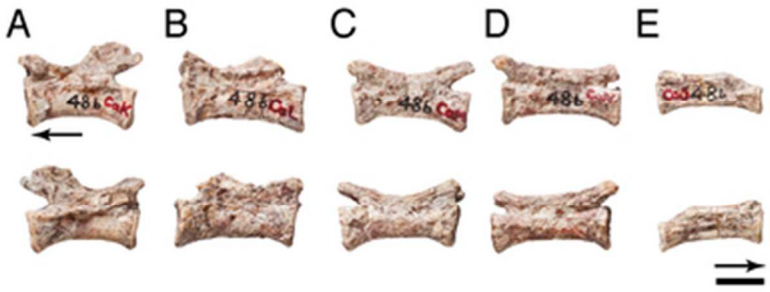

color

34x13mm (300 x 300 DPI)

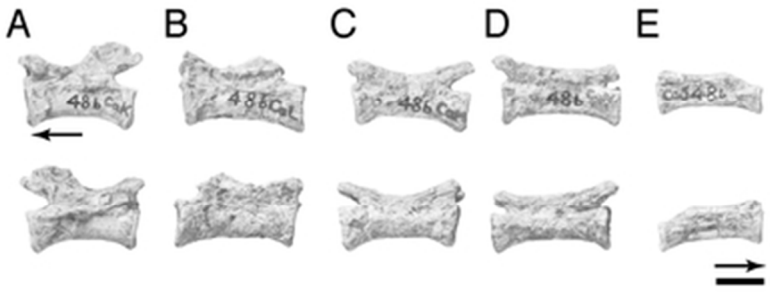

34x13mm (300 x 300 DPI)

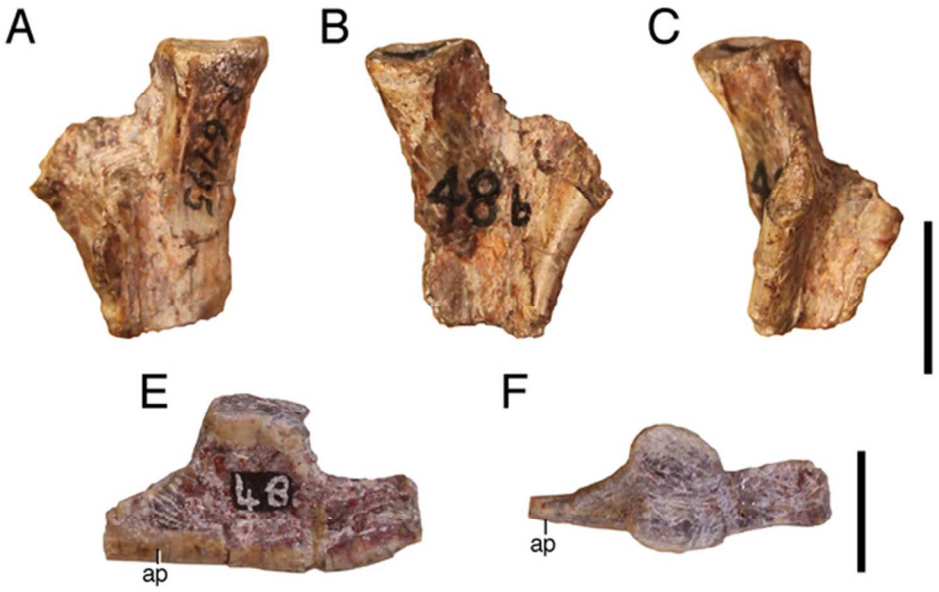

color

57x36mm (300 x 300 DPI)

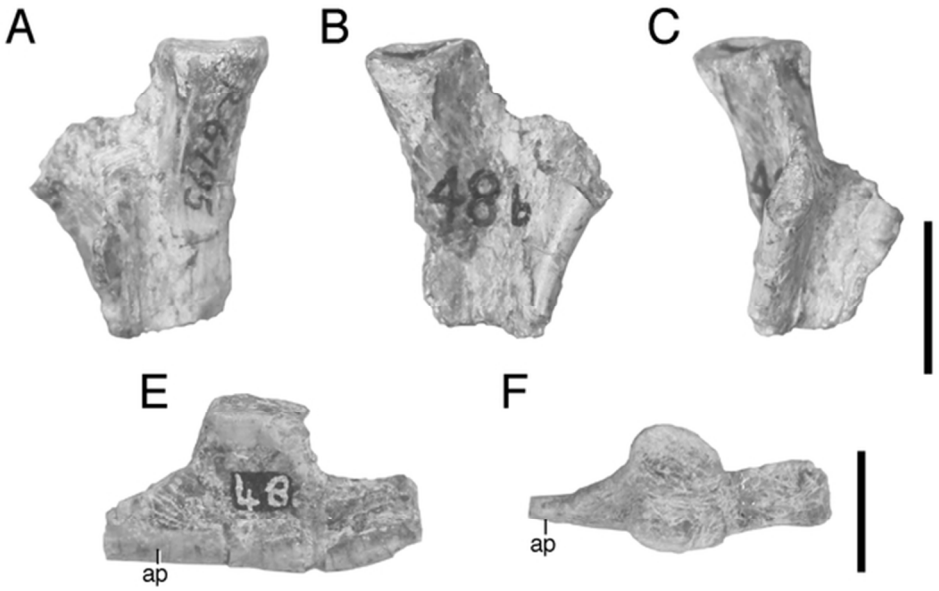

57x36mm (300 x 300 DPI)

color

157x275mm (300 x 300 DPI)

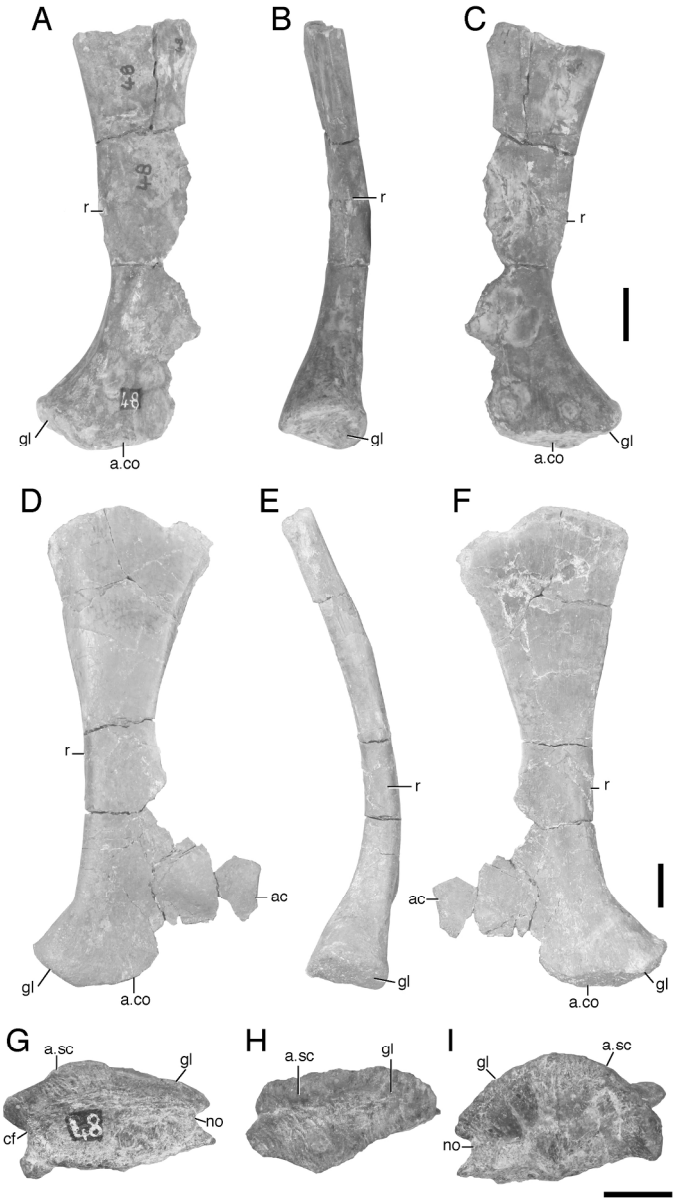

157x275mm (300 x 300 DPI)

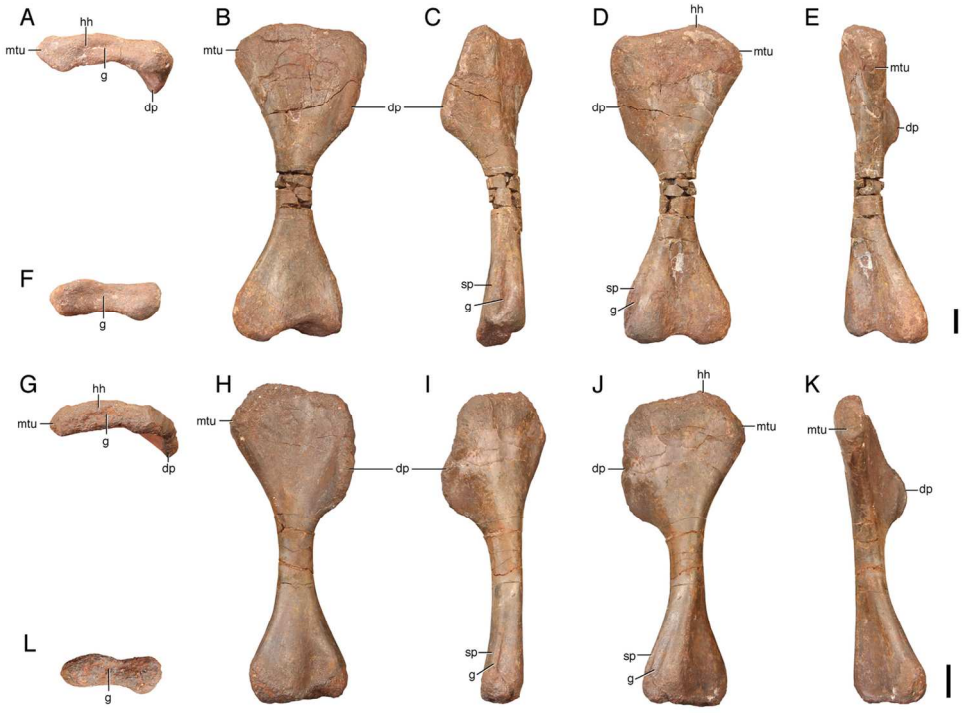

color

129x93mm (300 x 300 DPI)

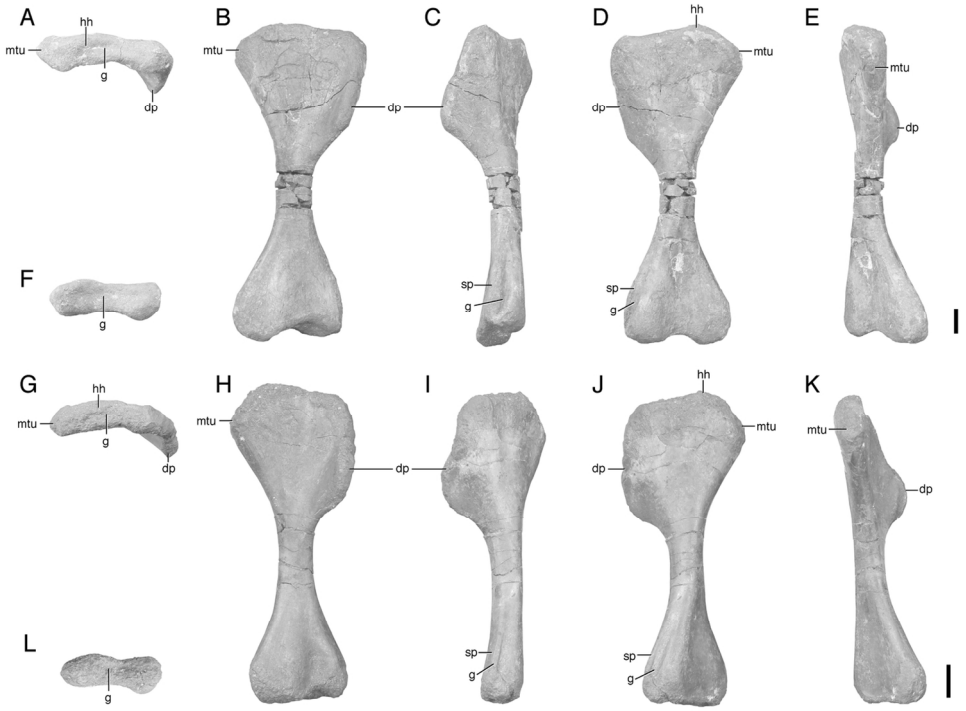

129x93mm (300 x 300 DPI)

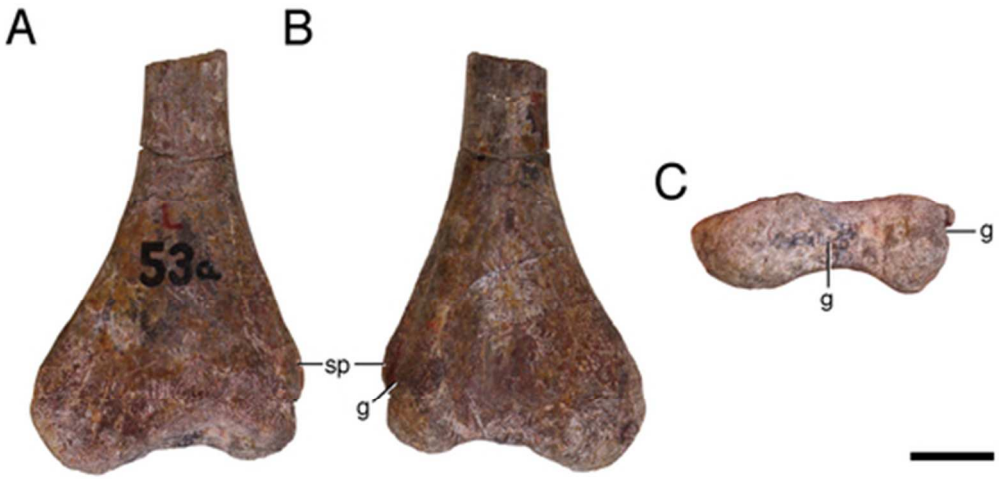

color

43x21mm (300 x 300 DPI)

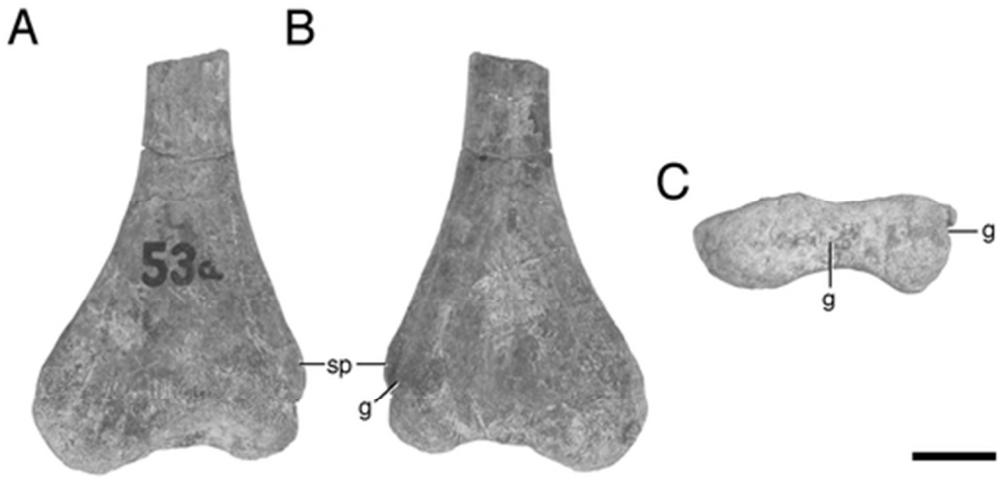

43x21mm (300 x 300 DPI)

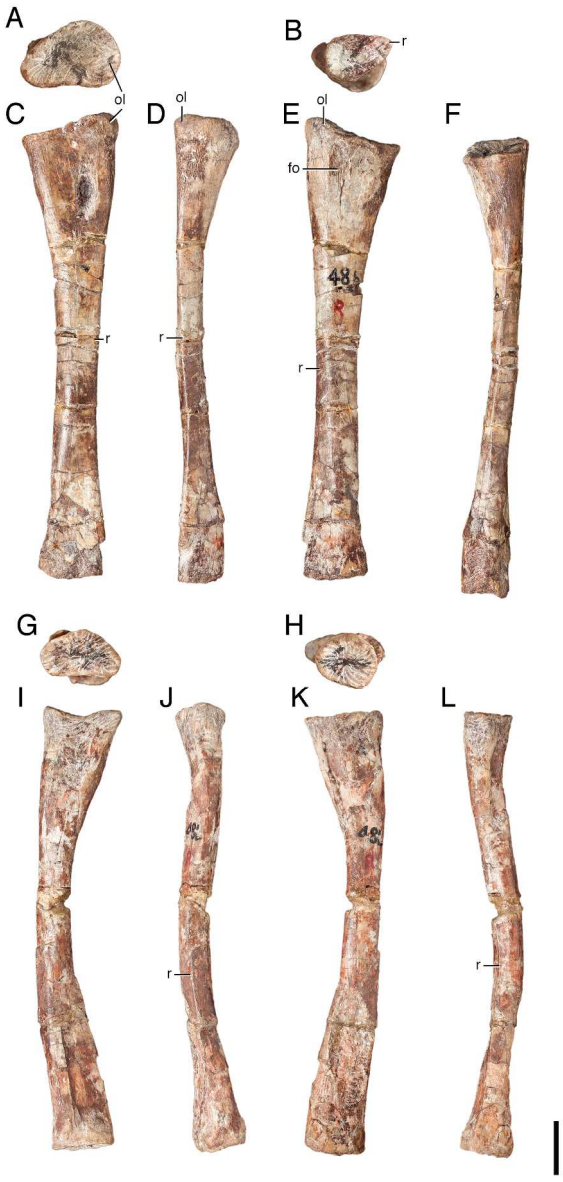

color

179x357mm (300 x 300 DPI)

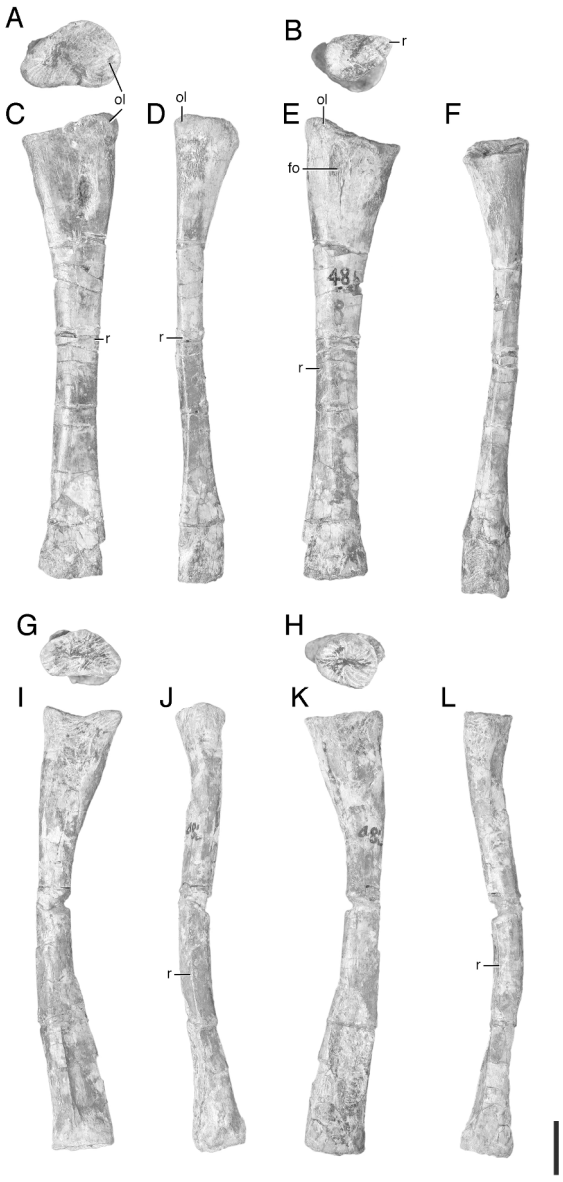

179x357mm (300 x 300 DPI)

color

67x55mm (300 x 300 DPI)

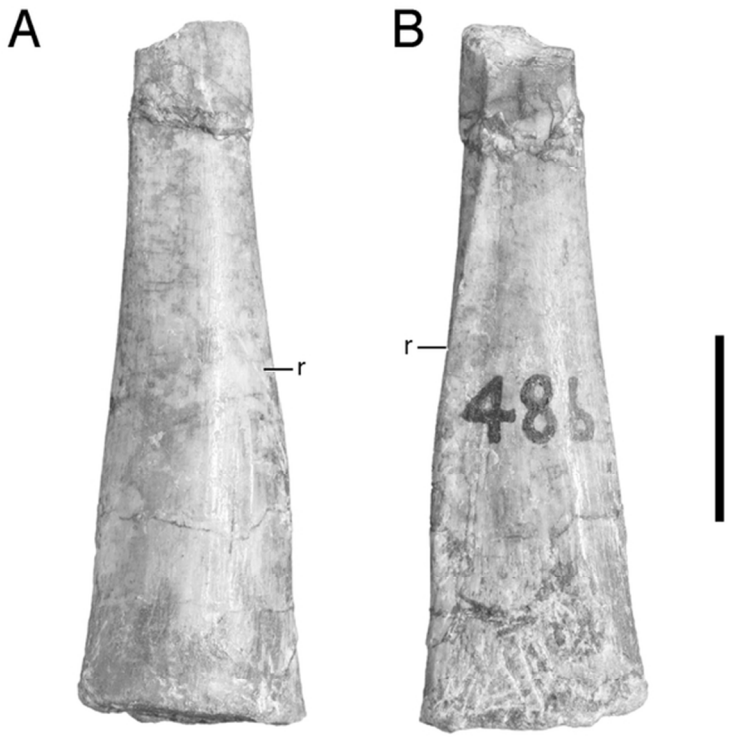

67x55mm (300 x 300 DPI)

color

49x26mm (300 x 300 DPI)

49x26mm (300 x 300 DPI)

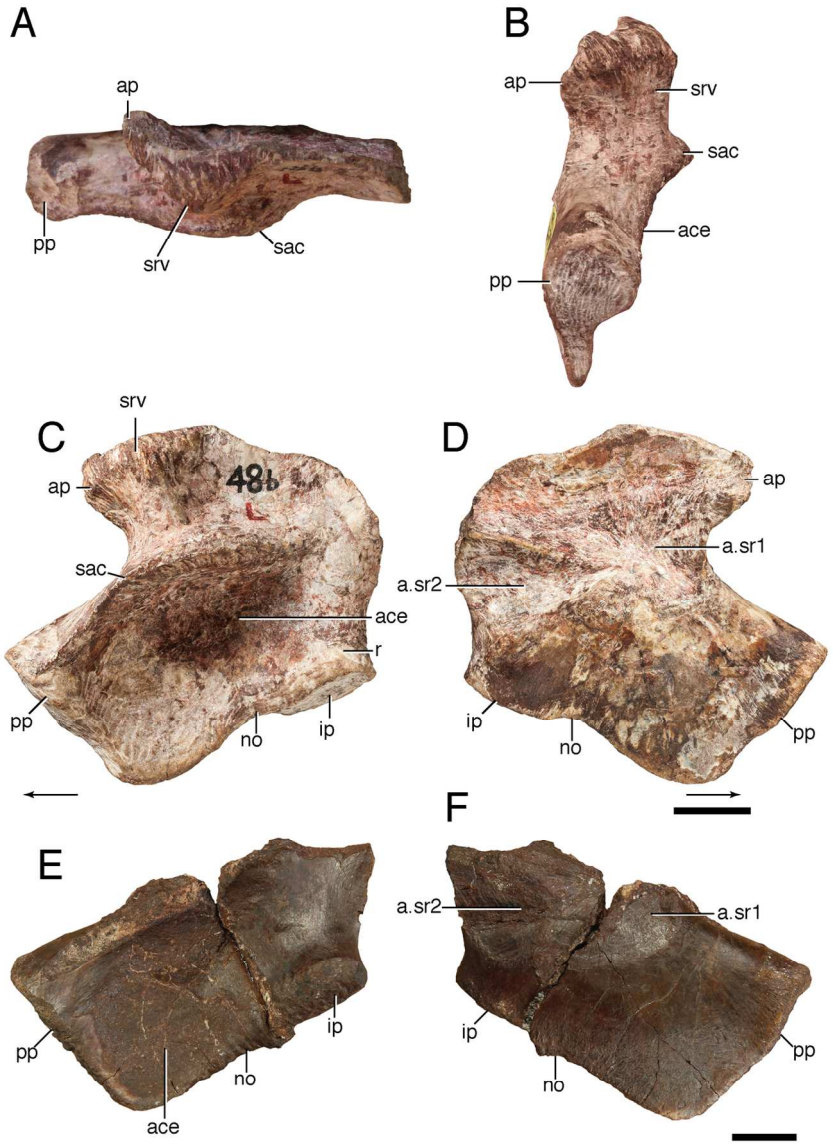

color

125x175mm (300 x 300 DPI)

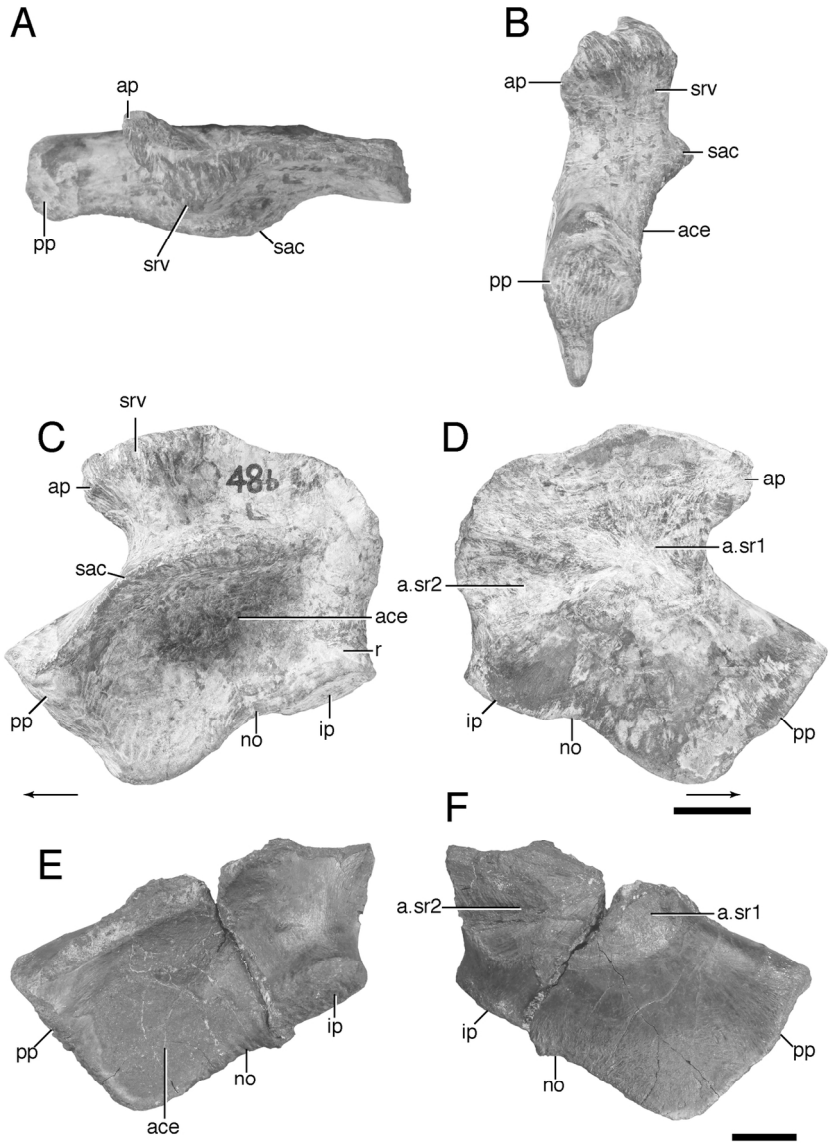

125x175mm (300 x 300 DPI)

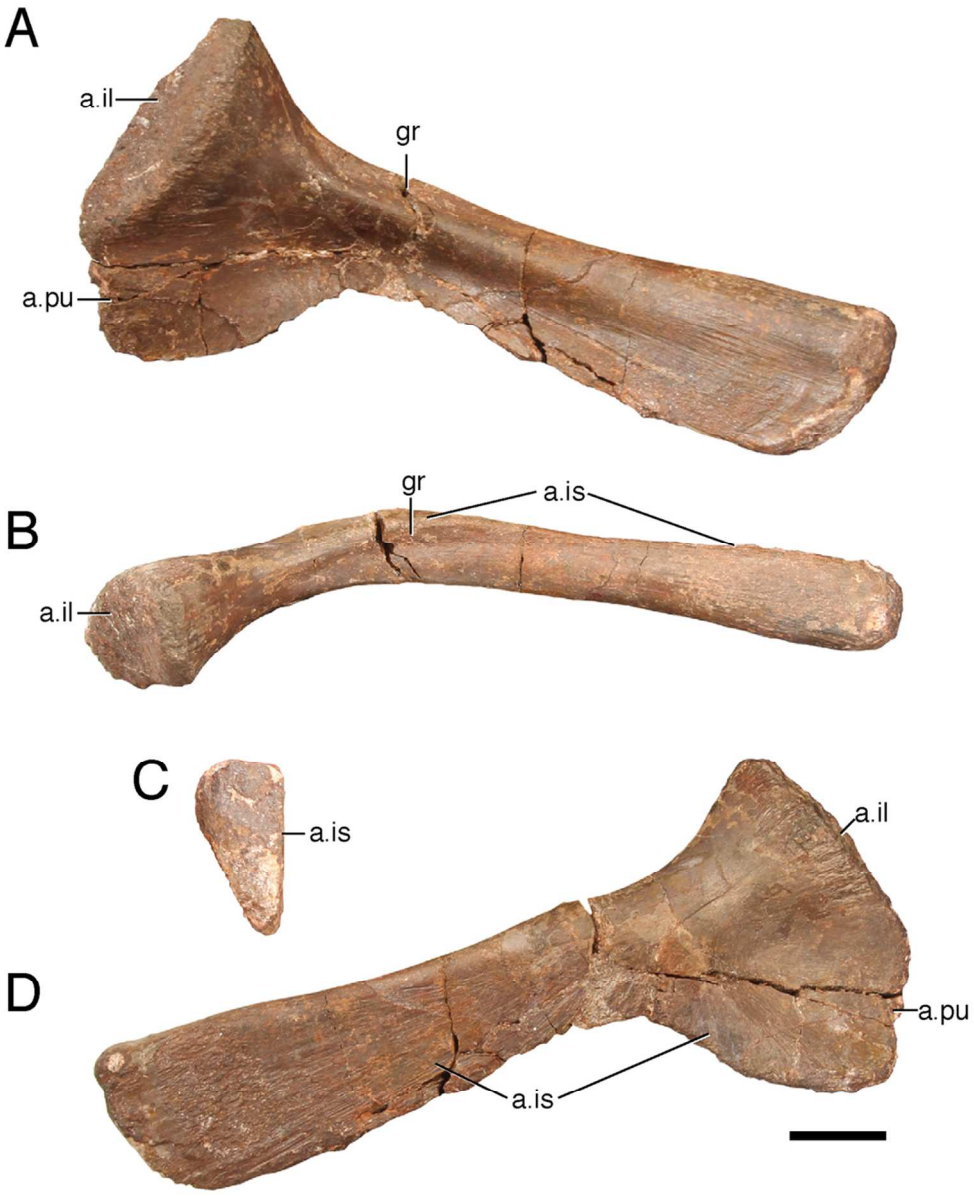

color

94x116mm (300 x 300 DPI)

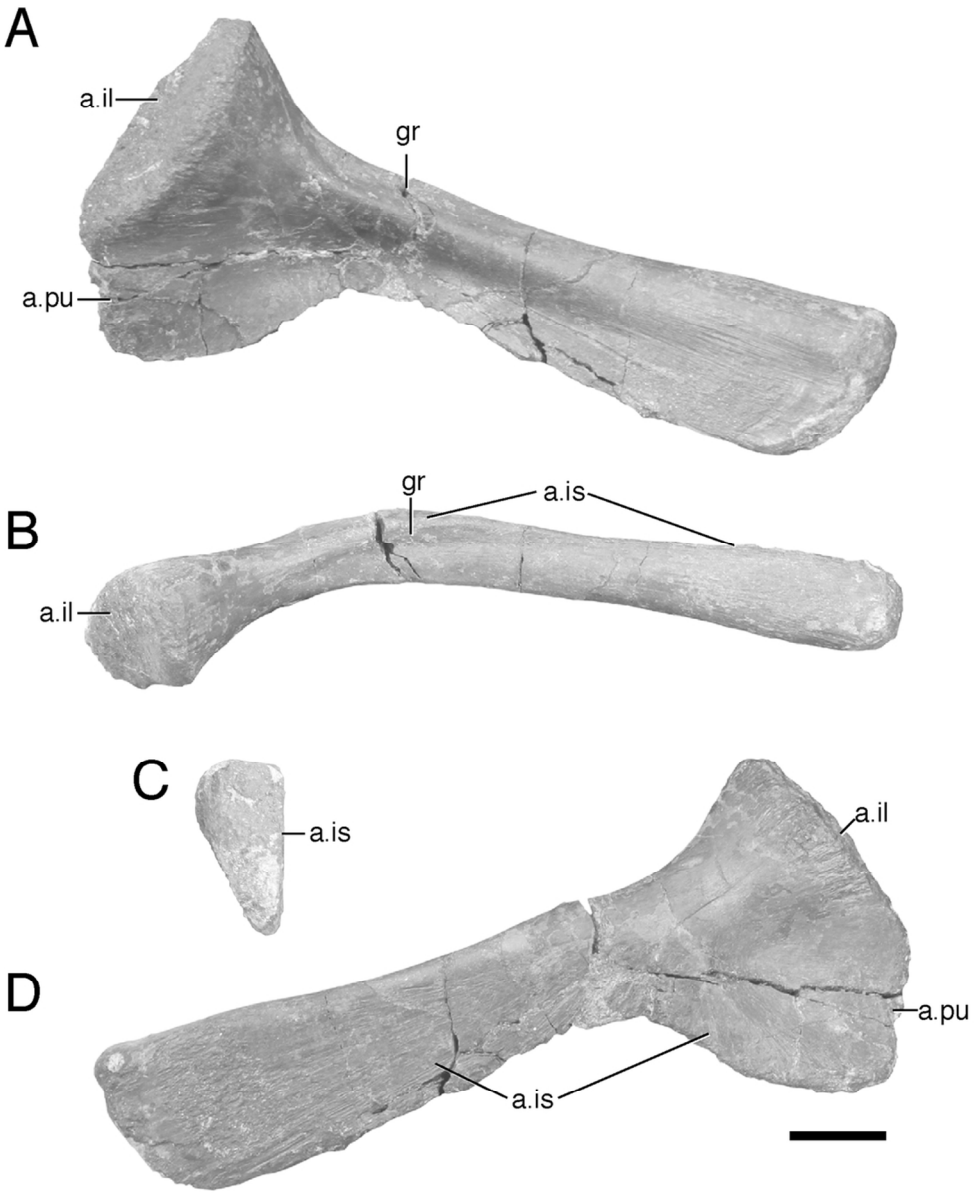

94x116mm (300 x 300 DPI)

color

155x134mm (300 x 300 DPI)

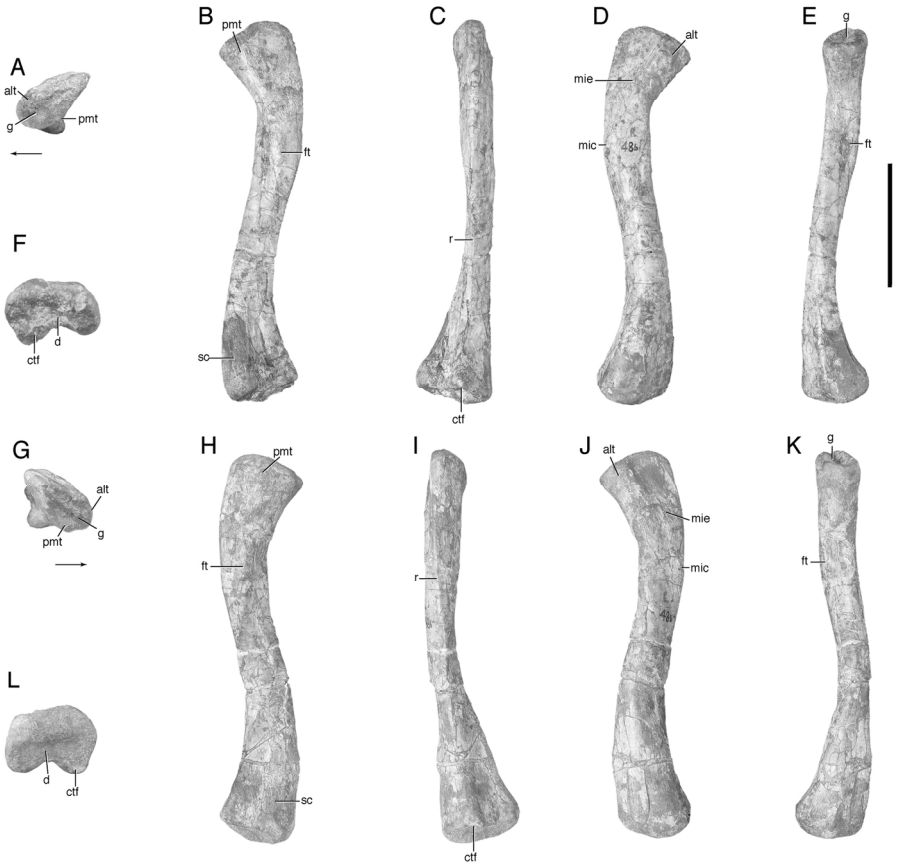

155x134mm (300 x 300 DPI)

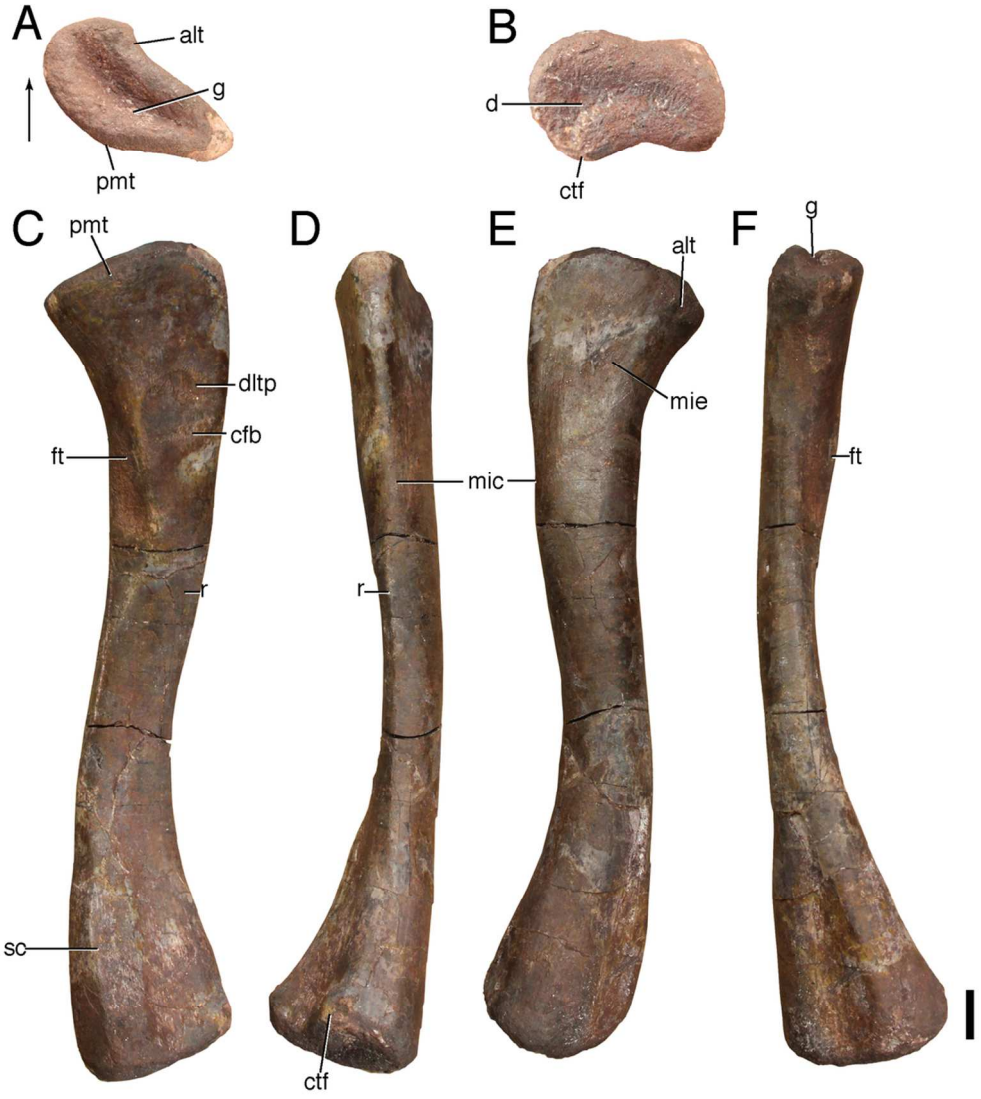

105x123mm (300 x 300 DPI)

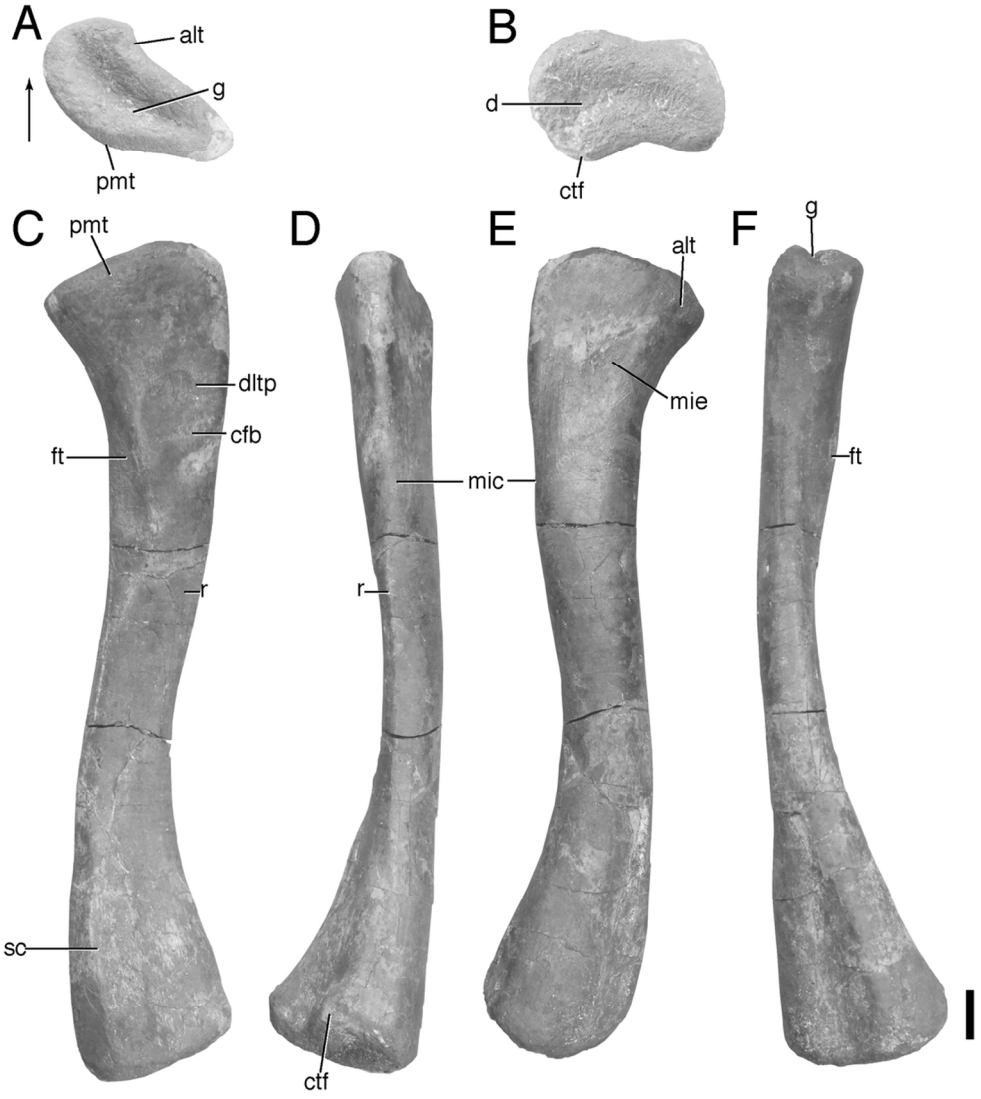

105x123mm (300 x 300 DPI)

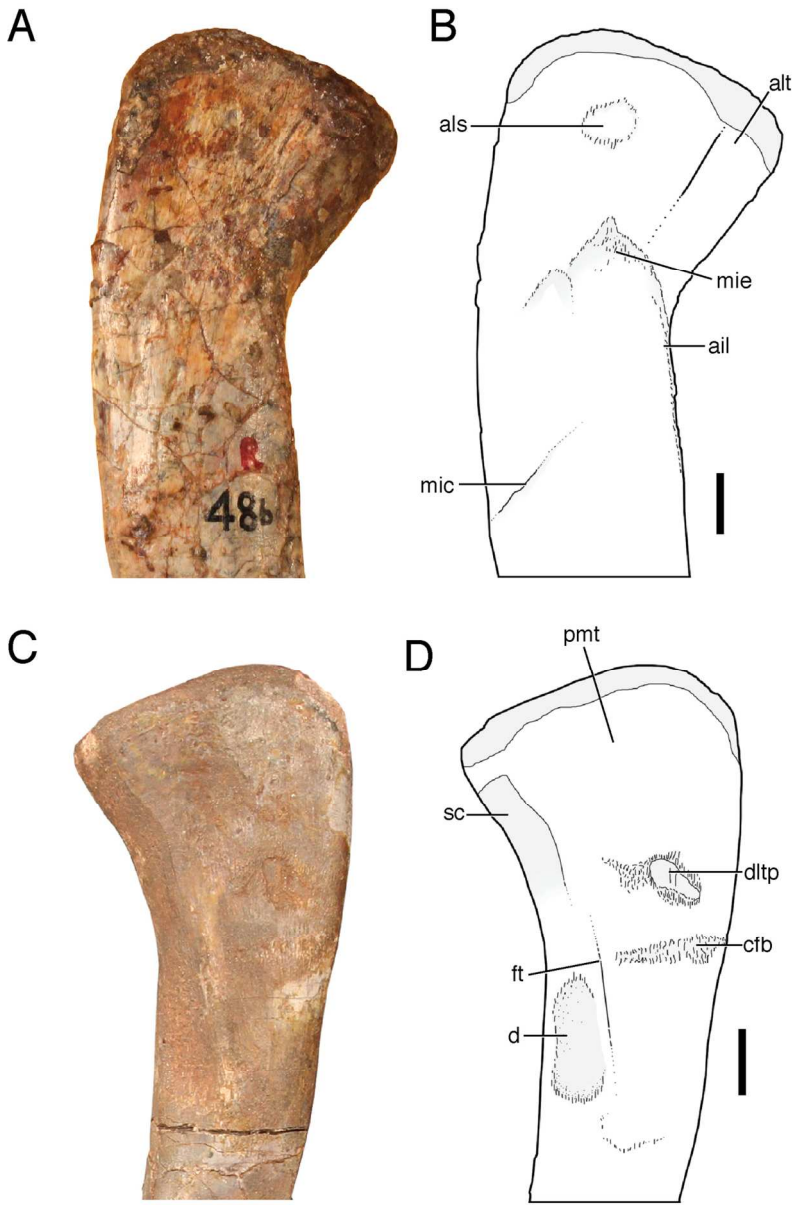

color

115x172mm (300 x 300 DPI)

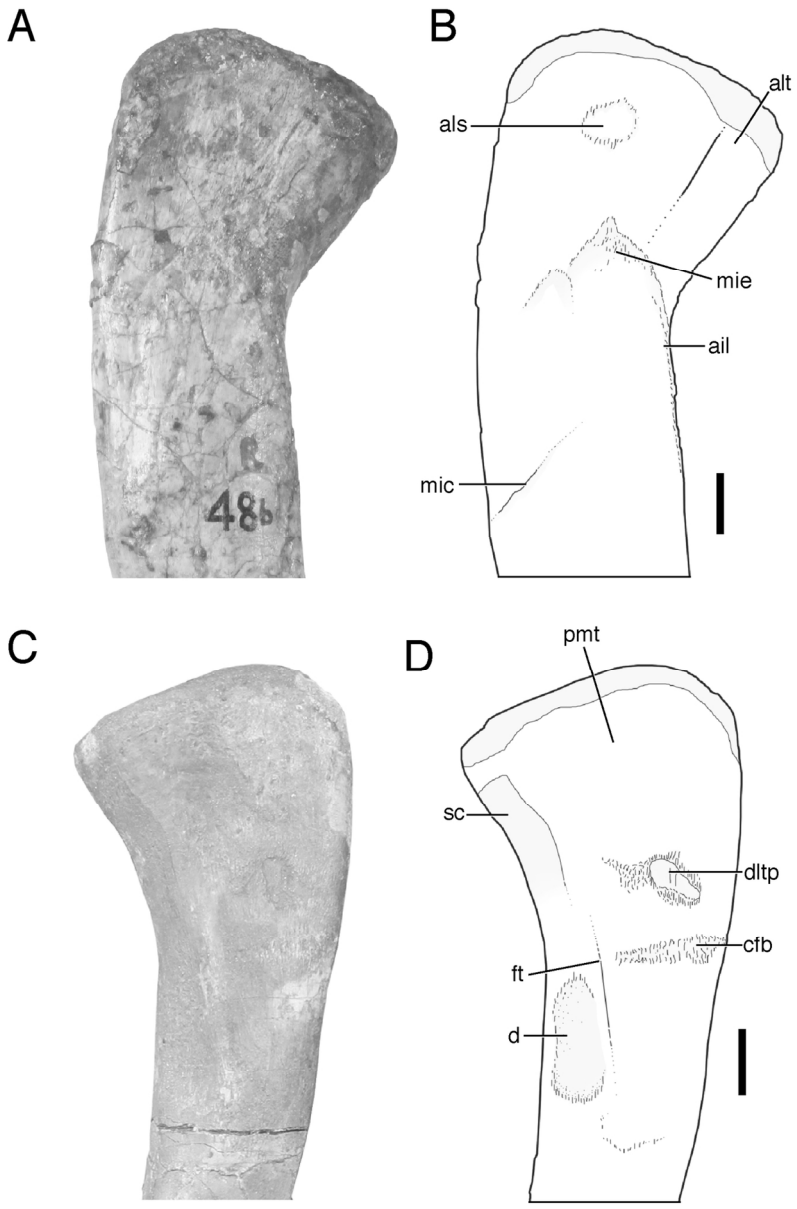

115x172mm (300 x 300 DPI)

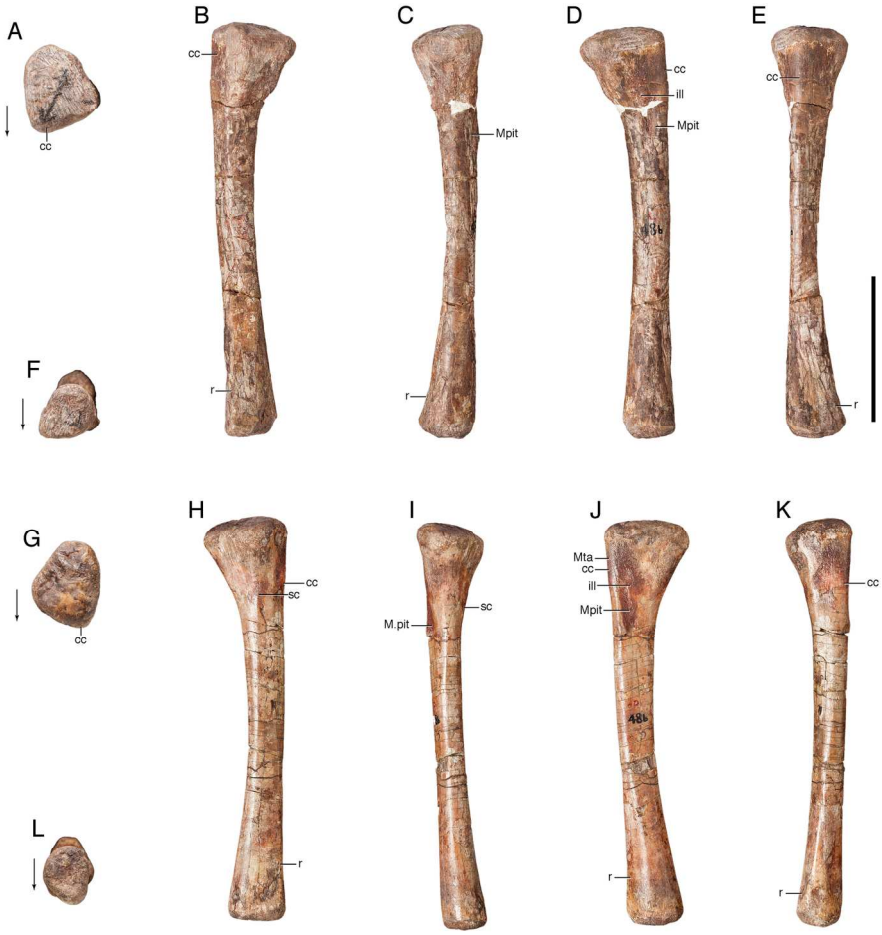

color

170x162mm (300 x 300 DPI)

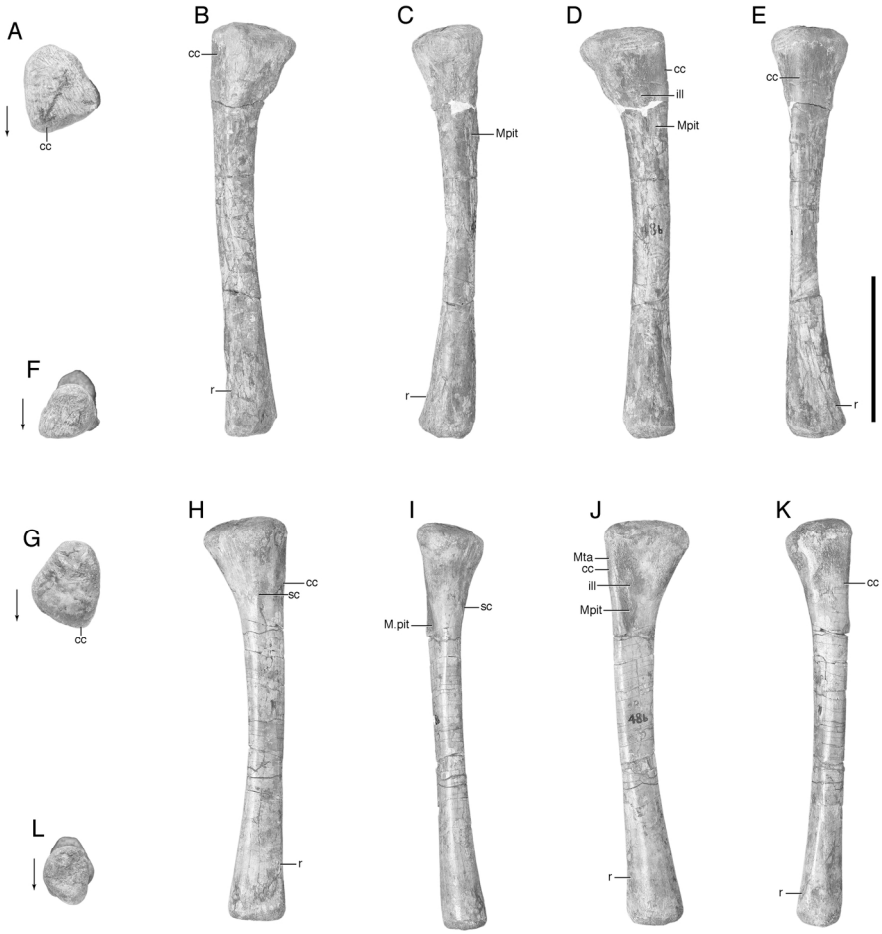

170x162mm (300 x 300 DPI)

color

117x154mm (300 x 300 DPI)

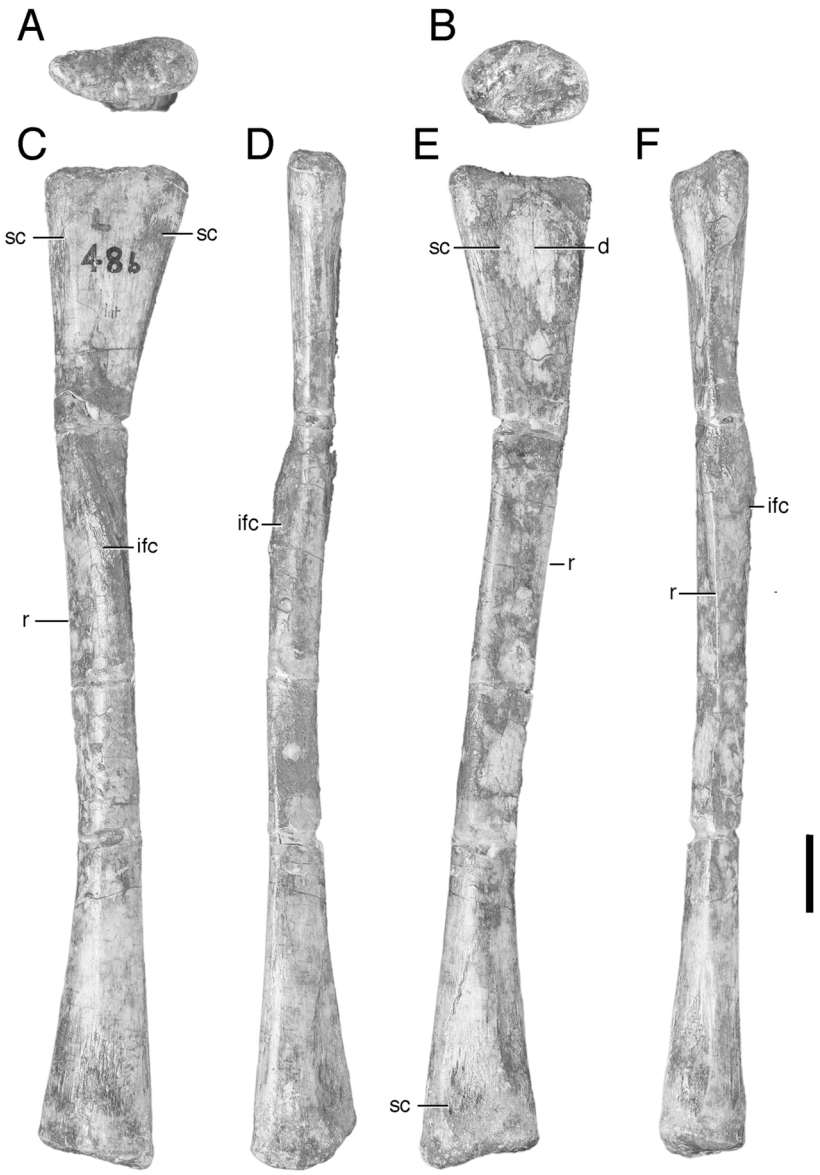

117x154mm (300 x 300 DPI)

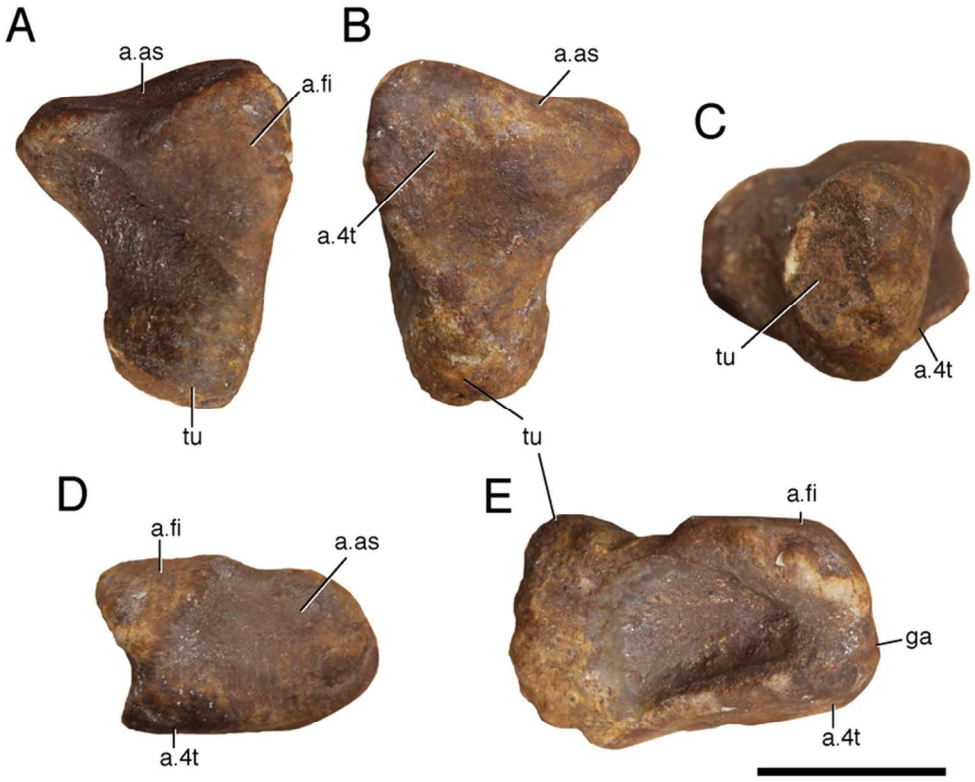

color

75x62mm (300 x 300 DPI)

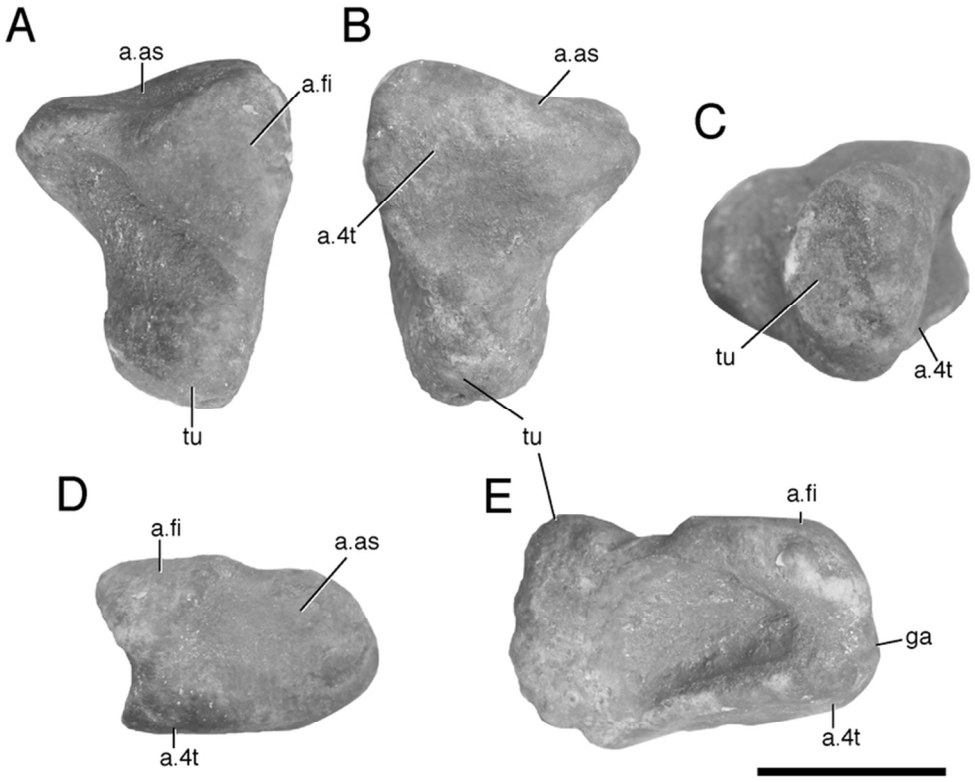

75x62mm (300 x 300 DPI)

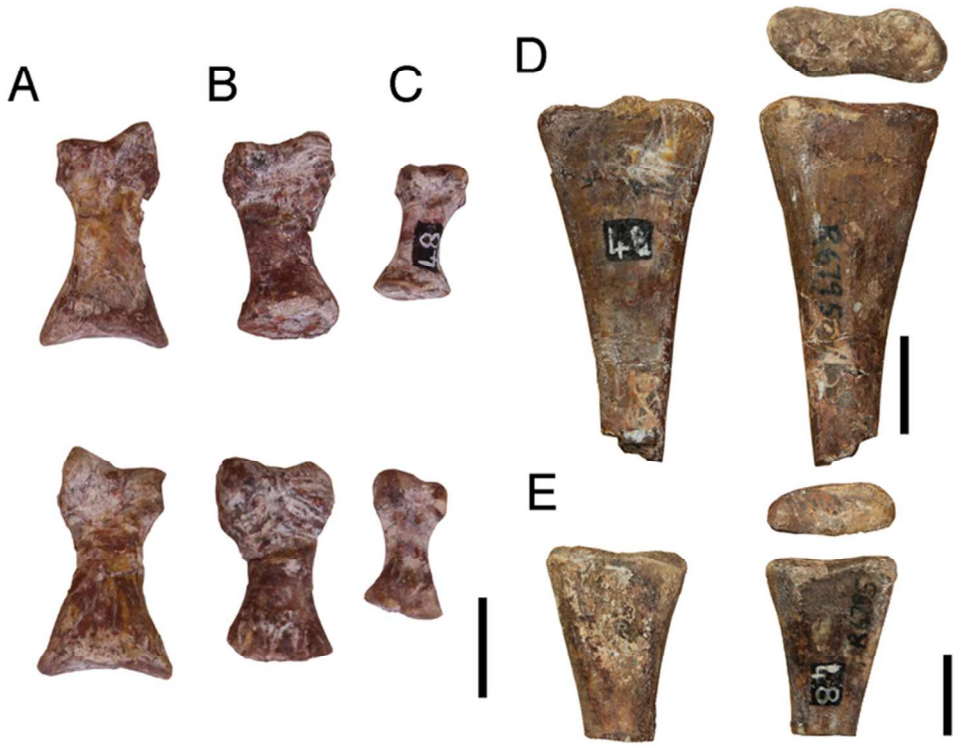

color

66x52mm (300 x 300 DPI)

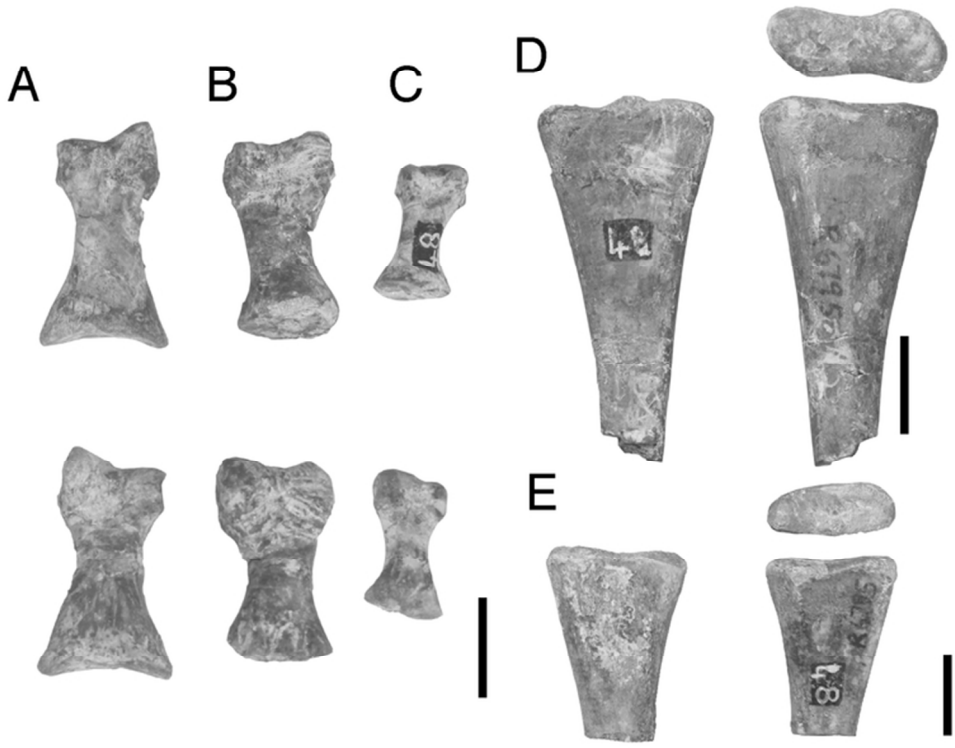

66x52mm (300 x 300 DPI)

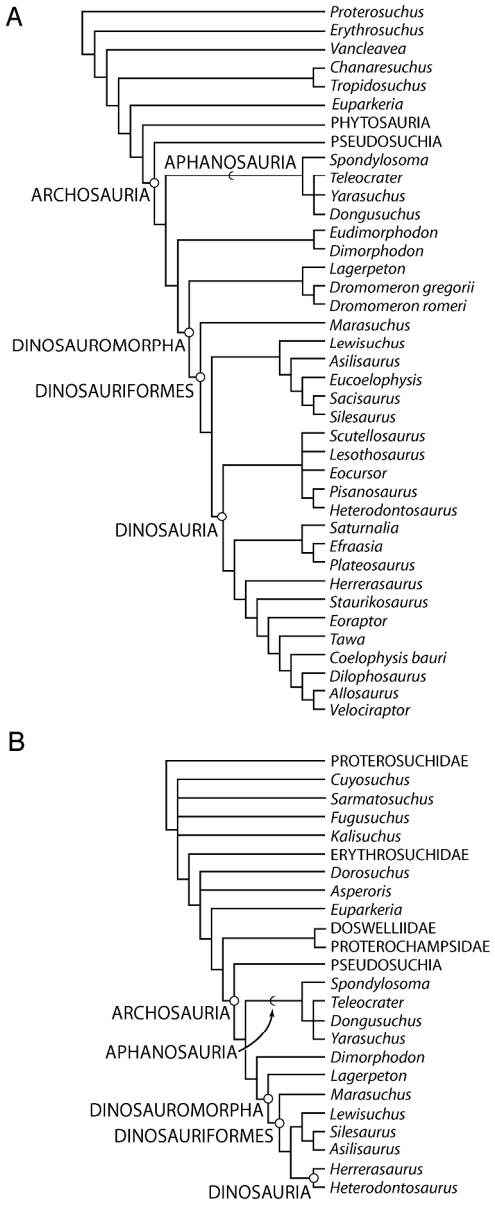

192x427mm (300 x 300 DPI)

color

102x57mm (300 x 300 DPI)

102x57mm (300 x 300 DPI)

TABLE 1. Measurements of the cervical, dorsal, and caudal vertebrae of the holotype of *Teleocrater rhadinus* (NHMUK PV R6795). The proposed order of vertebrae within the column follows that proposed by Charig (1956) and reflects some uncertainly in the exact positions of the vertebrae. **Abbreviations: Cd**, caudal vertebra; **CHA**, height of anterior centrum articular surface; **CHP**, height of posterior centrum articular surface; **CL**, centrum length; **CMW**, centrum minimum transverse width; **Cv**, cervical vertebra; **CWA**, width of anterior centrum articular surface; **CWP**, width of posterior centrum articular surface; **D**, dorsal vertebra. All measurements are provided in mm. Measurements that are too distorted/incomplete to include are denoted by a hyphen.

Vertebra	CL	CHA	CWA	CHP	CWP	CMW
CvA	53	-	-	14	13	8
CvB	32	14	15	14	15	7
DA	26	14	15	15	15	7
DB	25	14	15	15	16	7
DC	24	14	17	13	17	8
DD	25	13	15	13	15	7
DE	28	14	16	13	16	7
DF	30	13	17	14	18	6
DG	26	14	16	15	18	8
DH	21	14	17	14	17	9
DI	22	17	20	15	18	10

TABLE 1. (continued)

DJ	21	16	-	17	18	9
DK	21	16	17	16	17	10
CdA	24	14	13	14	13	7
CdB	23	13	12	12	12	7
CdC	23	12	12	11	11	6
CdD	23	11	11	10	11	6
CdE	23	11	11	11	11	5
CdF	23	10	10	11	10	5
CdG	24	9	9	10	9	5
CdH	25	10	9	12	9	5
CdI	23	10	10	10	10	5
CdJ	22	10	10	10	10	6
CdK	22	9	9	9	9	5
CdL	25	10	10	10	10	6
CdM	24	9	9	9	9	5
CdN	25	10	10	8	9	5
CdO	22	7	6	6	7	3

TABLE 2. Measurements of the fore- and hind limb elements of *Teleocrater rhadinus* (NHMUK PV R6795: holotype). All measurements are provided in mm.

Element/measurement	
Right radius	
Length	88
Length of proximal end	16
Length of distal end	12
Midshaft circumference	22
Right ulna	
Length	92
Length of proximal end	19
Length of distal end	13
Midshaft circumference	22
Right femur	
Length	170
Length of proximal end	35
Length of distal end	35
Midshaft circumference	51

TABLE 2. (continued)

Left femur	
Length	170
Length of proximal end	35
Length of distal end	35
Midshaft circumference	53
Right tibia	
Length	145
Length of proximal end	30
Length of distal end	20
Midshaft circumference	40
Left tibia	
Length	145
Length of proximal end	30
Length of distal end	21
Midshaft circumference	41
Left fibula	
Length	143
Length of proximal end	20
Length of distal end	17
Midshaft circumference	27

TABLE 2. (continued)

TABLE 3. Measurements of the cervical, dorsal, and sacral vertebrae of referred material of *Teleocrater rhadinus*. **Abbreviations: CHP**, height of posterior centrum articular surface; **CL**, centrum length; **CMW**, centrum minimum transverse width. All measurements are provided in mm.

Element	Specimen number	CL	CHP	CMW
Axis	NMT RB504	27	10	6
Anterior cervical	NMT RB505	41	13	8
Anterior cervical	NMT RB506	33	11	8
Middle cervical	NMT RB511	39	16	8
Middle cervical	NMT RB512	55	22	8
Posterior cervical	NMT RB514	23	14	7
Anterior dorsal	NMT RB500	21	15	7
Posterior dorsal	NMT RB516	23	15	8
Sacral 2	NMT RB519	20	17	7

TABLE 4. Measurements of the pectoral girdle, fore-, and hind limb elements of specimens referred to *Teleocrater rhadinus*. All measurements are provided in mm. Those marked with an '*' are estimated due to abrasion/breakage.

Element/measurement	
Right scapula (NMT RB480)	
Length	92
Proximal length	50*
Distal length	32
Diameter at constriction	17
Left humerus (NMT RB476)	
Length	112
Proximal length	48
Distal length	42
Circumference at midshaft	340
Left humerus (NMT RB477)	
Length	87
Proximal length	38
Distal length	32
Circumference at midshaft	32

TABLE 4. (continued)

Left ulna (NMT RB485)	
Length	85
Proximal length	16
Distal length	13
Circumference at midshaft	21
Left ulna (NMT RB486)	
Length	83
Proximal length	17
Distal length	14
Circumference at midshaft	23
Right femur (NMT RB498)	
Length	160
Proximal length	35
Distal length	33
Circumference at midshaft	46
Left tibia (NMT RB481)	
Length	129
Proximal length	30
Distal length	20

TABLE 4. (continued)

Circumference at midshaft	33
Right fibula (NMT RB482)	
Length	153
Proximal length	20
Distal length	20
Circumference at midshaft	30
Metacarpal ?II (NMT RB484)	
Length	23
Proximal length	8
Distal length	7
Circumference at midshaft	10